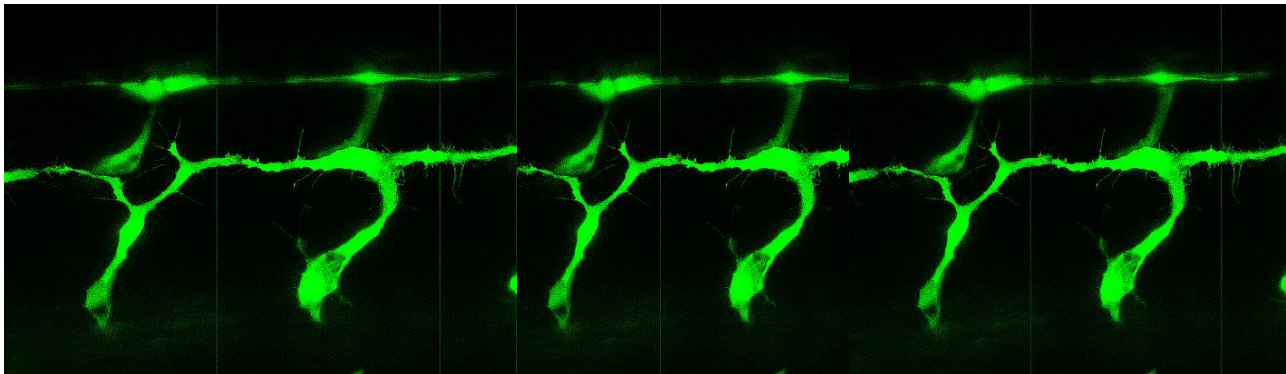Cover Page

Universiteit Leiden

Author: Rian, Hanan
Title: Functions of P38 and ERK kinases in zebrafish early development
Issue Date: 2014-01-15

Functions of P38 and ERK kinases in zebrafish early development

Hanan Rian

Functions of P38 and ERK kinases in zebrafish early development

Hanan Rian

Functions of P38 and ERK kinases in zebrafish early development

PROEFSCHRIFT

Ter verkrijging van de graad van Doctor aan de Universteit Leiden, op gezag van de Rector Magnificus prof.mr. C.J.J.M. Stolker, volgens besluit van het College voor Promoties te verdedigen op woensdag 15 Januari 2014 klokke 13:45 uur

door

Hanan Rian

Geboren te Winterswijk

31 januari 1984

Promotiecommissie

Promotor: Prof. dr.H.P.Spaink

Co-promotor: Dr. B. E. Snaar-Jagalska

Overige leden:

Prof. Dr. C.J. ten Cate

Prof. dr. Jaap Brouwer

Prof. Dr. J. den Hertog

Prof. Dr. G.J. Wiegertjes (Wageningen University)

Contents

CHAPTER I INTRODUCTION

1.1 Mitogen activated protein kinases (MAPK) in general

Cells communicate in multicellular organisms; by secreting and sensing signals, in order to adjust their behavior to the environment. Extracellular signals such as cytokines and growth factors bind to cell surface receptors and trigger the activation of multiple protein signal transduction cascades that mediate cellular responses such as proliferation, differentiation, apoptosis and motility. The Mitogen-activated protein kinase (MAPK) family is a group of homologous proteins forming several linear signal transduction pathways functioning in translating environmental cues into cellular behaviour **Fig1**. MAPKs exhibit their function in the form of sequential phophorylation events leading to two outcomes. The formation of functional signalling complexes in the nucleus to influence gene regulatory networks underlining cellular transformations induced by the environment. Alternatively, MAPKs could be retained in the cytoplasm and influence activity of cytoplasmic proteins [1,2].

Fig1: *MAPK pathways.* The MAPK family consist of the ERK, JNK and P38 subfamilies. Most of the MAPK family members are functional within a MAPKKK-MAPKK-MAPK signaling cascade that is stimulated by members of the small GTPase family such as RAS,RAC,CDC42 and RHO. Small GTPases are kept in an GTP bound active state by Guanine nucleotide exchange factors (GEFs) which relay the signal from membrane bound activated receptors. Activated MAPK could translocate to the nucleus and influence gene expression networks. *Liu et al. 2007,Nature Reviews Immunology*
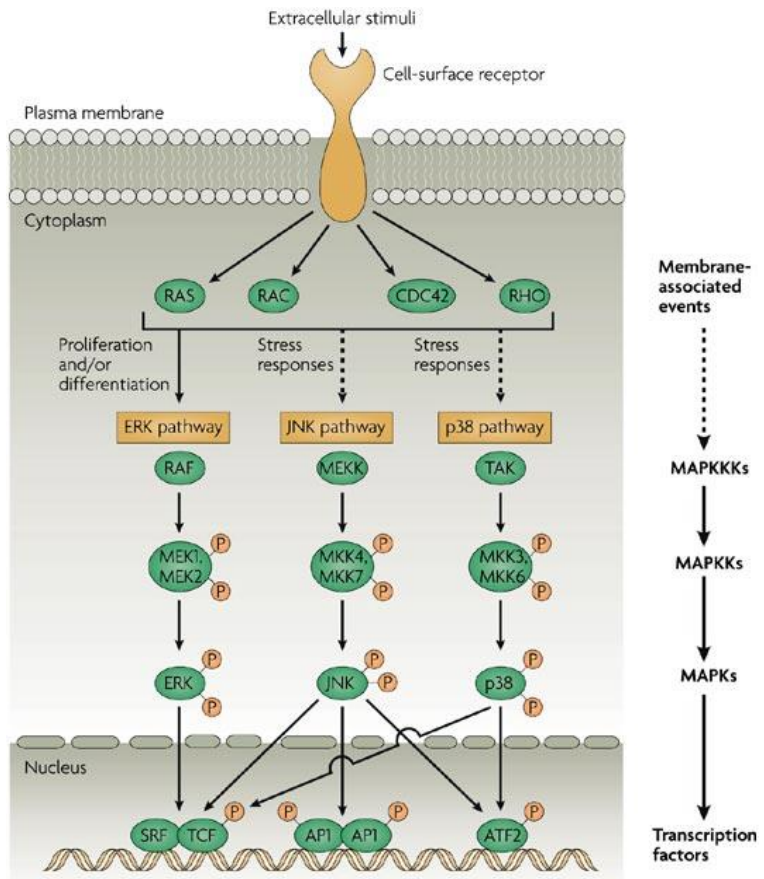
MAPK are classified into three subfamilies according to the middle amino-acid residue of the conserved Thr-X-Tyr dual-phosphorylation motif; the extracellular signal regulated kinases (Erk1,2,3,4,5,6,7) with a Thr-Glu-Tyr, the c-Jun amino-terminal kinases (Jnk1/2/3) have a Thr-Pro-Tyr motif and the P38 MAPK (α,β,γ, and

11

Δ) a Thr-Gly-Tyr. Phosphorylation of the Thr-X-Tyr motif activates the MAPK and occurs either by an upstream MAPK Kinase (MAPKK) or by autophosphorylation[2,3]. The MAPKK, (also called Mek) are in turn phosphorylated at Ser/Thr residues by upstream MAPKK Kinases (MAPKKK or Mekk) which could be activated by small GTP-binding proteins of the Ras/Rho family which relay signals from receptor tyrosine kinases (Rtk), integrins or G-protein coupled receptors[4-6].

MAPKs control the activity of numerous transcription factors and cytoplasmic proteins, including other kinases, by phosphorylation of Ser/Thr residues [7-9]. Transcription factor phosporylation occurs in the nucleus after translocation of MAPK as monomers [10]. MAPK could also form dimers and functional complexes with scaffold proteins to regulate signal transduction events in the cytoplasm. Scaffolding proteins are adaptor or anchoring proteins that bind multiple signalling proteins and create a functional complex at a particular subcellular location **Fig2**[11]. The cellular response is mediated by the duration of MAPK activity which depends on a dynamic exchange of phosphate groups on the dual phosphorylation
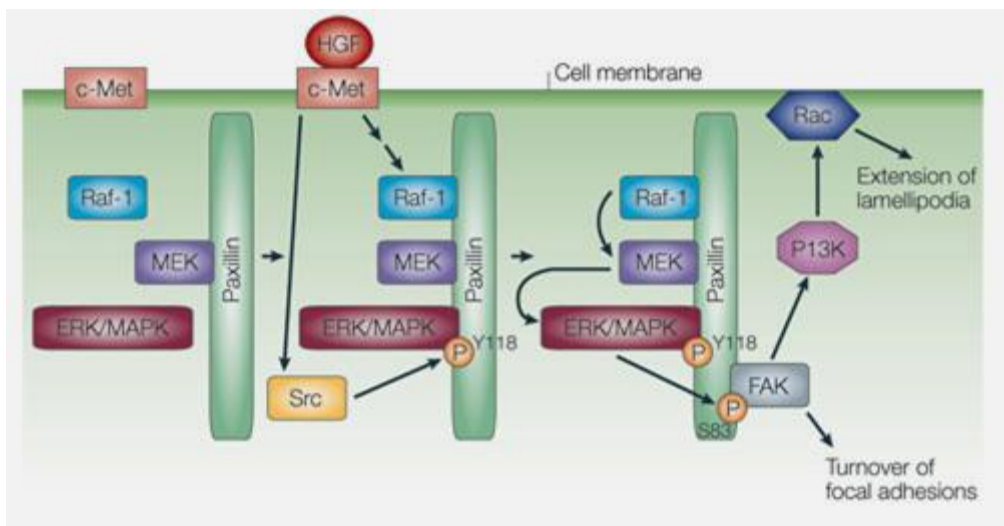
Fig2: Spatio-temporal regulation of the MAPK phosphorelay system by Scaffold proteins. MAPK signaling cascades can be organized into functional complexes at a specific subcellular location by interaction with scaffolding proteins. Paxillin is a scaffold protein recruiting the RAF-MEK-ERK cascade to focal adhesions which are large, dynamic protein complexes through which the cytoskeleton of a cell connects to the extracellular matrix. Following c-met activation, by the hepatocyte growth factor (HGF), paxillin binds and recruits the MAPK cascade to focal adhesion where activated ERK phosphorylates paxillin at S83 creating a binding site for focal adhesion kinase (FAK) at the scaffold and subsequent activation of phosphatidylinositol 3-kinase (PI3K) and Rac. This results in the extension of lamellipodia. *Walter Kolch 2005, Nature Reviews Molecular Cell Biology.*

motif by MAPK kinases and phosphatases[12]. MAPK phophatases (MKPs) inactivate the pathway by direct dephosphorylation of both the tyrosine and threonine residues of the dual phosphorylation motif[12]. Protein Tyrosine Phosphatases (PTPs) switch off the receptor signal through inactivation of upstream pathway members including RTK[13]. Finally, protein serine/threonine phosphatases (PSPs) act downstream of MAPK by removing phosphates of substrates. Interestingly, PP2A is a MEKK1 phosphatase which is activated by P38 during stress creating an inhibitory effect on Erk1/2 induced proliferation.

The MAPK family is conserved among eukaryotes and most vertebrates contain at least 14 MAPKs, 7 MAPKKs, and 20 MAPKKKs. Because of the characteristic conformation of both the MAPK activation loop containing the (Tyr-X-Thr) motif and the kinase pocket of MAPKKs this interaction is highly specific yet allows for some redundancy especially between closely identical isoforms from the same subfamily such as Erk1 and Erk2 or P38α and P38β. The 14 mammalian MAPKs can therefore be divided into four conventional MAPK signalling cascades and atypical MAPKs which are possibly constitutively active.

The first identified (canonical) cascade includes Erk1/2 which are specifically activated by Mek1/2 and initially discovered to be stimulated by growth factors (Egf, Pdgf, Igf and Fgf). The canonical MAPK pathway is stimulated after binding of Egf with its receptor. Ligand bound Egfr signals through adapter protein Grb2 and the Gef Sos to activate the small GTPase family member Ras. Ras transmits the signal to the MAPK cascade by recruiting Raf to the cell membrane for activation. Raf is a MAPKKK, the first kinase of the Erk1/2 cascade, which phosphorylates Mek1 and Mek2. Several other mitogen receptors, such as lpdgfr, Fgfr, Ngfr and Igfr, stimulate the pathway after ligand binding.

P38α,β,γ,Δ constitute the second cascade and are activated by Mek3 and Mek6 but also Mek4 which creates a crosstalk with the third cascade including Jnk1/2/3 and Mek7. Both P38α,β,γ,Δ and Jnk1/2/3 pathways are initially discovered to be stimulated by stress signals such as X-ray/UV irradiation, heat/osmotic shock, and oxidative/nitrosative stress as well as by proinflammatory cytokines. The fourth cascade with Erk5 and Mek5 is also activated by cellular stressors, cytokines and growth factors which are transmitted through Mekk2 and Mekk3. Erk5, also referred to as big MAPK kinase 1(Bmk1), has a larger C-terminal region containing an auto-inhibitory domain and nuclear localization signal[7,14-17]. **Fig1.**

Since the first discovery in 1990, research involving gene expression and functional analysis for identified members of the MAPK family is ongoing. Functional experiments with methods ranging from genetic engineering, pharmacological inhibition, siRNA or transgene expression are frequently used to outline specific and redundant functions of the various MAPK family members within certain contexts.

Some MAPK isoforms are widely expressed and functional in a great number of cell types ranging from embryonic to terminally differentiated lineages. In addition, MAPKs are discovered to be critically involved in severe disorders including cancer, Alzheimer, autoimmune/inflammatory diseases and also human genetic hereditary disorders [7,18-21]. How the existing closely related isoforms of a protein family, sharing sequence and functional domain similarities, take part in orchestrating cellular behaviours is in general a fundamental research topic with great scientific
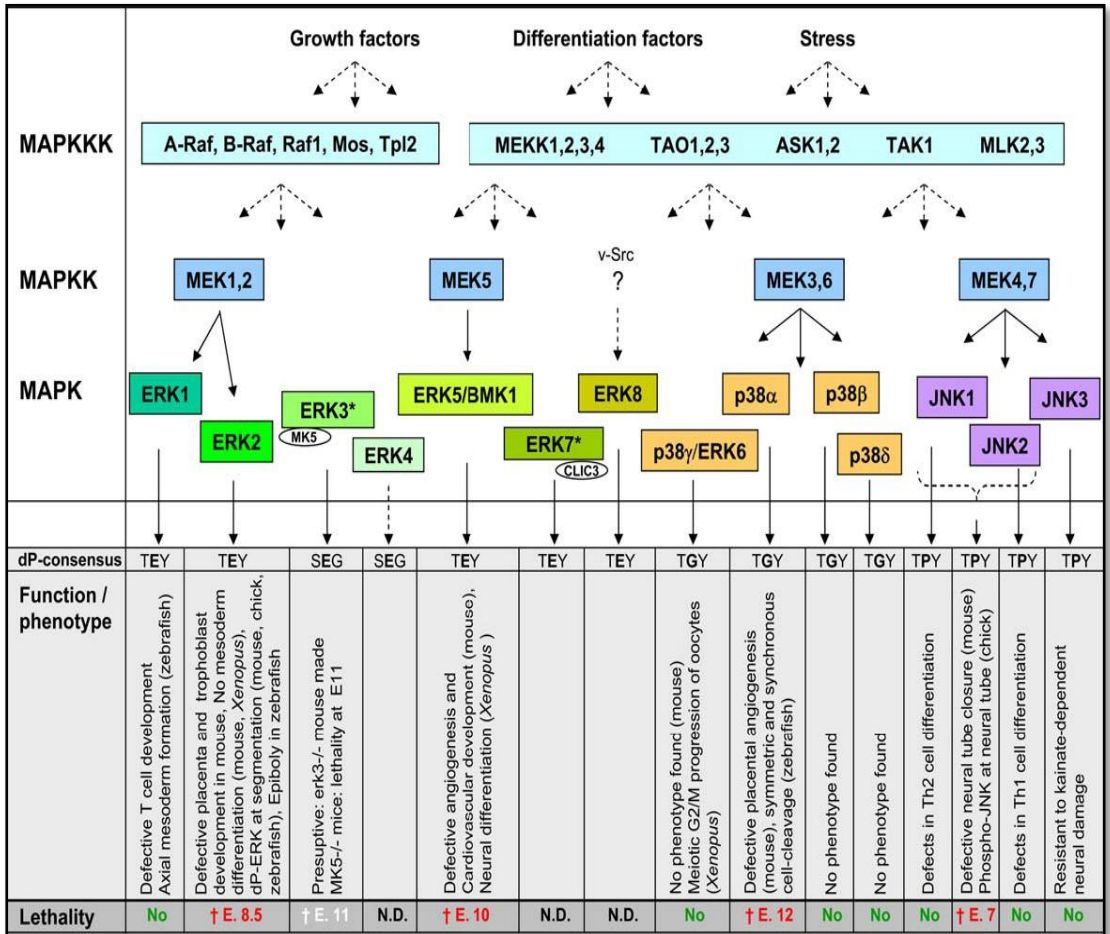
MAPKKK A-Raf, B-Raf, Raf1, Mos, Tpl2 | MEKK1,2,3,4 TAO1,2,3 ASK1,2 TAK1 MLK2,3

Growth factors — Differentiation factors — Stress

MAPKK MEK1,2 | MEK5 | v-Src ? | MEK3,6 | MEK4,7

MAPK ERK1, ERK2, ERK3* (MK5), ERK4 | ERK5/BMK1 | ERK8, ERK7* (CLIC3) | p38α, p38γ/ERK6, p38β, p38δ | JNK1, JNK2, JNK3

	ERK1	ERK2	ERK3*	ERK4	ERK5/BMK1	ERK8	ERK7*	p38α/p38γ-ERK6	p38β	p38δ(TGY)	JNK1	JNK2	JNK3	JNK (TPY)
dP-consensus	TEY	TEY	SEG	SEG	TEY	TEY	TEY	TGY	TGY	TGY	TGY	TPY	TPY	TPY	TPY
Function / phenotype	Defective T cell development Axial mesoderm formation (zebrafish)	Defective placenta and trophoblast development in mouse. No mesoderm differentiation (mouse, Xenopus). dP-ERK at segmentation (mouse, chick, zebrafish), Epiboly in zebrafish	Presuptive: erk3-/- mouse made MK5-/- mice: lethality at E11		Defective angiogenesis and Cardiovascular development (mouse), Neural differentiation (Xenopus)			No phenotype found (mouse) Meiotic G2/M progression of oocytes (Xenopus)	Defective placental angiogenesis (mouse), symmetric and synchronous cell-cleavage (zebrafish)	No phenotype found	No phenotype found	Defects in Th2 cell differentiation	Defective neural tube closure (mouse) Phospho-JNK at neural tube (chick)	Defects in Th1 cell differentiation	Resistant to kainate-dependent neural damage
Lethality	No	†E.8.5	†E.11	N.D.	†E.10	N.D.	N.D.	No	†E.12	No	No	No	†E.7	No	No

Fig3: The different MAPK cascades and their function in development. The identified MAPK pathways: ERK1/2, JNK1/2/3, p38α/β/γ/δ, ERK5, ERK3/4 and ERK7. The function, obtained by gene targeting or silencing studies are described for each MAPK. The lethality-index indicates if gene-disruption in mice resulted in a lethal developmental phenotype and at what day of development (†=lethal, No=not lethal, ND=not determined). erk3−/− mice neonates die within minutes after birth from acute respiratory failure. Recently (*Rousseau et al. 2010*) Erk4 is shown to be dispensable for mouse embryonic development. *Figure from Krens et al. 2006.*

value for molecular cell biology. Distinction of MAPK isoform signalling could also be beneficial in medical science related to MAPK associated diseases. Strategic invention of effective pharmaceuticals causing limited side effects requires facts of MAPK isoform specific signalling within relevant cellular and micro-environmental context.

1.2 MAPK in embryonic development

1.2.1 Lessons from *In vivo* and *In vitro* knock-out studies in mice.
In vivo functional distinction of MAPK family members has been achieved in particular with the gene-targeting technology in mice. Defects resulting from homologous recombination to disrupt the endogenous gene of interest are reported for most MAPK isoforms except Erk7 and Erk8 **Fig3**. Proteins indispensible for embryonic development could be functional in specific events such as patterning to establish the body plan or control pluripotent cell differentiation into lineages of cells and tissues. Functional studies could provide insight into the underlying mechanisms of human developmental genetic disorders.

Several studies have demonstrated Erk2, Erk5 and P38α to be essential for early vertebrate development and each fulfil a role that could not be compensated by other MAPK family members. Jnk1 and Jnk2 are fully functional redundant in regulation of early brain development. *Jnk*1-/- *Jnk*2-/- double knock-out mice die at E.11 due to defects in neural tube closure and deregulated neural apoptosis while embryos from single knock-outs showed no severe morphological abnormalities[22,23]. In contrast, a genetic study with embryonic stem cells (ESC) suggested that only the Jnk1 isoform was essential for neural differentiation induced by retinoic acid [24]. The expression of wnt-4 and wnt-6, inhibitors of ES cell neurogenesis, was found significantly elevated in JNK1(-/-) cultures relative to wild-type, JNK2(-/-), and JNK3(-/-) cultures. In addition, adult mice Jnk1 or Jnk2 single knock-out display defects of activated T lymphocyte differentiation into T-helper cells [25,26].

Erk2 plays a unique role during gastrulation, the differentiation of endoderm, mesoderm and ectoderm cell layers of embryonic blastocysts [27-29]. Gastrulation, the differentiation of endoderm, mesoderm and ectoderm cell layers of the blastocyst, is regulated by morphogens such as Fgf, Bmp, Wnt and Nodal which collectively orchestrate patterning and cell specification of the vertebrate and the invertebrate embryo. The Erk1/2 cascade functions downstream of Fgf and is involved in specification of the mesoderm, neural induction, anterior-posterior patterning and FGF formation during gastrulation[30]. Pluripotent mice ESC lacking either FGF4/ERK2 autocrine signalling resist mesodermal and neuronal induction

[31]. The Fgf-Erk pathway is an autoinductive stimulus for naive ES cells to exit the self-renewal programme and differentiate towards a state that is responsive to inductive cues for germ layer segregation[31,34,35]. The mesoderm defective phenotype was demonstrated *in vivo* with Erk2-deficient mice as well which also fail to induce the mesoderm cell fate[32]. Erk2 deficient embryos showed also increased apoptosis but proliferation was unaffected. In many somatic cell types, the Erk1/2 cascade is stimulated by mitogens and plays a prominent role in inducing proliferation. The mitogen stimulated ERK1/2 promotes proliferation by translocation to the nucleus for direct phosphorylation of transcription factors ets1, c-myc, c-jun, fos and indirect phosphorylation of CREB through p90RSK. Hyperactivation of the Erk1/2 cascade, as a result of upstream EGFR, RAS and RAF oncogene activity, is associated with uncontrolled proliferation of tumours. However undifferentiated mice ESC, sharing the same proliferative characteristics as transformed cells, do not require the Erk pathway for proliferation and expression of self-renewal markers Oct4, Nanog and Rex[33]. In fact, ESC and transformed cells can be propagated clonally, multiply in absence of serum and are not subject to contact inhibition or anchorage dependence. However attenuation of ERK signalling, by pharmacological inhibition of MEK activity or by ectopic expression of ERK phoshatases, facilitates self-renewal by reducing differentiation specifically in ESC.
Erk2 Knock-out in another *in vivo* background (C57BL/6 mice) leads also to embryonic lethality early in mouse development but after the implantation stage and reveals that Erk2 is essential for the formation of the placenta. Erk2-/- mice failed to form extra-embryonic ectoderm and the ectoplacental cone which differentiate from trophoblasts[36]. Erk2 is therefore involved in the first embryonic differentiation event where the blastocyst segregates into two cell lineages the trophoblast, which will specifically develop into extra-embryonic tissue forming the placenta, and the inner cell mass (ICM) which will predominantly give rise to the fetus.

Several studies using different background mice and knock-out approaches have shown that P38α knock-out is embryonic lethal within the first 12 days. Defects observed in P38α -/- mice include aberrant placental angiogenesis, increased apoptosis and massive reduction of the myocardium [27,37-39]. At the cellular level, P38α is abundantly present in ESC however knock-out did not affect endothelial, smooth muscle and neuronal cell differentiation. P38α-/- ESC have significantly increased cell adhesion to several extracelluar matrix proteins, correlating with elevated phosphorylation of focal adhesion kinase and paxillin. P38alpha -/- ESC also showed increased cell viability, correlating with increased expression of survivin and activation of AKT (protein kinase B)[40].

The Mek5/Erk5(Bmk1) cascade plays a role in embryonic development after the gastrulation stage. Erk5 deficient mice displays aberrant extra-embryonic (placental)

and embryonic blood vessel organization and maturation. Erk5 plays a role in controlling angiogenesis most likely by regulating endothelial cell survival. Histological and *In vitro* examination showed that endothelial cells lost their integrity, became round and eventually apoptotic. Also Cardiac development was largely retarded in Erk5-/- mice, and the heart failed to undergo normal looping [41].

1.2.2 MAPK in zebrafish development.

The disadvantage of the gene knock-out technology in mice is that it is time consuming and costly. The zebrafish is a much better alternative to screen for embryonic important genes. Synthetic antisense oligonucleotides known as morpholinos can be injected easily in batches of first stage zebrafish embryos for targeted knock-down of endogenous genes. A pair of adult zebrafish could lay 100 to 200 embryos according to a 10 hour light cyclus and batches of embryos of a particular stage can be obtained for experimentation. The ex-utero development and transparency of the embryo makes it possible to record phenotypes in wild type or transgenic fluorescent zebrafish lines. With the current available zebrafish tools molecular mechanisms could be identified and linked to cellular processes and morphological observations.

All 14 zebrafish MAPK genes are evolutionary conserved in zebrafish and analysis of phylogeny, based on zebrafish, mice, rat, xenopus, and human amino acid sequence similarity, shows that the different vertebrate MAPK cluster with their corresponding orthologs[28]. Most zebrafish MAPK are recently cloned and characterized by our laboratory using semi-quantitative RT-PCR expression analysis of different developmental stages and whole mount in situ hybridization for expression localization[42]. Further efforts for functional elucidation in zebrafish embryology have been performed for ERK1, ERK2, P38α and JNK1. The Current thesis described additional two MAPK members of the P38 subfamily: the P38β and P38δ isoforms.

FGF activation of the ERK1/2 cascade is also in the zebrafish embryo a critical molecular event during gastrulation. Zebrafish gastrulation occurs during epiboly a morphogenetic movement of the blastoderm over the interface of the yolk until fully covered. When the cells reach the equatorial region of the embryo the three cellular germ layers are formed depending on positional cues and distinct cell migratory properties provided by interplay of Bmp, Nodal, Wnt and Fgf morphogen gradients [43,44]. The Fgf protein family contains 23 members of which Fgf8, Fgf3, Fgf17b and Fgf24 are expressed at the margin of the migrating blastoderm during epiboly[45]. Erk1 and Erk2 are expressed throughout the blastoderm however activity is detected with Erk1/2 immuno-staining at the margin[46]. Morpholino knock-down of both MAPKs identifies Erk2 as a critical mediator of epiboly cell movements and differentiation of mesodermal cell fate[46]. Saturated Erk2 knock-

down prevents a large pool of embryos from initiating epiboly and the remaining from convergent extension movements that occur at 50% epiboly during the actual segregation of the germ layers. Transcriptional profiling of Erk2 morphants revealed downregulated mesoderm specific T-box transcription factors which are also known to be regulated by Fgf8[54]. Furthermore the Ap1 and Ets2 transcription factors are known Erk2 direct substrates and functional in Fgf induced mesoderm formation in xenopus[55,56]. Erk1 knock-down resulted only in a mild effect on epiboly progression without effect on mesoderm markers expression. P38α and its direct substrate Mapkapk2 are implicated in zebrafish epiboly as well [57,58]. However the molecular mechanism upstream and the downstream signaling during zebrafish gastrulation remain still unclear. Perhaps the Fgf pathway does also influence the P38α MAPK signaling. In somatic cells P38α can be activated by growth factors via the similar Grb2-Sos-Ras pathway which lead to the activation of the Raf-Mek1/2-Erk1/2 pathway from activated receptor tyrosine kinases. Growth factor stimulated Ras can also activate Cdc42 and Rac/Posh which will lead to activation of the Mixed Lineage Kinase Mlk2/3 which are MEKK upstream of P38 and also Jnk MAPKs[59]. The non-canonical Wnt pathway, also a major regulator of cell migration during gastrulation, could also recruit Rac to activate the Jnk module in Xenopus and mammalian cells [60]. Alterations in Rac or Jnk activity did disrupt Xenopus gastrulation and polarized cell movements. In zebrafish knock-down of Jnk1 did not result in severe defects in migration (unpublished data). Since functional redundancy of Jnk1 and Jnk2 was demonstrated previously in mice, the function in zebrafish epiboly might still be continued to be performed by Jnk2 despite reduced levels of Jnk1 in these embryos. Like in mice, a double Jnk1 and Jnk2 morpholino knock-down in zebrafish would reveal its possible function if this is the case. However this thesis focuses on the role of P38 and Erk2 MAPK in zebrafish early development.

Other early embryonic activities regulated by Fgf morphogens, and possibly the downstream Erk cascade, during gatrulation are dorso-ventral patterning, neural induction, endoderm formation and left-right assymmetry [30,47-49]. Over activation of Fgf8/Fgfr1/Ras/Mek signaling pathway leads to regional expansion of Bmp antagonists Chordin, Noggin and Follistatin expression which mark the dorsal side. Consequently the expression of Bmp ventral markers Bmp2b and Bmp4 is significantly reduced[49]. Dorsalized embryos appear extremely elongated which was the case after over activating a member of the Fgf8/Fgfr1/Ras/Raf/Mek cascade [47,50-52]. Neural induction is the process whereby naive ectodermal cells are instructed to adopt a neural fate. The ectoderm gives rise to both the neural tissue and the epidermis. Impeding FGF signaling results in a shift of posterior ectodermal markers from neural to epidermal. Dominant negative RAS blocks induction of posterior neural markers [53]. Conversely, over expression of Fgf3 expands posterior neural tissue. Anterior neural tissue, along with posterior

18

neuronal fate, fails to develop when inhibiting both FGF and Nodal signaling during zebrafish gastrulation. Specification of the neural plate requires repression of BMP signaling in the dorsal ectoderm. The FGF-MEK-ERK pathway induces expression of BMP antagonists and is able to block BMP binding to the receptor. However, an alternative pathway is also suggested since FGF signaling was able to repress BMP expression in absence of protein synthesis. The interaction of FGF/ERK pathway with BMP and Nodal signaling is also crucial for endoderm formation. While the ectoderm germ layer arises from the animal pole region of the embryo, the mesoderm and endoderm progenitors are located at the margin at the expression region of Nodal and Fgf. The endoderm progenitors arise from the first four rows of marginal cells, while the mesoderm develops from the entire marginal region. Endoderm specification is repressed in regions with both FGF/Erk and Bmp expression. Although FGF expression ovelaps the most vegetal marginal cells which develop into endoderm, BMP morphogens are absent in this region. Left-right assymmetry of the brain, heart and gut is regulated in the zebrafish by a ciliated epithelium inside a fluid-filled organ called Kupffer's vesicle which arise from dorsal forerunner cells during gastrulation. Multiple Kupffer's vesicles migrate ahead from the migrating margin establishing a directional fluid flow resulting in asymmetrical gene expression that leads to asymmetrical organogenesis. The fibroblast growth factor (FGF) signalling regulates cilia length and function in diverse epithelia during zebrafish and *Xenopus* development. Morpholino knockdown of FGF receptor 1 (Fgfr1) in zebrafish cell-autonomously reduces cilia length in Kupffer's vesicle and perturbs directional fluid flow required for left–right patterning of the embryo. Expression of a dominant-negative FGF receptor (DN-Fgfr1), treatment with SU5402 (a pharmacological inhibitor of FGF signalling) or genetic and morpholino reduction of redundant FGF ligands Fgf8 and Fgf24 reproduces this cilia length phenotype.

1.3 Structural comparison of P38 and ERK MAPK

The effect of MAPK signalling into different possible cellular outcomes depends on presence of kinases and phosphatases that regulate the on and off switching of the MAPK [61,62]. The mechanism of MAPK activation is much more understood since the crystal structures of both the low-activity, (unphosphorylated) and high-activity (phosphorylated) forms are resolved with X-ray crystallography **Fig4**. Especially research focused on Erk2 structural changes following phosphorylation provided insight into a common mechanism controlling activation and substrate specificity for protein kinases in general [61-65]. Folded protein kinases appear in two spherical lobes; the N-lobe and the C-lobe with the catalytic site in between **Fig4a**. The N- and C-lobes rotate apart to release substrates or together to align the catalytic site residues located at the interface of the two lobes [66]. The proper juxtaposition of active site residues on both lobes enables phosphoryltransfer from ATP to
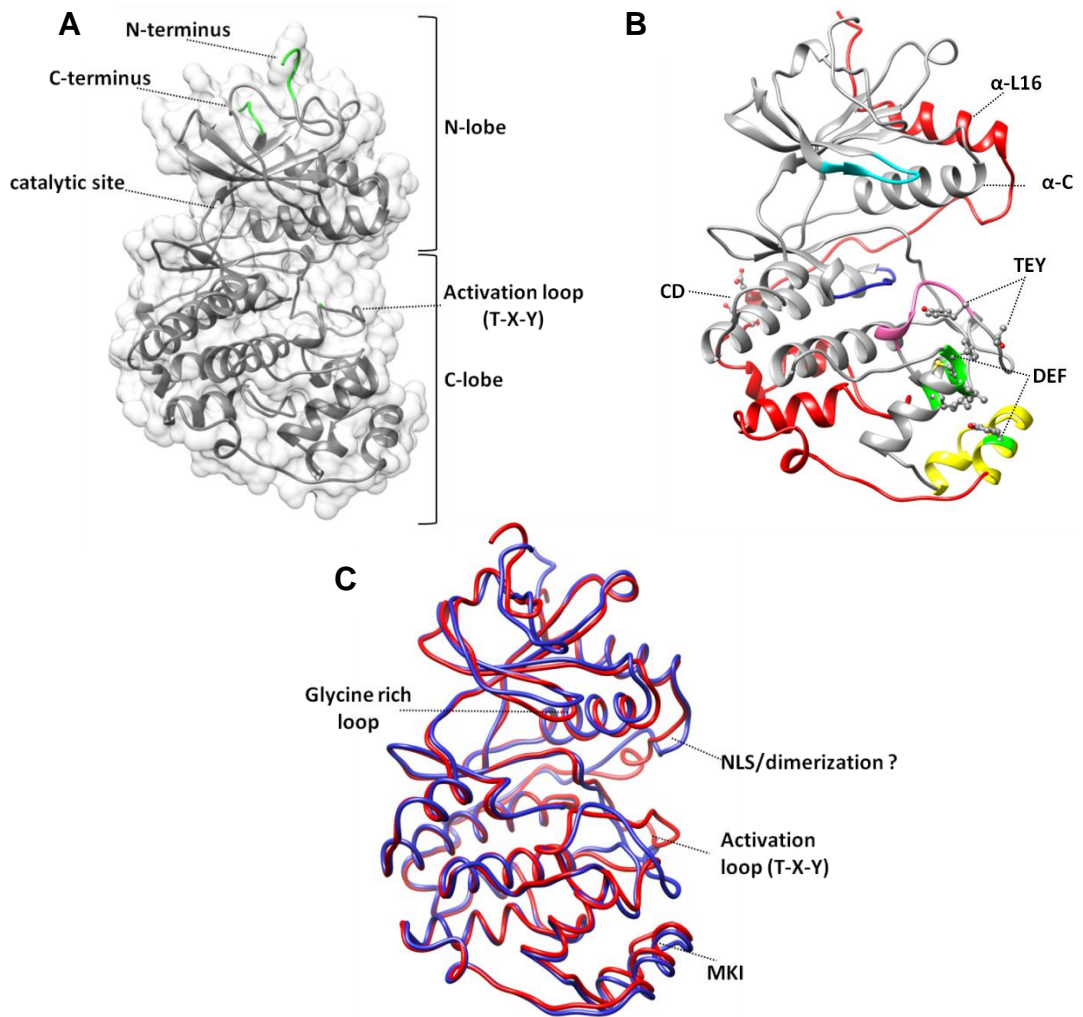
Fig4: Predicted three-dimensional structure of zebrafish Erk2. Homology models are obtained of unphosphorylated and phosphorylated zERK2 using 1ERKA and 2ERKA respectively (PDB). **A** Surface and ribbon figure showing protein features common to other protein kinases including cyclin-dependent kinase-2 (CDK2), cAMP-dependent protein kinase (PKA), phosphorylase kinase (PHK) and the Tyr kinase domain of the insulin receptor (IRK). Except the tyrosine residue of the dual phosphorylation site which is unique for MAPKs. **B** MAPK have two allosteric docking sites**.** The CD-site (ball and stick residues) is located on the C-terminal extension (red) and the groove for DEF domain docking is located between α-helix G, the MAPK insert (yellow) and activation loop. The P+1 site (pink) is also involved in substrate kinase interaction. Catalytic residues are located in the glycine rich loop (cyan), catalytic loop (blue) and α-helix C. **C** Superposition of unphosphorylated and phosphorylated zERK2. Phosphorylation of Thr-183 and Tyr-185 results in reorientation of the activation loop, glycine rich loop and MAPK insertion consequently leading to MAPK activation. Images made with UCSF Chimera http://www.cgl.ucsf.edu/chimera.

substrate. In the C-lobe the activation site of the kinase and allosteric docking sites for interacting proteins are situated. The C-terminal region folds back spans both domains and terminates in close approximation of the N-terminus **Fig4b (red)**. This C-terminal extension is longer in MAPK kinases and is important for stable protein folding and recognition of interacting proteins. The N-lobe of MAPKs consist of a several loops, a β-sheat and 2 helices α-helix C and α-helix L16. The latter being part of the C-terminal extension. Some residues of the catalytic site for ATP binding are located in α-Helix C. The C-lobe is mainly composed of α-helices but contains also several short β-strands and loops with catalytic residues that are clustered in the catalytic loop **Fig4b (blue)**. The catalytic loop is allosterically controlled by Loop 12 (activation loop) at the surface of the C-lobe.

Loop 12 contains the dual-phosphorylation site Thr-183 and Tyr-185 (TEY motif rat Erk2 numbering) for kinase activation. Upon phosphorylation the activation loop changes conformation making the MAPK kinetically active and accessible for substrates **Fig4c.** Thr-183 and Tyr-185 induce conformational changes differentially and contribute therefore separately to the activation of the protein. Tyr-185 is unique for MAPKs which is part of a highly conserved P+1 sequence (YVATRWYR) **Fig4b (pink)**. After phosphorylation the P+1 sequence forms an pocket for interaction with the phosphoacceptor site on substrates. MAPK phosphorylate substrates at Serine and Threonine residues next to a Proline residue (P+1). This interaction is inhibited by the side chain of unphosphorylated Tyr-185 which occupies the pocket. Phosphorylation of the Thr-X-Tyr motif induces rearrangements of hydrogen bonds and ionic contacts with other residues and cause the tyrosine side chain to face the surface of the molecule. This process opens the P+1 pocket for Proline and places the Ser/Thr residue of the substrate to the correct position for phospho-transfer[67]. Phospho-Thr-183 rearranges active site residues by forming direct ionic contacts with arginine residues in α-helix C (Arg-68), in the catalytic loop (Arg-146) and in the activation loop (Arg-170). These interactions create two extended networks of interacting amino acids that connect the activation loop with α-helix C and the C-terminal extension while changing the orientation of the N-terminal and C-terminal domains. Phosphorylated Tyr-185 increases the accessibility for substrates binding.

In addition the C-domain contains two allosteric docking sites that confer specificity for substrates referred to as the CD-site and a DEF/ED domain docking site. The CD-site is a docking site located on the C-terminal extension accessible for substrates containing a DEJL motif with consensus sequence Arg/Lys2-Xaa2–6-Faa-Xaa-Faa (where Faa are the hydrophobic residues Leu, Ile or Val). In the CD domain of MAPKs, two or three acidic amino acids (D330, D327 zERK2) forms an acidic cluster which is crucial for docking to a cluster of basic amino acids commonly present in MAPK-docking sites. MAPK substrates could also contain a

DEF/ED site (Phe-X-Phe) and dock in a hydrophobic groove **Fig4b (green)** between the loop the activation loop, α-helix G and the MAPK insertion **Fig4b (yellow)**[61,68-70] [71].

The existing structural differences between P38 and Erk influence the affinity for substrate binding and underlie therefore the specification of their biological function. The first obvious structural differences is the change in conformation of the activation loop which is 6 residues shorter in P38 than Erk2 causing a replacement of the Thr and Tyr phosphorylation sites. This could lead to differences in the binding affinity of activators (MEKs) and substrates. The length of the activation loop also plays an important role in controlling autophosphorylation. Other structural differences are observed when looking at the α-Helix C in the N-terminal domain which is rotated in P38 in respect to its position in Erk2. In addition the interactions between the C-terminal extension (α-Helix L16) and the other part of the N-terminal domain are weaker. These differences result in a relatively open ATP binding site in P38.

1.4 Scope of the thesis

The documented 30 years of research focus on the MAPK protein family is a rich source of information on molecular roles linked to cellular behaviour. Activation of MAPK cascades leads to precise cellular responses depending on intrinsic cell-type specific factors and the nature and abundance of the extracellular signal(s) in the cellular microenvironment. We are interested in the molecular mechanisms of MAPK signalling that facilitate proper development of the zebrafish embryo. The first stages of embryonic development involves divers, often in parallel occurring, cellular behaviours that contribute to the formation of the body plan such as proliferation, cell fate decisions, adjustment of cell motility and adhesiveness. Most MAPK family members are expressed at an early stage of development and might be part of the underlying mechanisms. Using four different approaches (**Chapter 2-5**) we aimed, with the present study, to contribute to the elucidation of Erk1/2 and P38 MAPK molecular mechanisms during zebrafish early development.

Description of the Erk/MAPK three-dimensional protein structure, identification of pathway components and biochemical studies describing signal amplitude, duration and localization in divers biological systems where of great value for explaining how a single MAPK cascade could be involved in different cellular behaviours. Models of distinguished MAPK transient, oscillatory, bistable and ultrasensitive signalling shed light into the multitasking capacity of Erk2. Further enrichment of this knowledge will add to our understanding of the imbalanced Erk2 signalling observed in tumorigenesis and provide a fundament for treatment design and prediction. To adjust Erk2 kinetic activity amino-acid substitutions were introduced and the effect

22

on downstream signalling and gene transcription were assayed based on well established molecular mechanisms. We constructed constitutive active zebrafish Erk2 mutants that will be used for identification of new signalling events in the context of embryology (**Chapter 2**). In future genomic incorporation of the mutants and engineering of zebrafish transgenic lines with tissue specific stable expression would be valuable for modelling Erk2 associated diseases.

Analysis of P38/MAPK isoform specific expression in organ tissues and during different time points of the developing zebrafish embryo is a first step for detailed functional elucidation of this cascade. With the second experimental chapter we completed expression analysis of all P38 isoforms by expression analysis of the P38β and P38δ isoforms. Like most MAPK, expression of both transcripts was detectable within the first 24 hours of zebrafish development and at 1dpf, when the body plan was completed, expression was most saturated in the brain compartments. The P38β transcript was maternally present and stably expressed during the first stages of development. P38δ expression started after zygotic transcription and varied in different stages (**Chapter 3**).

We performed also a comparative study between P38α and Erk2 MAPK since both are essential in a similar process during development. Morpholino knock-down of either P38α or Erk2 disrupts epiboly an embryonic process involving germ layer segregation which occurs in zebrafish from 5 to 10hpf. Transcriptome analysis of P38α and Erk2 morphants at high/oblong stage, approximately an hour before initiation of epiboly, revealed large, partly overlapping pools of genes functional in different aspects of early development such as morphogen pathway, cell adhesion and migration. Interestingly, some genes functional in later established tissues of the immune system or nervous system were affected by P38α or Erk2 knock-down. In addition, inhibition of endogenous P38α expression affects a significant pool of ribosomal proteins. We hypothesize that this molecular link can be attributed to the role of P38α in maintaining cellular integrity during stress (**Chapter 4**).

Mammalian P38α deficiency resulted in aberrant placental angiogenesis and many *in vitro* studies in endothelial cells mapped P38α downstream of Vegf a key growth factor for endothelial proliferation and vascular remodelling. We questioned whether this role was conserved in zebrafish by unsaturated morpholino knock-down in Tg:fli+eGFP zebrafish. We addressed the role of P38α in zebrafish angiogenesis and found that P38α depletion had no effect on vasculogenesis but disrupted outgrowth of intersegmental vessels (ISV) from the dorsal aorta in the trunk of the zebrafish embryos. Angiogenesis of intersegmental vessels was completely blocked after treatment with the P38 inhibitor Birb796. With transcriptional analysis we investigated whether P38α regulates expression of angiogenic factors (**Chapter 5**)

Reference List

1. Kyriakis JM, Avruch J: Mammalian MAPK signal transduction pathways activated by stress and inflammation: a 10-year update. *Physiol Rev* 2012, 92:689-737.

2. Plotnikov A, Zehorai E, Procaccia S, Seger R: The MAPK cascades: Signaling components, nuclear roles and mechanisms of nuclear translocation. *Biochimica et Biophysica Acta (BBA) - Molecular Cell Research* 2011, 1813:1619-1633.

3. Kim L, Del RL, Butcher BA, Mogensen TH, Paludan SR, Flavell RA, Denkers EY: p38 MAPK autophosphorylation drives macrophage IL-12 production during intracellular infection. *J Immunol* 2005, 174:4178-4184.

4. Chen Q, Kinch MS, Lin TH, Burridge K, Juliano RL: Integrin-mediated cell adhesion activates mitogen-activated protein kinases. *J Biol Chem* 1994, 269:26602-26605.

5. Katz M, Amit I, Yarden Y: Regulation of MAPKs by growth factors and receptor tyrosine kinases. *Biochim Biophys Acta* 2007, 1773:1161-1176.

6. Naor Z, Benard O, Seger R: Activation of MAPK cascades by G-protein-coupled receptors: the case of gonadotropin-releasing hormone receptor. *Trends Endocrinol Metab* 2000, 11:91-99.

7. Bogoyevitch MA, Kobe B: Uses for JNK: the many and varied substrates of the c-Jun N-terminal kinases. *Microbiol Mol Biol Rev* 2006, 70:1061-1095.

8. Trempolec N, Dave-Coll N, Nebreda AR: SnapShot: p38 MAPK signaling. *Cell* 2013, 152:656.

9. Yoon S, Seger R: The extracellular signal-regulated kinase: Multiple substrates regulate diverse cellular functions. *Growth Factors* 2006, 24:21-44.

10. Casar B, Pinto A, Crespo P: Essential role of ERK dimers in the activation of cytoplasmic but not nuclear substrates by ERK-scaffold complexes. *Mol Cell* 2008, 31:708-721.

11. Pullikuth AK, Catling AD: Scaffold mediated regulation of MAPK signaling and cytoskeletal dynamics: a perspective. *Cell Signal* 2007, 19:1621-1632.

12. Caunt CJ, Keyse SM: Dual-specificity MAP kinase phosphatases (MKPs): shaping the outcome of MAP kinase signalling. *FEBS J* 2013, 280:489-504.

13. Barr AJ, Knapp S: MAPK-specific tyrosine phosphatases: new targets for drug discovery? *Trends Pharmacol Sci* 2006, 27:525-530.

14. Abe MK, Kuo WL, Hershenson MB, Rosner MR: Extracellular signal-regulated kinase 7 (ERK7), a novel ERK with a C-terminal domain that regulates its activity, its cellular localization, and cell growth. *Mol Cell Biol* 1999, 19:1301-1312.

15. Cuadrado A, Nebreda AR: Mechanisms and functions of p38 MAPK signalling. *Biochem J* 2010, 429:403-417.

16. Zebisch A, Czernilofsky AP, Keri G, Smigelskaite J, Sill H, Troppmair J: Signaling through RAS-RAF-MEK-ERK: from basics to bedside. *Curr Med Chem* 2007, 14:601-623.

17. Nithianandarajah-Jones GN, Wilm B, Goldring CE, Muller J, Cross MJ: ERK5: structure, regulation and function. *Cell Signal* 2012, 24:2187-2196.

18. Kyriakis JM, Avruch J: Mammalian MAPK signal transduction pathways activated by stress and inflammation: a 10-year update. *Physiol Rev* 2012, 92:689-737.

19. Roberts PJ, Der CJ: Targeting the Raf-MEK-ERK mitogen-activated protein kinase cascade for the treatment of cancer. *Oncogene* 2007, 26:3291-3310.

20. Dhillon AS, Hagan S, Rath O, Kolch W: MAP kinase signalling pathways in cancer. *Oncogene* 0 AD, 26:3279-3290.

21. Rodriguez-Viciana P, Tetsu O, Tidyman WE, Estep AL, Conger BA, Cruz MS, McCormick F, Rauen KA: Germline mutations in genes within the MAPK pathway cause cardio-facio-cutaneous syndrome. *Science* 2006, 311:1287-1290.

22. Kuan CY, Yang DD, Samanta Roy DR, Davis RJ, Rakic P, Flavell RA: The Jnk1 and Jnk2 protein kinases are required for regional specific apoptosis during early brain development. *Neuron* 1999, 22:667-676.

23. Sabapathy K, Jochum W, Hochedlinger K, Chang L, Karin M, Wagner EF: Defective neural tube morphogenesis and altered apoptosis in the absence of both JNK1 and JNK2. *Mech Dev* 1999, 89:115-124.

24. Amura CR, Marek L, Winn RA, Heasley LE: Inhibited neurogenesis in JNK1-deficient embryonic stem cells. *Mol Cell Biol* 2005, 25:10791-10802.

25. Dong C, Yang DD, Wysk M, Whitmarsh AJ, Davis RJ, Flavell RA: Defective T cell differentiation in the absence of Jnk1. *Science* 1998, 282:2092-2095.

26. Yang DD, Conze D, Whitmarsh AJ, Barrett T, Davis RJ, Rincon M, Flavell RA: Differentiation of CD4+ T cells to Th1 cells requires MAP kinase JNK2. *Immunity* 1998, 9:575-585.

27. Aouadi M, Binetruy B, Caron L, Le Marchand-Brustel Y, Bost F: Role of MAPKs in development and differentiation: lessons from knockout mice. *Biochimie* 2006, 88:1091-1098.

28. Krens SF, Spaink HP, Snaar-Jagalska BE: Functions of the MAPK family in vertebrate-development. *FEBS Lett* 2006, 580:4984-4990.

29. Lanner F, Rossant J: The role of FGF/Erk signaling in pluripotent cells. *Development* 2010, 137:3351-3360.

30. Poulain M, Furthauer M, Thisse B, Thisse C, Lepage T: Zebrafish endoderm formation is regulated by combinatorial Nodal, FGF and BMP signalling. *Development* 2006, 133:2189-2200.

31. Kunath T, Saba-El-Leil MK, Almousailleakh M, Wray J, Meloche S, Smith A: FGF stimulation of the Erk1/2 signalling cascade triggers transition of pluripotent embryonic stem cells from self-renewal to lineage commitment. *Development* 2007, 134:2895-2902.

32. Yao Y, Li W, Wu J, Germann UA, Su MS, Kuida K, Boucher DM: Extracellular signal-regulated kinase 2 is necessary for mesoderm differentiation. *Proc Natl Acad Sci U S A* 2003, 100:12759-12764.

33. Binetruy B, Heasley L, Bost F, Caron L, Aouadi M: Concise review: regulation of embryonic stem cell lineage commitment by mitogen-activated protein kinases. *Stem Cells* 2007, 25:1090-1095.

34. Nichols J, Silva J, Roode M, Smith A: Suppression of Erk signalling promotes ground state pluripotency in the mouse embryo. *Development* 2009, 136:3215-3222.

35. Villegas SN, Canham M, Brickman JM: FGF signalling as a mediator of lineage transitions--evidence from embryonic stem cell differentiation. *J Cell Biochem* 2010, 110:10-20.

36. Saba-El-Leil MK, Vella FD, Vernay B, Voisin L, Chen L, Labrecque N, Ang SL, Meloche S: An essential function of the mitogen-activated protein kinase Erk2 in mouse trophoblast development. *EMBO Rep* 2003, 4:964-968.

37. Adams RH, Porras A, Alonso G, Jones M, Vintersten K, Panelli S, Valladares A, Perez L, Klein R, Nebreda AR: Essential role of p38alpha MAP kinase in placental but not embryonic cardiovascular development. *Mol Cell* 2000, 6:109-116.

38. Allen M, Svensson L, Roach M, Hambor J, McNeish J, Gabel CA: Deficiency of the stress kinase p38alpha results in embryonic lethality: characterization of the kinase dependence of stress responses of enzyme-deficient embryonic stem cells. *J Exp Med* 2000, 191:859-870.

39. Adams RH, Porras A, Alonso G, Jones M, Vintersten K, Panelli S, Valladares A, Perez L, Klein R, Nebreda AR: Essential role of p38alpha MAP kinase in placental but not embryonic cardiovascular development. *Mol Cell* 2000, 6:109-116.

40. Guo YL, Yang B: Altered cell adhesion and cell viability in a p38alpha mitogen-activated protein kinase-deficient mouse embryonic stem cell line. *Stem Cells Dev* 2006, 15:655-664.

41. Regan CP, Li W, Boucher DM, Spatz S, Su MS, Kuida K: Erk5 null mice display multiple extraembryonic vascular and embryonic cardiovascular defects. *Proc Natl Acad Sci U S A* 2002, 99:9248-9253.

42. Krens SF, He S, Spaink HP, Snaar-Jagalska BE: Characterization and expression patterns of the MAPK family in zebrafish. *Gene Expr Patterns* 2006, 6:1019-1026.

43. Schier AF, Talbot WS: Molecular genetics of axis formation in zebrafish. *Annu Rev Genet* 2005, 39:561-613.

44. Lepage SE, Bruce AE: Zebrafish epiboly: mechanics and mechanisms. *Int J Dev Biol* 2010, 54:1213-1228.

45. Mathieu J, Griffin K, Herbomel P, Dickmeis T, Strahle U, Kimelman D, Rosa FM, Peyrieras N: Nodal and Fgf pathways interact through a positive regulatory loop and synergize to maintain mesodermal cell populations. *Development* 2004, 131:629-641.

46. Krens SF, He S, Lamers GE, Meijer AH, Bakkers J, Schmidt T, Spaink HP, Snaar-Jagalska BE: Distinct functions for ERK1 and ERK2 in cell migration processes during zebrafish gastrulation. *Dev Biol* 2008, 319:370-383.

47. Furthauer M, Van CJ, Thisse C, Thisse B: Fgf signalling controls the dorsoventral patterning of the zebrafish embryo. *Development* 2004, 131:2853-2864.

48. Kudoh T, Wilson SW, Dawid IB: Distinct roles for Fgf, Wnt and retinoic acid in posteriorizing the neural ectoderm. *Development* 2002, 129:4335-4346.

49. Londin ER, Niemiec J, Sirotkin HI: Chordin, FGF signaling, and mesodermal factors cooperate in zebrafish neural induction. *Dev Biol* 2005, 279:1-19.

50. Anastasaki C, Rauen KA, Patton EE: Continual low-level MEK inhibition ameliorates cardio-facio-cutaneous phenotypes in zebrafish. *Dis Model Mech* 2012, 5:546-552.

51. Furthauer M, Thisse C, Thisse B: A role for FGF-8 in the dorsoventral patterning of the zebrafish gastrula. *Development* 1997, 124:4253-4264.

52. Furthauer M, Lin W, Ang SL, Thisse B, Thisse C: Sef is a feedback-induced antagonist of Ras/MAPK-mediated FGF signalling. *Nat Cell Biol* 2002, 4:170-174.

53. Koshida S, Shinya M, Nikaido M, Ueno N, Schulte-Merker S, Kuroiwa A, Takeda H: Inhibition of BMP activity by the FGF signal promotes posterior neural development in zebrafish. *Dev Biol* 2002, 244:9-20.

54. Krens SF, Corredor-Adamez M, He S, Snaar-Jagalska BE, Spaink HP: ERK1 and ERK2 MAPK are key regulators of distinct gene sets in zebrafish embryogenesis. *BMC Genomics* 2008, 9:196.

55. Kim J, Lin JJ, Xu RH, Kung HF: Mesoderm induction by heterodimeric AP-1 (c-Jun and c-Fos) and its involvement in mesoderm formation through the embryonic fibroblast growth factor/Xbra autocatalytic loop during the early development of Xenopus embryos. *J Biol Chem* 1998, 273:1542-1550.

56. Znosko WA, Yu S, Thomas K, Molina GA, Li C, Tsang W, Dawid IB, Moon AM, Tsang M: Overlapping functions of Pea3 ETS transcription factors in FGF signaling during zebrafish development. *Dev Biol* 2010, 342:11-25.

57. Holloway BA, Gomez de la Torre Canny, Ye Y, Slusarski DC, Freisinger CM, Dosch R, Chou MM, Wagner DS, Mullins MC: A novel role for MAPKAPK2 in morphogenesis during zebrafish development. *PLoS Genet* 2009, 5:e1000413.

58. Wagner DS, Dosch R, Mintzer KA, Wiemelt AP, Mullins MC: Maternal control of development at the midblastula transition and beyond: mutants from the zebrafish II. *Dev Cell* 2004, 6:781-790.

59. Gallo KA, Johnson GL: Mixed-lineage kinase control of JNK and p38 MAPK pathways. *Nat Rev Mol Cell Biol* 2002, 3:663-672.

60. Habas R, Dawid IB, He X: Coactivation of Rac and Rho by Wnt/Frizzled signaling is required for vertebrate gastrulation. *Genes Dev* 2003, 17:295-309.

61. Goldsmith EJ, Cobb MH, Chang CI: Structure of MAPKs. *Methods Mol Biol* 2004, 250:127-144.

62. Lee SJ, Zhou T, Goldsmith EJ: Crystallization of MAP kinases. *Methods* 2006, 40:224-233.

63. Chang CI, Xu BE, Akella R, Cobb MH, Goldsmith EJ: Crystal structures of MAP kinase p38 complexed to the docking sites on its nuclear substrate MEF2A and activator MKK3b. *Mol Cell* 2002, 9:1241-1249.

64. Goldsmith EJ, Min X, He H, Zhou T: Structural studies of MAP Kinase cascade components. *Methods Mol Biol* 2010, 661:223-237.

65. Wilson KP, Fitzgibbon MJ, Caron PR, Griffith JP, Chen W, McCaffrey PG, Chambers SP, Su MS: Crystal structure of p38 mitogen-activated protein kinase. *J Biol Chem* 1996, 271:27696-27700.

66. Zhang J, Zhang F, Ebert D, Cobb MH, Goldsmith EJ: Activity of the MAP kinase ERK2 is controlled by a flexible surface loop. *Structure* 1995, 3:299-307.

67. Canagarajah BJ, Khokhlatchev A, Cobb MH, Goldsmith EJ: Activation mechanism of the MAP kinase ERK2 by dual phosphorylation. *Cell* 1997, 90:859-869.

68. Cobb MH, Goldsmith EJ: How MAP kinases are regulated. *J Biol Chem* 1995, 270:14843-14846.

69. Dimitri CA, Dowdle W, MacKeigan JP, Blenis J, Murphy LO: Spatially separate docking sites on ERK2 regulate distinct signaling events in vivo. *Curr Biol* 2005, 15:1319-1324.

70. Goldsmith EJ: Three-dimensional docking in the MAPK p38alpha. *Sci Signal* 2011, 4:e47.

71. Klein AM, Zaganjor E, Cobb MH: Chromatin-tethered MAPKs. *Curr Opin Cell Biol* 2013, 25:272-277.

CHAPTER II

Generation of Constitutive Active ERK Mutants as Tools for Cancer Research in Zebrafish

Hanan Rian, S. F. Gabriel Krens, Herman P. Spaink, and B. Ewa Snaar-Jagalska

Abstract

The extracellular-signal-regulated-kinase (ERK) signaling pathway is essential for vertebrate development and is frequently deregulated in human, and zebrafish tumors. Previously, we cloned and characterized the zebrafish MAPK gene-family and showed that ERK2 is crucial for cell migration and early zebrafish embryogenesis. To further study ERK2 function we generated constitutively active mutant forms of the ERK proteins by introducing conserved point mutations. We validated the enhanced protein activity *in vitro* by transfection of constructs into zebrafish zf4 cells and demonstrated elevated phosphorylation levels of downstream targets p90RSK, CREB and MNK1, by ERK2$^{L84P/S162D}$ and ERK2$^{L84P/S162D/D330N}$ specifically. *In vivo* validation was performed by ectopic expression of corresponding mRNAs in the transgenic zebrafish FGF-ERK2 reporter fish line Tg(Dusp6:d2EGFP). Both mutant ERK2 isoforms induced elevated transgene expression compared to ERK2^{WT}, confirming increased kinase activity *in vivo.*

Phospho-kinomic analysis on peptide microarrays was performed to identify new targets in embryos injected with FGF8 or ERK2$^{L84P/S162D/D330N}$ mRNAs. We detected both FGF8 specific and common signalling targets. Interestingly, with both mRNAs we found increased phosphorylation levels of CDK1, which is critical for proper G2/M phase transition and mitotic entry in proliferation control. These results corroborate that constitutive activation of the ERK2 pathway leads to enhanced, possible oncogenic, proliferation.

Introduction

The mitogen-activated protein (MAP) kinases extracellular signal-regulated kinase 1 and 2 (ERK1 and ERK2) are crucial components of the regulatory machinery underlying normal and malignant cell proliferation. The rat sarcoma (RAS)/ rapidly accelerated fibrosarcoma (RAF)/ MAPK kinase (MEK)/ERK oncogenic pathway is induced by various growth factors and forms a convergence point of multiple signaling pathways to control essential cellular processes including migration, differentiation, growth and survival [1-5]. Approximately 30% of all human cancers display evidence of enhanced activation of the RAS/RAF/MEK MAPK pathway [6]. The pathway has been extensively studied in relation to tumor formation and this was greatly facilitated by the availability of constitutively active forms of RAS, RAF and MEK [7,8]. Expression of oncogenic RAS as well as constitutive active forms of RAF and MEK can lead to induced tumorigenic transformation of NIH 3T3 cells [9,10]. In addition, *in vivo* studies with transgenic mice models, expressing constitutive active MEK in the heart, lens chondrocytes or skin, displayed increased cell numbers or cell size and a delayed onset of cell differentiation [11]. Melanoma is a form of cancer with an extremely high frequency of deregulated RAF/MEK/ERK as 70% of the melanoma cases harbour increasing activity mutations in the RAF oncogene [12]. The activating mutation in B-RAF (BRAFV600E) found in human nevi drives generation of nevi in zebrafish when expressed in melanocytes. Coupled with the loss of the tumor-suppressor gene p53, nevi progress from benign clusters of melanocytes to malignant melanoma [13,14]. This indicates that pathology and molecular mechanisms of tumor formation between humans and zebrafish are similar and providing molecular tools for the establishing zebrafish cancer models for a better understanding of different pathogenesis [15-19].The same signaling pathways that orchestrate embryonic development are frequently deregulated during tumor progression. In fact these signaling pathways appear to add significantly to the aggressiveness of tumors. Proteins critical in embryogenesis can be reactivated in adult cells and play a role in allowing tumor cells to overcome barriers and to metastasize [20-22]. Recent studies in our laboratory have demonstrated that depletion of ERK2 in zebrafish disturbs cell migration mechanisms and causes developmental arrest in an early embryonic (blastula) stage. Although the apparent ERK1/2 gene expression levels appear to be constant during all stages of early zebrafish development, differences in ERK1/2 signal activity is first detected with whole mount immunohistochemistry in the enveloping layer (EVL) of the early blastula [23]. During epiboly ERK1/2 activity is induced at the margin by fibroblast growth factor (FGF) morphogens and controls convergent extension cell movements and mesoderm differentiation [23].

We expect that overactivation of ERK2 will increase the proliferation and migration properties of cells in the developing embryo, leading to aberrant developmental

programm and perhaps tumor formation. In this study we aim to focus on the ERK/MAPK level of the oncogenic RAS/RAF/MEK/ERK cascade by constructing zebrafish constitutive active mutants that are independent of negative feedback signaling and use these tools to understand the downstream molecular mechanisms that are involved in developmental processes, which also play a role in converting normal to uncontrolled cell proliferation. These results illustrate that zebrafish is a powerful vertebrate model that allows simultaneous study of embryonic development and tumor progression using multidisciplinary approaches.

Material & Methods

	Description	Sequence (5' > 3')	Reference
MAPK1/ ERK2	ERK2/L84P_fw	CTGCGTGAGATTAAAATCCCGCTCCGCTTCAAGC	RefSeq: NM_182888
	ERK2/L84P_rv	GCTTGAAGCGGAGCGGGATTTTAATCTCACGCAG	
	ERK2/S162D_fw	CGAGACCTGAAGCCAGACAACCTGTTGCTCAACAC	
	ERK2/S162D_rv	GTGTTGAGCAACAGGTTGTCTGGCTTCAGGTCTCG	
	ERK2/D330N_fw	CCTGGAGCAGTACTATGATCCTACAAATGAGCCTGTTGCTGAG	
	ERK2/D330N_rv	CTCAGCAACAGGCTCATTTGTAGGATCATAGTACTGCTCCAGG	
MAPK3/ ERK1	ERK1/L106P_fw	CTGAGAGAGATCAAAATCCCCCTGCGGTTCCATC	RefSeq: NM_201507
	ERK1/L106P_rv	GATGGAACCGCAGGGGGATTTTGATCTCTCTCAG	
	ERK1/S184D_fw	CAGAGACCTGAAGCCCGACAACCTTCTCATCAACAC	
	ERK1/S184D_rv	GTGTTGATGAGAAGGTTGTCGGGCTTCAGGTCTCTG	
	ERK1/D352N_fw	GCAGTACTATGACCCATCTAATGAGCCGGTAGCTGAGGAAC	
	ERK1/D352N_rv	GTTCCTCAGCTACCGGCTCATTAGATGGGTCATAGTACTGC	

Table1: Primer list for site directed mutagenesis.

Plasmid transformation and isolation

Transformation of DNA constructs was performed by adding 0,5 µl DNA to 50µl one shot TOPO 10F' competent *E.coli* cells (Invitrogen). The transformed cells were cultured on ampicilline LB agar plates (Luria-Bertani broth 1.5% agar 100mg/ml ampicilline) and the constructs were isolated with the Nucleobond Xtra midi/maxi plasmid DNA purification kit (Clontech laboratories inc).

Site directed mutagenesis

The Amino acid substitutions of interest in zERK1 and zERK2 were generated by site directed mutagenesis using the QuikChange[(R)] site directed mutagenesis kit (Stratagene). Primers (Sigma-Aldrich) were designed according to the guidelines of the supplied protocol and used for the mutagenesis reaction (*Table1*). A forward

and reverse primer is designed for each mutation. The primers (forward and reverse) overlap the mutation and have minimal 10 residues at each side of the mutation. The nucleotides complementary to the mutation site are changed to generate the desired substitutions. The four reaction steps of the site directed mutagenesis kit were performed with 10ng PCS2+zERK1 or PCS2+zERK2 DNA. Double and triple mutants were generated by repeating the four steps of the mutagenesis reaction with the single and double mutant DNA templates respectively. The Leucine to Proline substitution was generated by replacing CTC to a CCC codon in ERK1 and CTG to CCG in ERK2; the Serine to Aspartic acid substitution by replacing the TCA to GAC in both ERK1 and ERK2. Finally, the Aspartic acid to Aspargine substitution was obtained by GAT to AAT replacement in zERK1 and zERK2. Importantly, no other residues than the one of interest were found mutated. Sequencing analysis confirmed the successful introduction of all mutations. Importantly, no other residues than the one of interest were found mutated.

Transfection of PCS2+ERK1/2 (mut) in zf4 cells

The transfection experiments were performed with the FuGene HD transfection reagent (Roche). A transfection mix containing 1,5 µg construct DNA, the FuGene reagents and plain medium (without FCS) was applied to a confluent layer of cells in 0,5ml medium and incubated for 6h. To allow the cells to recover 1,0ml medium with FCS was added for overnight incubation. PCS2+ERK1 and PCS2+ERK2 (mutated) constructs were transfected in zf4 cells and after recovery starved for 6 ½ hour. The protein was isolated directly after starvation in 1X SDS sample buffer (Red Loading Buffer Pack 1723 Cell Signaling Technology[(R)]).

mRNA synthesis

The PCS2+ERK2_WT PCS2+ERK2* PCS2+ERK2** and PCS2+ERK2*** constructs were linearized with Apa1 prior mRNA synthesis with the mMessage mMachine kit (Ambion). 1 µg of the purified digest was used for the mRNA synthesis reaction with Sp6 RNA polymerase. Subsequently, 1 µl of Dnase was added to the reaction which is incubated for 30 min at 37 ºC. The mRNA samples were purified with the NucleoSpin RNA Clean-up kit (Nucleobond) and analysed by electrophoresis on a 1% Rnase-free agarosegel.

Microinjection in zebrafish embryos

1.0 nl ERK (mutant) mRNA (50ng/µl) was injected into one-cell stage Tg(Dusp6:d2EGFP) zebrafish embryos. Injected embryos were used for protein isolation at 5hpf, imaged with LEICA MZ12 or analyzed with COPAS XL from Union Biometrica.

Protein isolation from zebrafish embryos

(Injected) embryos of 5hpf where mechanical dechorionated and kept until protein isolation in agarose coated wells filled with 1X Danieau buffer. For isolation embryos were disrupted in Ca^{2+}/Mg^{2+} free solution and cells were subsequently washed with PBS. 1µl/embryos of 1X lysis buffer (1M Tris-Hcl pH7,4, 0,5M EDTA, 1 tablet protease inhibitor, 0,1M Na3VO4, 0,5M NaF) was added. 2ug protein from zebrafish embryos was used for western blotting.

Western blotting

Protein samples were loaded on a 10%acrylamide PAGE gel. The high range rainbow molecular weight marker (RPN756V, Amersham Biosciences) was used for band size determination. After blotting on a nitrocellulose membrane the blot was incubated with 1:1000 diluted Phospho-p90RSK Thr573 (9346), Phospho-p44/42 MAP Kinase Thr202/Tyr204 (9101), p44/42 MAP Kinase (9102), Phospho-Elk-1 Ser383 (9181), Phospho-CREB Ser133 (9198), Phospho-Mnk1 Thr197/202 (2111), and phospho-p90RSK Ser380 (9341) rabbit antibody (Cell Signaling technology[R]). The ECL western blotting detection reagents and analysis system (Amersham Biosciences) was used for chemoluminescence detection with secondary antibody the ECL™-HRP Linked Antirabbit IgG (Amersham). The blots are stripped with Western-Re-Probe™ Reagent (G-Biosciences) for re-staining.

Serine Threonine kinome profiling

Protein samples were prepared as described above except M-PER lysis buffer with phosphatase and protease inhibitors (PIERCE) was used. Samples were snapfreezed in liquid nitrogen and delivered to PamGene International BV for analysis. 1µg of each lysate was loaded on PamChip® arrays, with 144 immobilized peptide substrates in a porous ceramic membrane, and incubated in the presence of 400µl ATP. Functional readout is based on kinetic measurement of Ser/Thr phosphorylation occurring on the array using fluorescently labelled anti-phopho-antibodies. Data processing including image quantification, quality control, statistical analysis, visualization was performed using the Bionavigator software.

Results

<u>Conserved constitutive activating mutation sites in ERK2 orthologues over different evolutionary phyla.</u>

Previous large scale mutation screens of the *Drosophila melanogaster* gene rolled and *Saccharomyces cerevisiae* gene fus3 have facilitated the construction of the constitutive active rat orthologue ERK2 [24]. Three point mutations (L73P, S151D and D319N) were found to increase the kinase activity a 100-fold compared to the
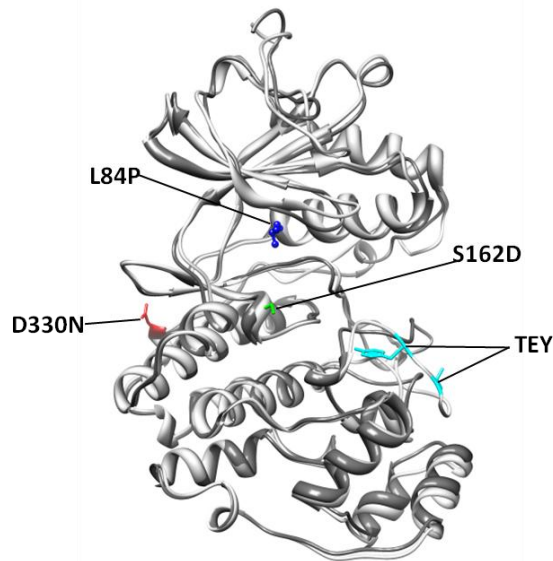

Fig1: Overlap of homology predicted protein models showing the active (grey) and inactive (white) zebrafish ERK2 protein structure . Phosphorylation of the dual phosphorylation site (TEY) causes structural rearrangement of the activation lip. The substitutions may cause rearrangements of intermolecular interactions between amino acids resulting in a smaller distance between the activation lip with the TEY motif and the catalytic site and facilitating autophosphorylation. The L83P site (blue) is located in α-helix C and S162D (green) in the catalytic loop, both in the active site of the kinase. The D330N (red) mutation is located in the CD-site which is a docking site for inhibitory phosphatases. The D330N substitution prevents ERK inhibitory phosphatases to bind. The atomic resolution models of zebrafish ERK2 were constructed with the zERK2 amino acid sequence (ENSAMBLE:ENSDARP00000038550) and based on three dimensional X-ray crystallography predictions PDB:1ERK and PDB:2ERK (phosphorylated). Homology modelling was performed using free online Swiss-model and models were illustrated with Chimera.

wild type rERK2 when introduced simultaneously. In addition, the L73P/S151D double mutant was 50-fold more active as detected in the *in vitro* test where the rates of phosphoryl transfer from [-32P] ATP to myelin basic protein were measured in 10-min assays. The mutations enhance ERK2 activity most likely by facilitating intramolecular autophosphorylation predominantly at Tyr-185 and to a lesser extent at Thr-183. As in the wild type, phosphorylation at both sites is required for full activation of ERK2 [24]. Considering the high conservation of MAPKs in vertebrates, these point mutations could possibly activate the zebrafish orthologue of rat ERK2 and since ERK1 and ERK2 are 90% identical the same mutations may also activate zERK1. Multiple alignment including the amino acid sequence of FUS3, ROLLED, rat ERK2 and zebrafish ERK1 and ERK2 showed an evolutionary conservation of the L73P, S151D and D319N mutation sites (*Table2)* [24-26]. The homology model illustrates positions of these conserved sites in zebrafish ERK2 molecule (*Fig1).*

organism	gene name	activating mutations			reference
Rat	rERK2/MAPK1	L73P	S151D	D319N	Emrick et al
Yeast	FUS3	L63P		D317N	Hall et al.
Drosophila	rolled (rl)			D334N	Brunner et al.
	zMAPK3/ERK1	L106P	S184D	D352N	
	zMAPK1/ERK2	L84P	S162D	D330N	
Zebrafish		_____ *			
		_____ **			
		_____ ***			

Table2: MAPK activating mutations. * Single mutant, ** Double mutant, *** Triple mutants of zebrafish ERK1 and ERK2.

The mutations that were found to activate rERK2 were introduced into pCS2+zERK1 and pCS2+zERK2 constructs by site directed mutagenesis. To determine whether single mutation or a combination of two or three mutation(s) would increase zERK activity we constructed single, double and triple mutants of both zERK1 and zERK2. Altogether six potential constitutive active ERK mutants were obtained; zERK1^{L106P}, zERK1$^{L106P/S184D}$, zERK1$^{L106P/S184D/D352N}$, zERK2^{L84P}, zERK2$^{L84P/S162D}$ and zERK2$^{L84P/S162D/D330N}$.
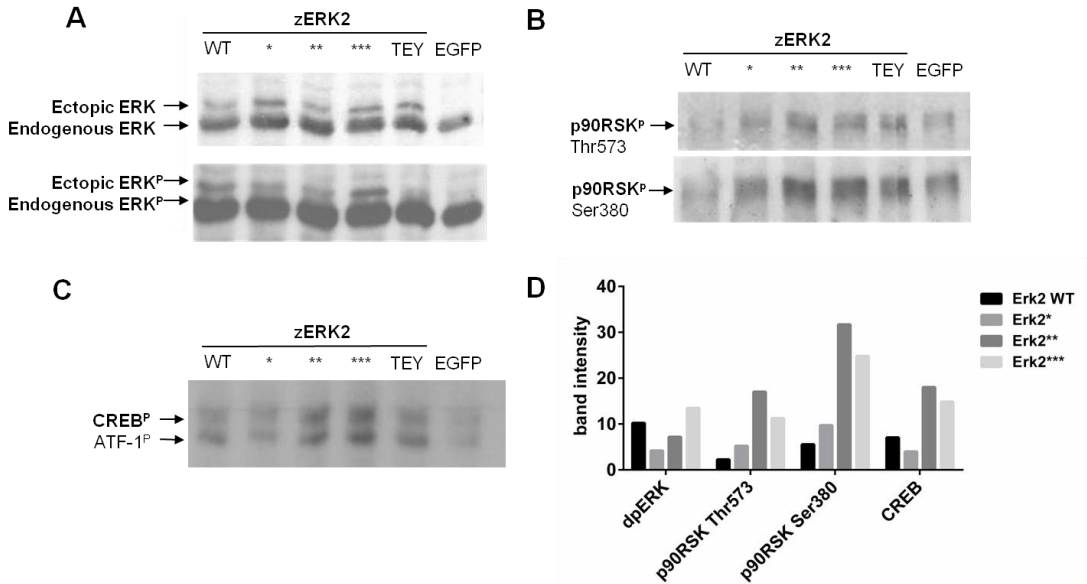
Fig2: Western blot detection of ERK1/2, P90RSK, and CREB phosphorylation in zf4 cells transfected with PCS2+ERK1 and PCS2+ERK2 (mutated) constructs. **A** Western blotting was performed with total ERK and dpERK. The Ectopic ERKs derived from synthetic mRNAs have a greater MW than the endogenous ERKs due to the introduction of a small linker, and can therefore be distinguished by size. The bands with higher molecular mass were also detected with anti-ERK1/2 antibody in cells transfected with ERK^{TEY} mutants but not with the anti-phspho-ERK1/2 antibody. This confirms that the bands with higher molecular weights are from the transfected ectopic ERK. **B** Western blot detection of phospho-p90Rsk with two different antibodies one targeted against Thr573 and another against Ser380. **C** Western blot detection with the phospho-Creb Ser133 antibody which cross-reacts with phospho-ATF. **D** Band intensities were measured for quantification of western blots (**A-C**) dp-ERK(ectopic) p-P90RSK and p-CREB band intensities were corrected for total ectopic ERK synthesis. Mutants were normalized against ERK1-WT or ERK2-WT. WT: protein samples from zf4 cells transfected with wtERK1 or wtERK2, *: single mutants ERK1^{L106P} ERK2^{L84P}, **: double mutants ERK1$^{L106P/S184D}$ ERK2$^{L84P/D162D}$, ***: triple mutants ERK1$^{L106P/S184D/D352N}$ ERK2$^{L84P/S162D/D330N}$, TEY: ERK1$^{T216A/Y218A}$ and ERK2$^{T194A/Y196A}$ 0: untransfected zf4 cells, EGFP: zf4 cells transfected with pcs2+EGFP.

ERK2 double and triple mutants phosphorylate downstream targets *in vitro* despite growth factor deprivation.

In cells transfected with ERK2 double and triple mutants substrate phosphorylation is enhanced *in vitro*, in the absence of growth factors. To compare the activity of ERK mutants and wild type (wt) proteins we performed a biochemical characterization experiment after transfection of corresponding plasmids into cultured zf4 cells (*Fig2).* The transfected cells were starved for 6½ h in cell culture medium without of FCS before protein isolation. Since the MAPK/ERK pathway is

known to be induced by growth factors we expected the activity of endogenous and ectopic ERK to be decreased to basal levels by starvation, enabling us to compare downstream signalling between wt and mutant ERK proteins. Subsequent western blotting with antibodies against total ERK showed that all transfected zebrafish ERK1 (data not shown) and ERK2 constructs were expressed in zf4 cells (*Fig2a*). In addition to the band of endogenous zERK, visible in all samples, a second band was detected in protein samples of ERK1 and ERK2 transfected cells but not in the control untransfected cells and the cells transfected with PCS2+eGFP. The extra bands have the exact molecular mass of the ectopic zERKs which are modified to have a 1,66 and 1,23 kD higher molecular mass then the endogenous zERK1 and zERK2 respectively. The bands of ectopic zERK1 (data not shown) and zERK2 were also visible after detection with antibody against phosphorylated ERK1/2 in samples of the ERK transfected cells. To be able to detect differences in the degree of target phosphorylation between mutant and wild type zERKs, antibodies against phosphorylated p90 ribosomal S6 kinase (p90RSK), *cAMP response element-binding* protein (CREB) and MAP kinase-activated protein kinase (MNK1) were used (*Fig2b-e*). Western blotting quantification and subsequent correction for ectopic ERK synthesis and normalization against wt ERK confirms the increased phosphorylation of the triple mutants of both ERK1 and ERK2. For the detection of phosphorylated p90RSK, two different antibodies were available, that cross reacted with the zebrafish ortologue, directed against distinct sites targeted by ERK. With both antibodies an increased phosphorylation of p90RSK was found in cells transfected with the double and triple mutants of zERK2 only when compared to cells with wt ERK1/2 overexpression. In addition, phosphorylation increase of the other ERK targets CREB and MNK1 was detected in the zERK2 double and triple mutant samples. No increase of either phosphorylated p90RSK, CREB or MNK1 was detected in cells transfected with wt or mutated ERK1 (data not shown).

CA-ERK2 and FGF8 induce transgene expression of Tg(Dusp6:d2EGFP).

Synthesized ERK2 wt and mutant mRNA was injected in 1-cell stage zebrafish embryos for *in vivo* validation of constitutive activation. Ectopic phosphorylated ERK was detectable in proteins samples collected at 5hpf with western blotting *(Fig3a)*. In addition, the ERK2 triple mutant was significantly more phosphorylated and the double mutant was slightly increased compared to the ectopic wt ERK2 and the ERK2 single mutant. Therefore we continued the validation of the double and triple ERK2 mutants *in vivo*, based on an ERK2 negative feedback mechanism, involving the downstream gene target dual specificity phosphatase (DUSP6) in Tg(Dusp6:d2EGFP) *(Fig3b)*. The FGF8 morphogen induces ERK activity at the dorsal site and the margin of the zebrafish embryo during epiboly. Subsequently ERK2 induces the expression of DUSP6 which is a dual specificity phosphatase that removes both activating phosphates of the ERK2 (Thr-Glu-Tyr) motif [27]. When

FGF8 mRNA was injected in Tg(Dusp6:d2EGFP) embryos the GFP signal increased and shifts from the dorsal site to the entire animal pole *(Fig3b)*. Batches
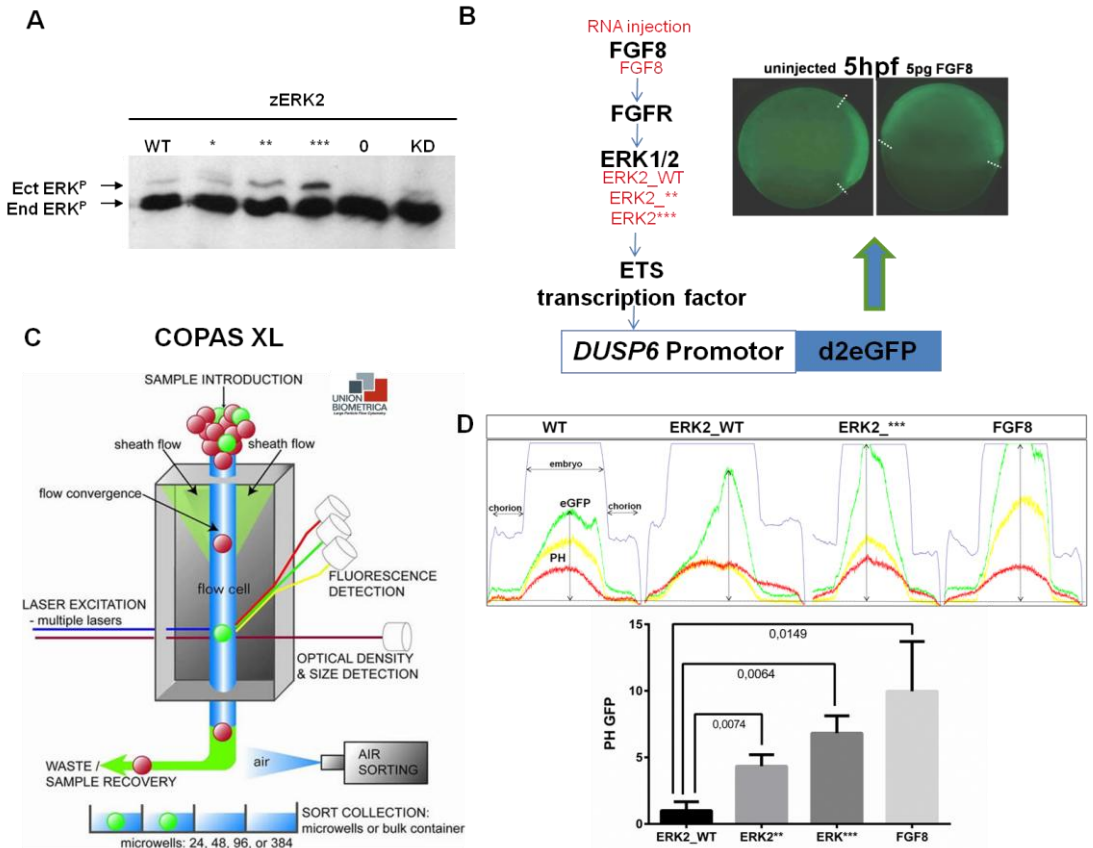
Fig3: In vivo ERK signaling activity analysis of ectopically expressed FGF or ERK isoforms. A western blot detection of dpERK on protein samples isolations from 5hpf embryos injected with 50pg WT or mutant ERK2 mRNA and isolated. **B** flowchart of the experimental procedure using the Tg(Dusp6:d2EGFP) and subsequent COPAS XL$_{Union\ Biometrica}$·analyis **C**. 5hpf old living embryos are passed through the COPAS flowcell and optical density/axial length (blue), GFP (green), YFP (yellow) and dsRED (red) fluorescence profiles are recorded Union Biometrica, Inc. **D**. Peak Height values (PH) of the GFP channel were collected for ERK2_WT, ERK2**, ERK2*** and FGF8 mRNA injected embryos, after corrected for auto-fluorescence/background of non-injected wild type embryos (see methods), and plotted in a bar graph as the mean value of three biological experiments, each with a minimum of 30 embryos/condition. Mean GFP PH values are normalized against ERK2_WT. Arrow bares represent standard deviations of the means of the three biological experiments, p-values were calculated by plying a t-test with Welch-correction.

of Tg(Dusp6:d2EGFP) embryos were injected with wt ERK2, ERK2 double mutant, triple mutant and FGF8 mRNA and analyzed with the COPAS XL which performs large scale GFP fluorescence detection of live embryos. Both mutants as well as FGF8 increased the eGFP signal in heterozygous Tg(Dusp6:d2EGFP) embryos at 5hpf *(Fig3c)*.

Kinome profiling reveals increased phosphorylation of the cell cycle progression protein CDK1 as a consequence of FGF8 and CA-ERK2 overexpression in zebrafish embryos.

To identify substrates that are in particular affected by ERK constitutive activation we performed a serine threonine phospho-kinome peptide array experiment comparing lysates of ERK2***, ERKWT and FGF8 injected embryos against an uninjected control. 111 peptides where phosphorylated by the zebrafish lysates and with model based clustering 7 clusters were distinguished from this pool *(Fig4a)*. Cluster 1 comprises peptides which are less phosphorylated due to FGF8 overexpression (supplementary Fig1a) while cluster 2 is showing the opposite effect of FGF8 specific targets which are increasingly phosphorylated *(Fig4b and Table 3)*. Cluster 3 and 4 represent peptides with decreased and increased phosphorylation respectively as a result of wt ERK2 overexpression. This might be the effects of negative feedback as a consequence of ERK overexpression that have less or no effect on the mutant. Cluster 5 and 7 are less phosphorylated peptides due to overactivation of the FGF-ERK pathway or due to injection. Cluster 6 consist of an interesting group of peptides which are increasingly phosphorylated by both FGF8 and the ERK2*** mutant *(Fig4c and Table4)*. The proliferation marker CDK1 (CDC2) is found among the cluster 6 peptides of which phosphorylation within amino acids 154-169 is significantly induced by FGF8 and ERK*** (p-value<0,05) compared to uninjected embryos.

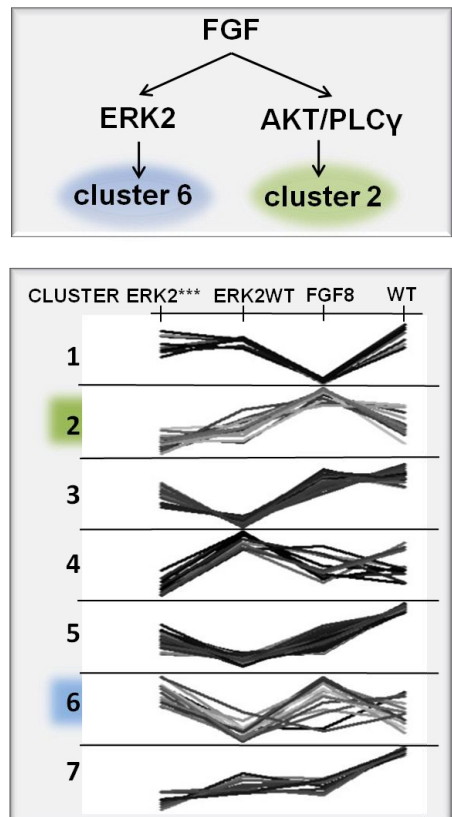**Fig4: Kinome profile clustering of embryos ectopically expressing ERK2WT, ERK2 triple mutant and FGF8.** Simplified representation of FGF-ERK signalling pathways to downstream specific target clusters (up). Clusters are based on a Bionavigator based clustering algotithm,that groups peptides into clusters according to treatment-based response similarities (down). AKT is Protein Kinase B (PKB), PLCγ is Phospholipase Cγ.

Table 3: Cluster 2 Peptides with increased phosphorylation specifically by FGF8 samples. Protein samples were prepared at 5 hpf. ANOVA and Dunnett's test are performed with a biological triplicate.

Peptide	Fold change (mean 2log values)				P values versus WT			P values versus ERK2_WT	
	WT	ERK2WT	ERK2***	FGF8	ERK2WT	ERK2***	FGF8	ERK2***	FGF8
ACM5_494_506	1.00	0.99	1.02	1.04	0.909	0.925	0.093	0.835	0.079
ACM5_498_510	1.00	0.98	1.01	1.08	0.897	0.730	0.119	0.637	0.143
ANDR_785_797	1.00	0.98	1.01	1.05	0.923	0.471	0.153	0.529	0.133
CA2D1_494_506	1.00	1.05	1.06	1.10	0.290	0.364	0.012†	0.864	0.056
ESR1_160_172	1.00	0.97	0.99	1.04	0.451	0.189	0.183	0.523	0.060
GPR6_349_361	1.00	0.96	1.01	1.02	0.382	0.465	0.609	0.876	0.189
GSUB_61_73	1.00	0.98	0.93	1.05	0.441	0.147	0.942	0.432	0.402
KS6A1_374_386	1.00	1.00	1.02	1.09	0.969	0.822	0.430	0.852	0.409
P53_12_24	1.00	1.07	0.97	1.58	0.906	0.543	0.472	0.472	0.543

† P values < 0.05.

Table 4: Cluster 6 peptides are increasingly phosphorylated by FGF8 or ERK2*** but not ERK2WT samples. ANOVA and Dunnett's test are performed with a biological triplicate.

Peptide	Fold change (from mean 2log)				P values versus WT			P values versus ERK2_WT	
	WT	ERK2WT	ERK2***	FGF8	ERK2WT	ERK2***	FGF8	ERK2***	FGF8
RBL2_655_667	1.00	0.93	1.11	1.31	0.772	0.671	0.205	0.482	0.135
PRKDC_2618_2630	1.00	0.98	1.17	1.63	0.734	0.618	0.267	0.412	0.165
PP2AB_297_309	1.00	0.88	1.11	1.27	0.270	0.307	0.510	0.058	0.104
MBP_222_234	1.00	0.94	1.19	1.05	0.697	0.055	0.591	0.032†	0.367
NEK3_158_170	1.00	1.21	1.27	1.50	0.516	0.093	0.031†	0.240	0.080
KCC2G_278_289	1.00	1.02	1.28	1.43	0.537	0.099	0.012†	0.040†	0.006†
CGHB_109_121	1.00	0.97	1.29	1.20	0.446	0.064	0.143	0.022†	0.047†
CDC2_154_169	1.00	0.95	1.11	1.15	0.982	0.041†	0.037†	0.042†	0.038†

† P values < 0.05.

Discussion

Three point mutations, that already were shown to activate rat ERK2, were sequentially introduced in zERK1 and zERK2 providing us with six mutants to be tested for increased activation [24]. The six mutants include the single mutants zERK1^{L106P} and zERK2^{L84P}, the double mutants zERK1$^{L106P/S184D}$ and zERK2$^{L84P/S162D}$ and finally the triple mutants zERK1$^{L106P/S184D/D352N}$ and zERK2$^{L84P/S162D/D330N}$. The Western blot results with total and dpERK antibodies show that all mutants were successfully expressed and phosphorylated in zf4 cells. In addition, Western blot analysis with dp-ERK after transfection of zf4 cells as well as mRNA injection in zebrafish embryos clearly showed increased TEY phosphorylation of zERK1 and zERK2 triple mutants *(Fig2a)*. Comparison to the wild type isoforms of the proteins shows that the ERK2 double mutant induced a slight increase in signaling to downstream targets, despite the poorly detectable increase of its TEY

TABLE 5: Cluster 2 gene ontology.

Peptide	Name protein	Functions
P53_12_24	Cellular tumor antigen p53. Tumor suppressor p53. Phosphoprotein p53. Antigen NY-CO-13	Protein import into nucleus, negative regulation of transcription from RNA polymerase II promoter, transcription factor activity, embryonic development, somitogenesis, release of cytochrome c from mitochondria, T cell proliferation involved in immune response, B/T cell lineage commitment, DNA binding chromatin binding, DNA double-strand break repair, apoptotic process, DNA damage response, ER overload response, cell cycle arrest, Ras protein signal transduction, multicellular organismal development, gastrulation, negative regulation of neuroblast proliferation, central nervous system development, cell aging, blood coagulation, rRNA transcription, X-ray response, gamma radiation
KS6A1_374_386	Ribosomal protein S6 kinase alpha-1.S6K-alpha 1. p90-RSK 1. pp90RSK1. p90S6K. RSK-1. MAPKAPK1A	Toll-like receptor signaling pathway, cell cycle, synaptic transmission, axon guidance, negative regulation of apoptotic process, regulation of translation in response to stress, regulation of DNA-dependent transcription in response to stress, innate immune response, cell differentiation positive regulation of transcription from RNA polymerase II promoter, nerve growth factor receptor signaling pathway, stress-activated MAPK cascade
GSUB_61_73	G-substrate. C7orf16.protein phosphatase 1. regulatory subunit 17 (PPP1R17)	Central nervous system development
GPR6_349_361	Sphingosine 1-phosphate receptor. G-protein coupled receptor 6	G-protein coupled receptor activity
ESR1_160_172	Estrogen receptor (ER). Estradiol receptor (ER-alpha). Nuclear receptor subfamily 3 group A member 1	Epithelial cell development, osteoblast development, sequence-specific DNA binding, transcription factor activity, steroid hormone receptor activity, DNA-dependent transcription initiation from RNA polymerase II promoter, beta-catenin binding, transcription factor binding, androgen metabolic process, chromatin remodeling complex, nitric-oxide synthase regulator, estrogen receptor signaling pathway, type 1 metabotropic glutamate receptor binding, response to estradiol stimulus, regulation of apoptotic
CA2D1_494_506	Voltage-dependent calcium channel subunit alpha-2/delta-1 precursor. CACNA2D1	Voltage-gated calcium channel complex, sarcoplasmic reticulum, T-tubule
ANDR_785_797	Androgen receptor. Dihydrotestosterone receptor. Nuclear receptor subfamily 3 group C member 4	In utero embryonic development, DNA binding, chromatin binding, transcription factor activity, androgen receptor activity, sex differentiation, beta-catenin binding, positive regulation of cell proliferation, male gonad development, prostate gland development, response to insulin stimulus, positive regulation of intracellular estrogen receptor signaling pathway, negative regulation of apoptotic process, positive regulation of MAPK cascade, positive regulation of insulin-like growth factor receptor signaling pathway, positive regulation of integrin biosynthetic process, negative regulation of epithelial cell proliferation, positive regulation of NF-kappaB transcription factor activity, prostate gland development
ACM5_498_510 ACM5_494_506	Muscarinic acetylcholine receptor M5. cholinergic receptor. muscarinic 5	

phosphorylation in transfected zf4 cells. Strikingly, the triple mutant of ERK2 revealed clear hyper- phosphorylation of ERK substrates p90RSK, CREB and MNK1 *(Fig2)*. This could have been a detection discrepancy of this assay as the double mutant appears to be indeed more phosphorylated at its dual phosphorylation site in zebrafish embryos *(Fig3a)*. In the absence of growth factor stimulation zERK2$^{L84P/S162D}$ and zERK2$^{L84P/S162D/D330N}$ maintained activity and phosphorylation of substrates in zf4 cells. We therefore continued investigation the constitutive active ERK2 double and triple mutants in heterozygous Tg(Dusp6:d2EGFP) at 5hpf and included FGF8 as a positive control. eGFP induction after FGF8 mRNA injection was demonstrated previously by *Molina et al* using fluorescent microscopy [28]. We were able to quantify increased eGFP fluorescence in batches of minimal 30 FGF8 mRNA injected embryos with the COPAS XL *(Fig3)*. During zebrafish epiboly FGF8 acts as a morphogen which induces the MEK/ERK pathway at the margin were it regulates the gene expression

of DUSP6 [29]. Therefore along with FGF8 we injected the ERK2 WT, double and triple mutants for in vivo quantitative fluorescent detection and conclude that the ERK2 double and triple mutants are more potent to induce downstream gene expression than the WT form. For the next experiment we proceeded further with the ERK2 triple mutant because the *in vivo* monitored increase in activity was more significant than that of the double mutant. In addition to the two substitutions that facilitate auto-phosphorylation, the triple mutant contains an extra substitution in the phosphatases interacting motif which prevents inactivation of ERK2 by feedback signaling, resulting in the highest phosphorylation activity level for the triple mutant isoform.

TABLE 6: Cluster 6 gene ontology.

Peptide	Name protein	Functions
RBL2_655_667	Retinoblastoma-like protein 2.p130.PRB2. RBR-2	Tumor suppressor, inhibitor of E2F-mediated transactivation, cell cycle regulation and proliferation, differentiation during human placental development
PRKDC_2618_2630	DNA-dependent protein kinase catalytic subunit (DNA-PKcs). DNPK1.p350	Apoptosis (FAS signaling pathway) Cell Cycle: G2/M Checkpoint, B-cell differentiation, telomere maintenance, DNA double strand break repair, transcription factor
PP2AB_297_309	Serine/threonine-protein phosphatase 2A catalytic subunit beta isoform. PP2A-beta. PPP2CB. PPM1B	Fibroblast growth factor receptor signaling pathway, negative regulation of Ras protein signal transduction, negative regulation of apoptotic process, proteasomal ubiquitin-dependent protein catabolic process
MBP_222_234	Myelin basic protein. Myelin A1 protein. Myelin membraneencephalitogenic protein	Protease binding, immune response, synaptic transmission, structural constituent of myelin sheath
NEK3_158_170	NimA-related protein kinase 3. HSPK 36	Protein serine/threonine kinase activity, cell cycle, mitosis, cell division
KCC2G_278_289	Calcium/calmodulin-dependent protein kinase type II gamma chain. CaM kinase II subunit gamma, CaMK-II subunit gamma. CAMK2G	G1/S transition of mitotic cell cycle, response to hypoxia, synaptic transmission, cytokine-mediated signaling pathway, insulin secretion
CGHB_109_121	Choriogonadotropin subunit beta precursor. CGB5. HCG. CG-beta	Hormone-mediated signaling pathway
CDC2_154_169	Cell division control protein 2 homolog.p34 protein kinase. Cyclin-dependent kinase 1. CDK1. CDC28A. P34CDC2	Cell cycle checkpoint, G1/S transition of mitotic cell cycle, MAPK cascade activation, microtubule cytoskeleton organization, toll-like receptor signaling pathway, cyclin-dependent protein kinase activity, spindle microtubule, DNA replication, DNA repair protein complex assembly, apoptotic process, DNA damage checkpoint, epidermal growth factor receptor signaling pathway, Ras protein signal transduction, pronuclear fusion, axon guidance, cell aging, insulin receptor signaling pathway, RNA polymerase II carboxy-terminal domain kinase activity, fibroblast growth factor receptor signaling pathway, gene expression, regulation of Schwann cell

The fibroblast growth factors are known to bind to their corresponding tyrosine kinase receptors and that relay the extracellular signals further to the ERK/MAPK pathway and the PI3/AKT pathway. Therefore, part of FGF downstream signaling should overlap with ERK2 downstream signaling. To identify this pool of substrates in zebrafish cell lysates isolated from 5 hours old embryos, using PamGene serine threonine kinome peptide arrays *(Fig4)*. Kinome profiles of embryos injected with FGF8, wt ERK2 and ERK2 triple mutant mRNA were compared against uninjected wt with model based clustering. The 7 clusters of peptides were identified of which

cluster 6 represents the overlapping pool of peptides induced by FGF8 and ERK2 triple mutant and cluster 2 the FGF8 targets independent of ERK/MAPK signaling. However the fold induction of phosporylation of each peptide compared to the uninjected control was quite low and often did not exceed the variation between the biological triplicates and therefore we could not demonstrate its significance using statistical tests. This is possibly due to the endogenous ERK2 signaling already present in the cell lysates. Despite this difficulty we found phosphorylation on the 154-162 amino acids of the peptide corresponding to the cell proliferation marker CDK1 (CDC2), to be significantly increased in embryo lysates overexpressing ERK2*** and FGF8. Direct interaction of active ERK2 with CDC2/CDK1 has not been demonstrated before, but, both kinases are key players in cell cycle regulation and known to promote G2/M transition and proliferation. In response to mitotic stimulation ERK2 is known to induce expression of cyclin D, which binds and activates CDK4 and CDK6. In addition, activated ERK2 increased the expression of cyclin A, which binds to either CDK1 or CDK2 [30]. The cyclinA/B-CDK1 complex becomes fully functional after dephosphorylation of inhibitory Tyr15 and Thr14 residues and phosphorylation of Thre-161 on CDK1 by Cdk Activating Kinases (CAK) [31,32]. The molecular mechanism connecting ERK2 and CAK, leading to increased thr-161 phosphorylation of CDK1, remains to be identified.

Conclusion

In this study we have successfully constructed two constitutive active zebrafish ERK2 mutants zERK2[L84P/S162D] and zERK2[L84P/S162D/D330N] which continue to drive downstream signaling during growth factor deprivation *in vitro* and which are more potent to relay signals to the nucleus and induce target gene transcription *in vivo*. In addition, cell proliferation can be induced by zERK2[L84P/S162D/D330N] as elevated ERK2 signals increase the phosphorylation of CDK1, a key protein involved in promoting cell cycle progression. Future research will be focusing on the possible long term effect of constitutive ERK2 activation by developing transgenic zebrafish lines that drive constitutive active ERK2 isoforms under the control of the melanocyte-specific promotors *mitfa* or *kita*. Analysis of the specific downstream molecular mechanisms that are involved in oncogenic transformation will attribute to the specific role of MAPK signaling, when compared to other systems such as the BRAF (BRAFV600E) transgenic fish line.

Reference List

1. McCubrey JA, Steelman LS, Chappell WH, Abrams SL, Wong EWT, Chang F, Lehmann B, Terrian DM, Milella M, Tafuri A et al.: Roles of the Raf/MEK/ERK pathway in cell growth, malignant transformation and drug resistance. *Biochimica et Biophysica Acta (BBA) - Molecular Cell Research* 2007, 1773:1263-1284.

2. Roberts PJ, Der CJ: Targeting the Raf-MEK-ERK mitogen-activated protein kinase cascade for the treatment of cancer. *Oncogene* 2007, 26:3291-3310.

3. Yoon S, Seger R: The extracellular signal-regulated kinase: Multiple substrates regulate diverse cellular functions. *Growth Factors* 2006, 24:21-44.

4. Zebisch A, Czernilofsky AP, Keri G, Smigelskaite J, Sill H, Troppmair J: Signaling through RAS-RAF-MEK-ERK: from basics to bedside. *Curr Med Chem* 2007, 14:601-623.

5. Zhang W, Liu HT: MAPK signal pathways in the regulation of cell proliferation in mammalian cells. *Cell Res* 2002, 12:9-18.

6. Hoshino R, Chatani Y, Yamori T, Tsuruo T, Oka H, Yoshida O, Shimada Y, Ari-i S, Wada H, Fujimoto J et al.: Constitutive activation of the 41-/43-kDa mitogen-activated protein kinase signaling pathway in human tumors. *Oncogene* 1999, 18:813-822.

7. Askari N, Diskin R, Avitzour M, Yaakov G, Livnah O, Engelberg D: MAP-quest: could we produce constitutively active variants of MAP kinases? *Mol Cell Endocrinol* 2006, 252:231-240.

8. Mansour SJ, Matten WT, Hermann AS, Candia JM, Rong S, Fukasawa K, Vande Woude GF, Ahn NG: Transformation of mammalian cells by constitutively active MAP kinase kinase. *Science* 1994, 265:966-970.

9. Cowley S, Paterson H, Kemp P, Marshall CJ: Activation of MAP kinase kinase is necessary and sufficient for PC12 differentiation and for transformation of NIH 3T3 cells [abstract]. *Cell* 1994, 77:841

10. Kolch W, Heidecker G, Lloyd P, Rapp UR: Raf-1 protein kinase is required for growth of induced NIH/3T3 cells. *Nature* 1991, 349:426-428.

11. Scholl FA, Dumesic PA, Khavari PA: Effects of active MEK1 expression in vivo [abstract]. *Cancer letters* 2005, 230:1

12. Karasarides M, Chiloeches A, Hayward R, Niculescu-Duvaz D, Scanlon I, Friedlos F, Ogilvie L, Hedley D, Martin J, Marshall CJ et al.: B-RAF is a therapeutic target in melanoma. *Oncogene* 2004, 23:6292-6298.

13. Patton EE, Widlund HR, Kutok JL, Kopani KR, Amatruda JF, Murphey RD, Berghmans S, Mayhall EA, Traver D, Fletcher CD et al.: BRAF mutations are sufficient to promote nevi formation and cooperate with p53 in the genesis of melanoma. *Curr Biol* 2005, 15:249-254.

14. Patton EE, Zon LI: Taking human cancer genes to the fish: a transgenic model of melanoma in zebrafish. *Zebrafish* 2005, 1:363-368.

15. Amatruda JF, Patton EE: Genetic models of cancer in zebrafish. *Int Rev Cell Mol Biol* 2008, 271:1-34.

16. Amatruda JF, Shepard JL, Stern HM, Zon LI: Zebrafish as a cancer model system. *Cancer Cell* 2002, 1:229-231.

17. Goessling W, North TE, Zon LI: New waves of discovery: modeling cancer in zebrafish. *J Clin Oncol* 2007, 25:2473-2479.

18. Lam SH, Wu YL, Vega VB, Miller LD, Spitsbergen J, Tong Y, Zhan H, Govindarajan KR, Lee S, Mathavan S et al.: Conservation of gene expression signatures between zebrafish and human liver tumors and tumor progression. *Nat Biotechnol* 2006, 24:73-75.

19. Stoletov K, Klemke R: Catch of the day: zebrafish as a human cancer model. *Oncogene* 2008, 27:4509-4520.

20. Abbott DE, Postovit LM, Seftor EA, Margaryan NV, Seftor RE, Hendrix MJ: Exploiting the convergence of embryonic and tumorigenic signaling pathways to develop new therapeutic targets. *Stem Cell Rev* 2007, 3:68-78.

21. Hendrix MJ, Seftor EA, Seftor RE, Kasemeier-Kulesa J, Kulesa PM, Postovit LM: Reprogramming metastatic tumour cells with embryonic microenvironments. *Nat Rev Cancer* 2007, 7:246-255.

22. Moustakas A, Heldin CH: Signaling networks guiding epithelial-mesenchymal transitions during embryogenesis and cancer progression. *Cancer Sci* 2007, 98:1512-1520.

23. Krens SF, He S, Lamers GE, Meijer AH, Bakkers J, Schmidt T, Spaink HP, Snaar-Jagalska BE: Distinct functions for ERK1 and ERK2 in cell migration processes during zebrafish gastrulation. *Dev Biol* 2008, 319:370-383.

24. Emrick MA, Hoofnagle AN, Miller AS, Eyck LFT, Ahn NG: Constitutive Activation of Extracellular Signal-regulated Kinase 2 by Synergistic Point Mutations. *Journal of Biological Chemistry* 2001, 276:46469-46479.

25. Hall JP, ChERKasova V, Elion E, Gustin MC, Winter E: The osmoregulatory pathway represses mating pathway activity in Saccharomyces cerevisiae: isolation of a FUS3 mutant that is insensitive to the repression mechanism. *Mol Cell Biol* 1996, 16:6715-6723.

26. Brunner D, Oellers N, Szabad J, Biggs WH, III, Zipursky SL, Hafen E: A gain-of-function mutation in Drosophila MAP kinase activates multiple receptor tyrosine kinase signaling pathways. *Cell* 1994, 76:875-888.

27. Tsang M, Maegawa S, Kiang A, Habas R, Weinberg E, Dawid IB: A role for MKP3 in axial patterning of the zebrafish embryo. *Development* 2004, 131:2769-2779.

28. Molina GA, Watkins SC, Tsang M: Generation of FGF reporter transgenic zebrafish and their utility in chemical screens. *BMC Dev Biol* 2007, 7:62.

29. Tsang M, Maegawa S, Kiang A, Habas R, Weinberg E, Dawid IB: A role for MKP3 in axial patterning of the zebrafish embryo. *Development* 2004, 131:2769-2779.

30. MacCorkle RA, Tan TH: Mitogen-activated protein kinases in cell-cycle control. *Cell Biochem Biophys* 2005, 43:451-461.

31. Coulonval K, Kooken H, Roger PP: Coupling of T161 and T14 phosphorylations protects cyclin BÇôCDK1 from premature activation. *Molecular Biology of the Cell* 2011, 22:3971-3985.

32. Krek W, Nigg EA: Cell cycle regulation of vertebrate p34cdc2 activity: identification of Thr161 as an essential in vivo phosphorylation site. *New Biol* 1992, 4:323-329.

CHAPTER III

Characterization and expression analysis of two novel zebrafish P38 isoforms

H. Rian, Z. Forghany, S.F.G Krens[2], H.P Spaink and B. Ewa Snaar-Jagalska

Abstract

The P38 MAPK subfamily consists of four isoforms (P38α, P38β, P38γ, and P38δ) that play a role in proliferation, differentiation and stress responses. P38 signaling is found to be deregulated in pathologies like Alzheimer, cancer, rheumatoid arthritis and asthma.

The Zebrafish orthologs of most MAPK genes have recently been identified, however two isoforms of the p38 family remained to be detected. In this study, two novel zebrafish p38 (β, δ) cDNAs were cloned, which translated into 361 and 362 amino acid proteins, respectively, with approximately 56% identity. Comparison of the amino acid sequences of all zebrafish P38 MAPKs by multiple sequence alignment indicated conservation of the dual phosphorylation site TXY motif, DFG site, ED site and CD domain in all zebrafish P38 isoforms. The catalytic region, with the glycine-rich loop, hinge region and α-Helix C, is more than 83% identical between the P38α and P38β isoforms. Mutation prone residues are mainly localized at the MAP Kinase insert and α-Helix G. Semi-quantitative reverse transcriptase-PCR revealed an ubiquitous expression pattern of zebrafish p38β throughout embryogenesis, whereas p38δ levels were variable. Unlike p38δ, p38β was maternally expressed and both genes were expressed in the adult zebrafish. To localize the expression whole mount in situ hybridization was performed from 1- to 5- dpf. p38β mRNA was detectable in the heart, lens, notochord and the telencephalon, diencephalon, presumptive forebrain ventricle, the midbrain tegmentum, mid-hindbrain boundary and rhombencephalon of the brain. P38δ was aslo expressed in the notochord, the telencephalon, diencephalon, midbrain tegmentum and rhombomeres of the hindbrain. In addition p38β mRNA was concentrated in the chondrocranium, pectoral fins, neural retina, the gut and at somite boundaries.

Phylogenetic analysis revealed that zebrafish p38 isoforms cluster with their corresponding orthologues in human, mice, rat, *Xenopus* and medaka. Like in mammals, the zebrafish P38α and P38β are the most similar isoforms.

Altogether, this study reports the identification of two novel zebrafish P38 isoforms and the analysis of their specific spatial and temporal expression patterns during early zebrafish development.

Introduction

The four mammalian P38 MAPKs, α(MAPK14), β(MAPK11), γ(MAPK12) and δ(MAPK13) are representative MAPKs of one of the three main subfamilies of the Mitogen Activated Protein Kinases (MAPK). The other two subfamilies are the extracellular-signal regulated protein kinases (ERK) and the c-Jun amino terminal kinases (JNK). MAPK family is conserved in evolution through the plant and animal kingdom and constitutes one of the major eukaryotic signalling families that transmit extracellular signals from the cell-surface to the nucleus. They contribute to the ability of cells to receive and respond to environmental cues. The repertoire of their substrates includes cytoskeleton proteins as well as transcription factors controlling global gene expression (Johnson, Lapadat, 2002; Kim, Choi, 2010; Roux, Blenis, 2004). These proteins have been implicated in numerous cellular functions including cell growth, migration, proliferation, differentiation, survival and development, and mis-regulated MAPK signaling has been engrossed in many human diseases.

The three subfamilies are distinguished according to the middle amino-acid residue of the conserved Thr-Xxx-Tyr (TXY) dual-phosphorylation motif with TGY being specific for the P38 subfamily. Phosphorylation of the TXY motif activates MAPKs and occurs by upstream MAPKK which in turn are activated by MAPKKK. MAPKK undergo a highly selective interaction with specific MAPKs which could be explained by structural differences of the activation loop containing the TXY motif. MAPKK3 and MAPKK6 interact specifically with the P38 subfamily whereas MAPKK4 binds to the P38α isoform and to JNK MAPKs facilitating crosstalk between these two subfamilies (Zarubin, Han, 2005; Cuadrado, Nebreda, 2010).

The P38 family was initially associated with stress responses since the first identified isoform Hog1/P38α in yeast was rapidly phosphorylated after LPS stimulation or hyper osmotic shock. Additionally, P38α activation in higher eukaryotes is stimulated by stress factors such as heat, pro-inflammatory cytokines, UV irradiation etc (Fearns et al. 2000). In response to these stimuli P38α regulates cellular protective mechanisms including the biosynthesis of pro-inflammatory cytokines (IL-1, IL-6, IL-8, TNFα, COX-2 and IFN-γ) and inhibits the anti-inflammatory and immunosuppressive activities of the glucocorticoid receptor (Lee et al. 1994; Wang, 2004). In addition, the P53 tumor supressor is among the P38α substrates providing a link with the cell cycle checkpoints (Thornton, Rincon, 2009). The P38 subfamily is often found to play a key role in the pathogenesis of disorders such as cancer, rheumatoid arthritis, asthma and Alzheimer, which are a consequence of aberrant functioning of cell cycle progression and immune or inflammatory responses (Coulthard et al. 2009; Cuenda, Rousseau, 2007; Chung, 2011; Munoz, Ammit, 2010) .

Many studies have been performed using the pyridinyl imidazole inhibitors SB203580 and SB202190 which inhibit P38α and β equally, with no significant effect on γ and δ, therefore knowledge on the functional distinction between these two isoforms is elusive. The essential role of the P38α isoform in development was demonstrated in knock-out mice resulting in homozygous embryonic lethality caused by severe defects in placental angiogenesis (Mudgett et al. 2000). In contrast, mice lacking P38β, P38γ and P38δ were viable, fertile and did not show any obvious phenotypes.

Although all P38 isoforms are activated by environmental stress and pro-inflammatory cytokines, P38α is suggested to be the main isoform regulating cytokine production. Mice lacking p38β showed no defects in the cytokine production or immune function after LPS stimulation or after crossing with a mouse line ectopically expressing the systemic cytokine TNFα (Beardmore et al. 2005). Nevertheless a specific metabolic role of P38β has been reported in the regulation of the mTORC1 pathway during energy stress involving intracellular ATP depletion (Kalender et al. 2011). Antagonistic roles of the P38 isoforms were demonstrated, for example P38δ has an opposing role in P38α induced activation of the osmoprotective transcription factor TonEBP/OREBP in HEK293 cells treated with high concentrations of NaCl (Zhou et al. 2008; Pramanik et al. 2003). In addition, P38δ plays a specific role in the regulation of skin homeostasis and tumorigenesis (Eckert et al. 2003; Schindler et al. 2009).

As previously described (Krens et al. 2006a), the zebrafish genome encodes for members of all MAPK subfamily: ERK, JNK and p38 and the functions of ERK1/2 and JNK in embryogenesis are intensively studied (Krens et al. 2006b). However, only a few reports have investigated the role of p38 family in zebrafish. Ectopic expression by injection of a dominant negative (DN) form of p38α indicated that asymmetric distribution of p38α activation contributes to symmetric and synchronous cell cleavage (Fujii et al. 2000). Furthermore, DN p38α phenocopies the *betty boop* (MAPKAPK2) mutant phenotype by inducing premature constriction of the blastoderm margin, in a YSL specific manner in zebrafish pre-gastulation embryos (Holloway et al.2009).

In this study we report the cloning and characterization of novel members of the p38 subfamily p38β and p38δ and describe their spatial and temporal expression patterns during early zebrafish development.

Material & Methods

Zebrafish husbandry
Zebrafish (Danio rerio) wild type line was maintained under standard conditions and guidelines given in the zebrafish book (Westerfield 200). Embryos were kept at 28.5°C and staged in hours post fertilization (hpf) according to (Kimmel et al. 1995).

3.2 cDNA synthesis and Cloning of p38 β/δ genes
Total RNA was isolated from adult Teubingen zebrafish, using Trizol Reagent protocol (GIBCOBRL, Life technologies™). cDNA synthesis was performed with iScript™ cDNA Synthesis Kit (Bio-Rad) and was amplified with Phusion® High-Fidelity DNA Polymerase and gene specific primers of P38β fw: 5' CGGAAAACATGGCGACAAGAC 3' rv: 5' TGCGCTCAGTTTTATTGTTCAACC 3' and p38δ fw: 5' CTAAATGGAGTCTCGGGTGG 3' rv: CTAGGACATGGTGAGTGAGTGTGTT. Subsequently the full CDS flanking sequences were cloned into pCR-BluntII-TOPO (Invitrogen) and transformed in one shot Top10 chemically competent E.coli. Several clones were verified with restriction analysis and DNA sequencing.

3.3 Sequence alignments and phylogenetic analysis
Phylogenetic analysis was performed based on multiple alignments of p38 MAPKs from different species; human (h), rat (r), mouse (m), Xenopus (x), zebrafish (z) and medaka fish (med). ENSEMBLE protein codes: hp38α: ENSP00000229795 hp38β: ENSP00000333685 hp38γ: ENSP00000215659 hp38δ: ENSP00000211287 mp38α:ENSMUSP00000004990 mp38β:ENSMUSP00000132439 mp38γ:ENSMUSP00000086207 mp38δ: ENSMUSP00000004986 rp38α:ENSRNOP00000000617 rp38β: ENSRNOP00000009325 rp38γ: ENSRNOP00000046455 rp38δ: ENSRNOP00000000621 xp38α: ENSXETP00000000926 xp38β: ENSXETP00000048165 xp38γ: ENSXETP00000048167 xp38δ: ENSXETP00000000923 medP38α.1: ENSORLP00000008135 medP38α.2: ENSORLP00000020176 medp38β: ENSORLP00000011217 medp38γ.1: ENSORLP00000020405 medp38γ.2 ENSORLP00000011305 medp38δ: ENSORLP00000000486 zp38αA: ENSDARP00000040361 zp38γ: ENSDARP00000011298 zP38αb.1 ENSDARP00000035686, zP38αb.2 ENSDARP00000040146

RNA isolation and reverse transcriptase PCR
Total RNA was extracted from embryos at different stages of development using Trizol reagent (Invitrogen) phenol-chloroform and phase-lock gel. RNA quality control was performed by agarose gel electrophoresis. Expression patterns during development of P38β and P38δ were determined by RT-PCR with SuperScript™ III

One-Step RT-PCR System with Platinum® Taq DNA polymerase (Invitrogen) and the full CDS-flanking primers used for cloning. β-actin was used as a control fw 5' ggcacccagcacaatgaagat 3' rv 5' aagtcatagtccgcctagaagcat 3'.

<u>In situ hybridization</u>
Anti-sense digoxigenin labeled RNA probes were synthesized from the full length cDNA cloned in pCR-BluntII-TOPO. The constructs were linearized and antisense probes were synthesized using the DIG RNA Labeling Kit (Roche) and T7, sp6 RNA polymerase (Maxiscript kit, Ambion) according to the orientation of the gene in the TOPO construct. Zebrafish embryos were harvested at 24 and 48hpf, dechorionated and fixed overnight in 4% paraformaldehyde in PBS at 4°C. In situ hybridization was performed as described previously (Westerfield 200).

Results & Discussion

<u>Cloning of zebrafish p38β and p38δ</u>
To obtain the cDNA of p38β and p38δ, gene specific primers were designed based on the ensemble predictions zgc:86905 and im:7136778 (Zv8), respectively (Table 1). Several clones were sequenced for both p38β and p38δ. One single p38δ transcript was obtained of 1089bp encoding for a 362 amino acid (a.a.) protein with a 99.4% identical sequence to im: 7136778. Since there was only one transcript found, the splicing of p38δ RNA is most likely to occur uniformly. In contrast, three P38β transcripts were obtained of which two, with a size of 1086bp and 1087bp, are mostly identical. The full protein (361a.a) is translated from the 1086bp transcript. The second transcript contains a single nucleotide insertion that changes the reading frame and results in an early truncation of the protein. The third transcript of 1263bp contains a retained intron of 170bp with an early stop codon, resulting in a truncated protein. The obtained clones were sequenced and the complete coding sequences of the newly identified transcripts p38β.2(1087bp) and p38β.3(1263bp) were submitted to GenBank: JQ513868 and JQ513869 respectively.

<u>Multiple sequence alignment of zebrafish P38 isoforms</u>
After the cloning of the zebrafish P38β and P38δ all isoforms were compared in a multiple sequence alignment (Fig1). Previously, the crystal structures of the human orthologues have been resolved and most functional domains are identified (Wilson et al.1996; Patel et al. 2009). Functional differences between the different P38 isoforms have been assigned to specific amino acids. Comparison of the sequences to other species revealed that these domains and residues are preserved in the analogous positions in zebrafish P38 MAPKs. The comparison of the primary

structure between isoforms, the dual phosphorylation site, catalytic site and protein-protein interaction sites are indicated in the alignment (Fig1).

As observed in most kinases, the N-terminal and C-terminal regions of the protein

Name	Synonyms	LG	Transcripts	Ensemble	Size CDS (bp)	Exons	Size (a.a)
P38αa	MAPK14a SAPK2A	8	1	ENSDART00000040362	1086	12	361
P38αb	MAPK14b SAPK2A	11	1	ENSDART00000030921	1086	12	361
			2	ENSDART00000132768	1047	11	348
			3	ENSDART00000040147	1086	12	361
P38β	MAPK11 PRKM11 SAPK2 zgc:86905	4	1**	ENSDART00000032857	1086	12	361
			2*	–	1087	12	–
			3*	–	1263	13	–
P38γ	MAPK12 ERK6 SAPK3 zgc:101695	18	1	ENSDART00000018502	1092	12	363
P38δ	MAPK13 im:7136778	8	1**	ENSDART00000081341	1089	12	362

Table 1. The zebrafish contains all isoforms of the P38 subfamily of MAPKs.
We confirmed the presence of the first P38β transcript and identified novel alternative transcripts coding for truncated proteins. No additional transcripts of P38δ have been identified. P38αA and P38αB are duplicated genes found in zebrafish. The linkage group corresponds with chromosome number, based on the Ensemble website.* Sequences submitted to Genbank: mapk11_2 JQ513868 and mapk11_3 JQ513869. ** Full coding transcripts of P38β and P38δ.

are folded into two small lobes and the catalytic domain is situated at the interface of these two lobes (Fig1B). The dual phosphorylation motif (TXY) is located on the activation lip at the C-terminal lobe. The position of the activation lip changes upon phosphorylation and induces additional conformational changes of mostly hydrogen interactions between residues. The N' and C' lobe rotate 5^0 towards each other (P38α) aligning the catalytic residues in the hinge region, glycine-rich loop and α-Helix C. The phenylalanine of the DFG motif, which sterically interferes with ATP binding in the non –phosporylated form, changes its position, thereby enabling the MAPK to become fully active (Zhang et al. 2011).

The dual phosphorylation motif and DFG site are conserved between all zebrafish P38 isoforms and are located in a highly conserved region, as indicated by the use of a blue font color (Fig1A). The existing amino acid differences in the glycine-rich loop, hinge region and α-Helix C are often found between P38α/β and P38γ/δ isoforms. The catalytic site is more than 80% conserved between the P38α and

P38β isoforms. SB203580 and SB202190 inhibitors target the catalytic site and are known to be selective for P38α/β this is likely to be similar in zebrafish. The 175th a.a (histidine in zP38α) is the only highly variable residue in the region of the catalytic and activation domains. However, a possible contribution of this particular residue to the conformation of the activation lip or to the kinase activity is not reported yet. The D177L substitution, two residues upstream, is found to increase the activity of all isoforms except P38δ (Diskin et al. 2007).

The two allosteric docking sites, CD domain and ED site have been found to be important for binding of activators, inactivating phosphatases and substrates (Tanoue et al. 2001). In the folded structure these sites are in close proximity and are part of a hydrophobic docking groove that is recognised by motifs on interacting proteins. Both domains consist predominantly of acidic amino acids and are conserved in zebrafish P38 MAPKs.

In mammals, two MEKK independent mechanisms are known to specifically activate P38α. P38α is capable of auto-activation upon binding with the TGF-β-activated protein kinase 1-binding protein 1 (TAB1) or after phosphorylation of Tyr323 by Zeta-chain-associated protein kinase 70 (ZAP-70), a kinase that is thought to occur specifically in antigen receptor stimulated lymphocytes and natural killer cells (Cuadrado, Nebreda, 2010). TAB1 interacts with several residues in the C-terminal domain inside as well as outside the allosteric docking sites (Ile117, Gln121, Thr219 and Ile276 in zP38α) (Zhou et al. 2006). In zebrafish, TAB1 interacting residues are also conserved in P38α. In contrast, Tyr323 is replaced by phenylalanine in zebrafish P38αA, but is present in P38αB isoform and in other P38 isoforms. Tyr323 is located in loop16 which spans both the C' lobe and the N' lobe. Recently identified activating mutations reveal the importance of this loop for the kinase activity since mutations of phe328 render all isoforms active, except P38δ (Diskin et al. 2007). The F325S substitution increases the activity of P38δ however this residue is not conserved in zebrafish.

The least conserved protein region includes the MAPK insertion, α-Helix G and the L16 loop. The MAPK insertion (MKI), a feature characteristic for MAPKs and cyclin-dependant kinase 2 (CDK2) related kinases, is located at the C'-lobe and consist of two perpendicular positioned α-helixs connected by a short loop. The function of the MKI domain is possibly involved in lipid binding (Diskin et al. 2008).

P38β and P38δ expression during zebrafish development
To determine the expression dynamics of p38β and p38δ genes through the course of zebrafish development, we performed semi-quantitative RT-PCR analysis on RNA isolated from 18 developmental stages (Fig2). The p38β is
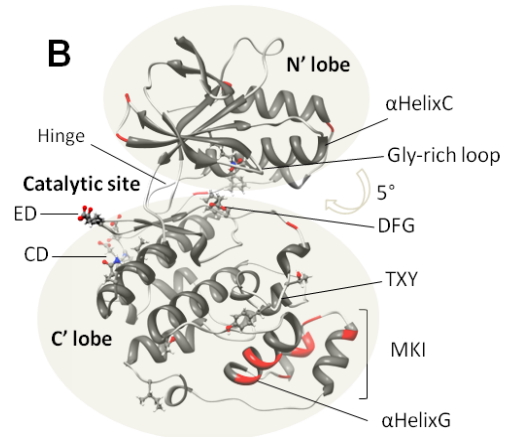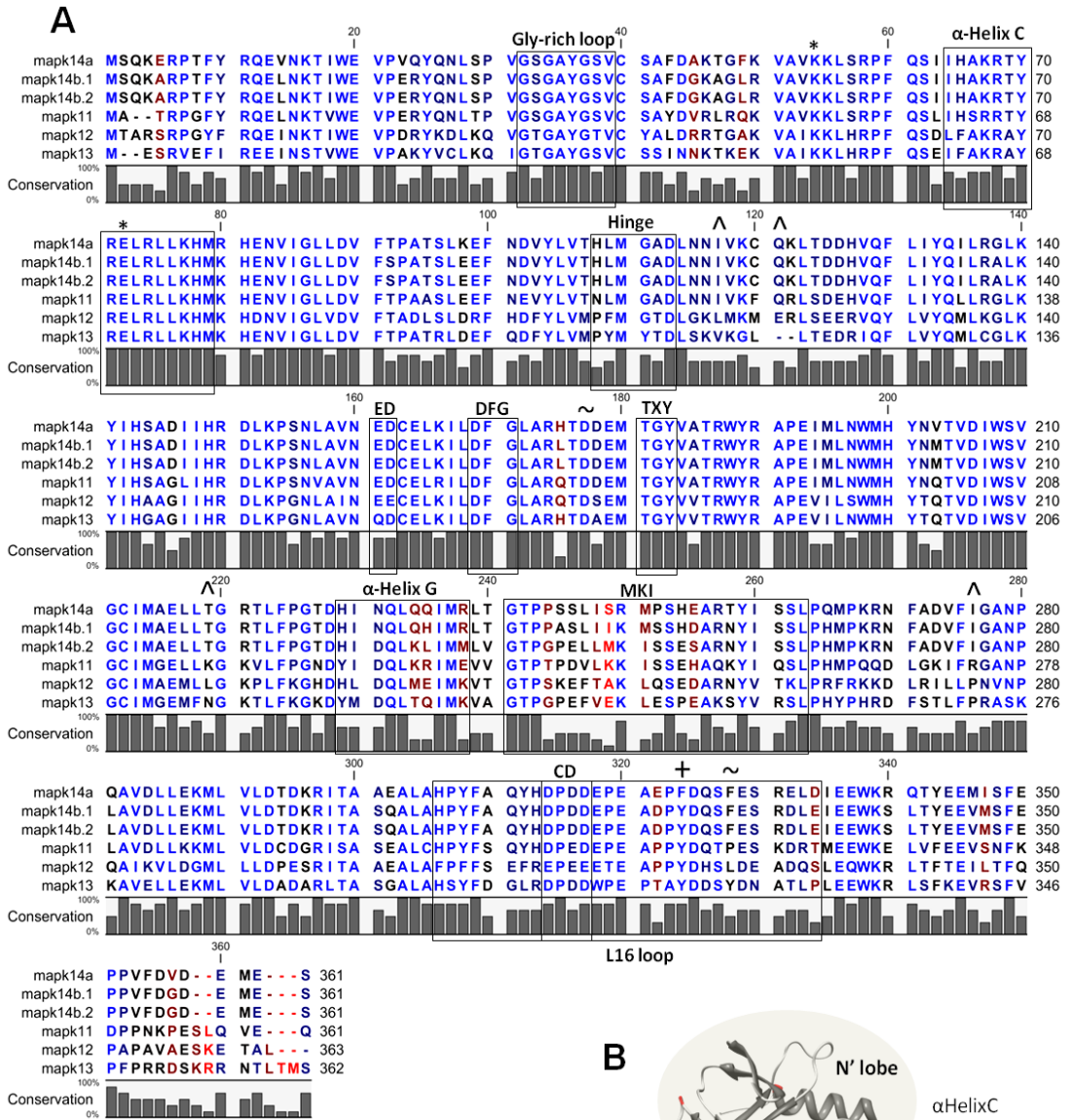
A

Gly-rich loop / α-Helix C (positions 20, 40, 60; * markers)

```
                                 20                40                   60        α-Helix C
mapk14a    MSQKERPTFY RQEVNKTIWE VPVQYQNLSP VGSGAYGSVC SAFDAKTGFK VAVKKLSRPF QSIIHAKRTY 70
mapk14b.1  MSQKARPTFY RQELNKTIWE VPERYQNLSP VGSGAYGSVC SAFDGKAGLR VAVKKLSRPF QSIIHAKRTY 70
mapk14b.2  MSQKARPTFY RQELNKTIWE VPERYQNLTP VGSGAYGSVC SAFDGKAGLR VAVKKLSRPF QSIIHAKRTY 70
mapk11     MA--TRPGFY RQELNSTVWE VPERYQNLTP VGSGAYGSVC SAYDVRLRQK VAVKKLSRPF QSLIHSRRTY 68
mapk12     MTARSRPGYF RQEINKTIWE VPDRYKDLKQ VGTGAYGTVC YALDRRTGAK VAIKKLHRPF QSDLFAKRAY 70
mapk13     M--ESRVEFI REEINSTVWE VPAKYVCLKQ IGTGAYGSVC SSINNKTKEK VAIKKLHRPF QSEIFAKRAY 68
```
Conservation 100% / 0%

Hinge (positions 80, 100, 120, 140; *, ^ markers)

```
             80                     100          Hinge          120              140
mapk14a    RELRLLKHMR HENVIGLLDV FTPATSLKEF NDVYLVTHLM GADLNNIVKC QKLTDDHVQF LIYQILRGLK 140
mapk14b.1  RELRLLKHMK HENVIGLLDV FSPATSLEEF NDVYLVTHLM GADLNNIVKC QKLTDDHVQF LIYQILRALK 140
mapk14b.2  RELRLLKHMK HENVIGLLDV FSPATSLEEF NDVYLVTHLM GADLNNIVKC QKLTDDHVQF LIYQILRALK 140
mapk11     RELRLLKHMK HENVIGLLDV FTPAASLEEF NEVYLVTNLM GADLNNIVKF QRLSDEHVQF LIYQLLRGLK 138
mapk12     RELRLLKHMK HDNVIGLVDV FTADLSLDRF HDFYLVMPFM GTDLGKLMKM ERLSEERVQY LVYQMLKGLK 140
mapk13     RELRLLKHMK HENVIGLLDV FTPATRLDEF QDFYLVMPYM YTDLSKVKGL --LTEDRIQF LVYQMLCGLK 136
```
Conservation 100% / 0%

ED / DFG / ~ / TXY (positions 160, 180, 200)

```
                   160         ED        DFG      ~     TXY           200
mapk14a    YIHSADIIHR DLKPSNLAVN EDCELKILDF GLARHTDDEM TGYVATRWYR APEIMLNWMH YNVTVDIWSV 210
mapk14b.1  YIHSADIIHR DLKPSNLAVN EDCELKILDF GLARLTDDEM TGYVATRWYR APEIMLNWMH YNMTVDIWSV 210
mapk14b.2  YIHSADIIHR DLKPSNLAVN EDCELKILDF GLARLTDDEM TGYVATRWYR APEIMLNWMH YNMTVDIWSV 210
mapk11     YIHSAGLIHR DLKPSNVAVN EDCELRILDF GLARQTDDEM TGYVATRWYR APEIMLNWMH YNQTVDIWSV 208
mapk12     YIHAAGIIHR DLKPGNLAIN EECELKILDF GLARQTDSEM TGYVVTRWYR APEVILSWMH YTQTVDIWSV 210
mapk13     YIHSAGIIHR DLKPGNLAVN QDCELKILDF GLARHTDAEM TGYVVTRWYR APEVILNWMH YTQTVDIWSV 206
```
Conservation 100% / 0%

α-Helix G / MKI / ^ markers (positions 220, 240, 260, 280)

```
           ^ 220              α-Helix G      240         MKI            260              280
mapk14a    GCIMAELLTG RTLFPGTDHI NQLQQIMRLT GTPPSSLISR MPSHEARTYI SSLPQMPKRN FADVFIGANP 280
mapk14b.1  GCIMAELLTG RTLFPGTDHI NQLQHIMRLT GTPPASLIIK MSSHDARNYI SSLPHMPKRN FADVFIGANP 280
mapk14b.2  GCIMAELLKG RTLFPGTDHI DQLKLIMMLV GTPGPELLMK ISSESARNYI SSLPHMPKRN FADVFIGANP 280
mapk11     GCIMAELLKG KVLFPGNDYI DQLKRIMEVV GTPTPDVLKK ISSEHAQKYI QSLPHMPQQD LGKIFRGANP 278
mapk12     GCIMAEMLLG KPLFKGHDHL DQLMEIMKVT GTPSKEFTAK LQSEDARNYV TKLPRFRKKD LRILLPNVNP 280
mapk13     GCIMGEMFNG KTLFKGKDYM DQLTQIMKVA GTPGPEFVEK LESPEAKSYV RSLPHYPHRD FSTLFPRASK 276
```
Conservation 100% / 0%

CD / + / ~ / L16 loop (positions 300, 320, 340)

```
                   300          CD        320     +      ~              340
mapk14a    QAVDLLEKML VLDTDKRITA AEALAHPYFA QYHDPDDEPE AEPFDQSFES RELDIEEWKR QTYEEMISFE 350
mapk14b.1  LAVDLLEKML VLDTDKRITA SQALAHPYFA QYHDPDDEPE ADPYDQSFES RDLEIEEWKS LTYEEVMSFE 350
mapk14b.2  LAVDLLEKML VLDTDKRITA SQALAHPYFA QYHDPDDEPE ADPYDQSFES RDLEIEEWKS LTYEEVMSFE 350
mapk11     LAVDLLKKML VLDCDGRISA SEALCHPYFS QYHDPEDEPE APPYDQTPES KDRTMEEWKE LVFEEVSNFK 348
mapk12     QAIKVLDGML LLDPESRITA AEALAFPFFS EFREPEEETE APPYDHSLDE ADQSLEQWKR LTFTEILTFQ 350
mapk13     KAVELLEKML VLDADARLTA SGALAHSYFD GLRDPDDWPE PTAYDDSYDN ATLPLEEWKR LSFKEVRSFV 346
```
Conservation 100% / 0%

L16 loop

(position 360)

```
           360
mapk14a    PPVFDVD--E ME---S 361
mapk14b.1  PPVFDGD--E ME---S 361
mapk14b.2  PPVFDGD--E ME---S 361
mapk11     DPPNKPESLQ VE---Q 361
mapk12     PAPAVAESKE TAL--- 363
mapk13     PFPRRDSKRR NTLTMS 362
```
Conservation 100% / 0%

B

N' lobe — αHelixC — Gly-rich loop — 5° — DFG — TXY — MKI — αHelixG
Hinge — Catalytic site — ED — CD — C' lobe

Figure 1. Multiple sequence alignment of zebrafish P38 isoforms. A) Amino acid sequence of zebrafish p38 MAPKs were aligned with CLC DNA Workbench 5.7.1. The color gradient marks the conservation: with red the most variable residue and blue highly conserved residues. Functional domains and motifs are boxed and important residues are indicated: * catalytic residues, ^ TAB1 interaction site, + ZAP70 phosphorylation site ~ catalytic activity increasing mutation sites. The same functional domains and residues are displayed on the homology model of zebrafish P38α to illustrate the position in the folded protein (B). Highly variable residues are indicated (red). To obtain the zebrafish P38α folded protein structure homology modeling was performed with Swiss-Model on the web server of the Swiss institute of bioinformatics http://www.isb-sib.ch and based on the crystal structure of the human orthologue of inactive P38α (PDB 1R39). Molecular graphics image were produced using the UCSF Chimera package from the Resource for Biocomputing, Visualization, and Informatics at the University of California, San Francisco (supported by NIH P41 RR001081).

ubiquitously expressed from the zygote on, throughout zebrafish development and eventually in the adult zebrafish. In contrast, p38δ is not maternally deposited and shows a dynamic expression pattern, as it increases at early blastula stage (16 cells-sphere cells), decreases during gastrulation and early somitogenesis, and increases again until 48hpf, thereafter its expression becomes undetectable. The p38δ is expressed in the adult zebrafish.

Expression of the two p38α genes and p38γ during the same developmental stages was reported previously (Krens et al. 2006a). The p38αA and p38γ have the same ubiquitous expression as p38β while p38αB expression peaks from 16 cells to 30% epiboly.
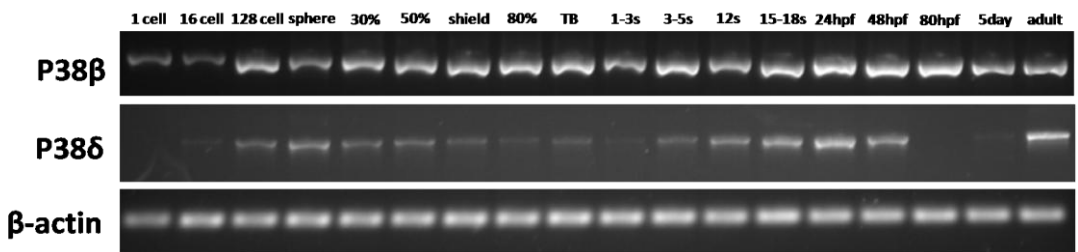

Figure 2. RT-PCR of P38β and P38δ during zebrafish development. Gene specific primers were designed flanking the full coding sequences and used for RT-PCR analysis of p38β and p38δ expression from cleavage until hatching stages. RNA isolated from the zygote and adult tissue was used to determine possible maternal expression and expression in mature adult zebrafish, respectively. β-actin expression was used as a control.

<u>Whole mount in situ hybridization of p38β and p38δ at 24hpf and 48hpf</u>

Whole mount in situ hybridization using antisense digoxigenin labeled RNA probes was performed to localize the expression of p38β (Fig 3) and p38δ (Fig 4) from 1 to 5 dpf. At 1dpf p38β is highly expressed in the in the heart, lens, notochord and specific parts of the brain. In the forebrain p38β is expressed in the dorsal rostral cluster of the telencephalon and in the ventral diencephalon. furthermore the dorsal view of the 1dpf p38β in situ shows an concentrated expression at two perpendicular anatomical lines in the forebrain one on the left-right axis and second one, connected to the first, at the posterior side of the eyes on the left-right axis. Since from 16hpf the forebrain ventricle start to appear at this position p38β could be expressed and perhaps functional in the formation in the presumptive forebrain ventricle. Furthermore p38β is expressed in the midbrain tegmentum of the mesencephalon and although expressed in the entire the rhombencephalon a highly divined expression can be distinguished located at the position of the upper rhombic
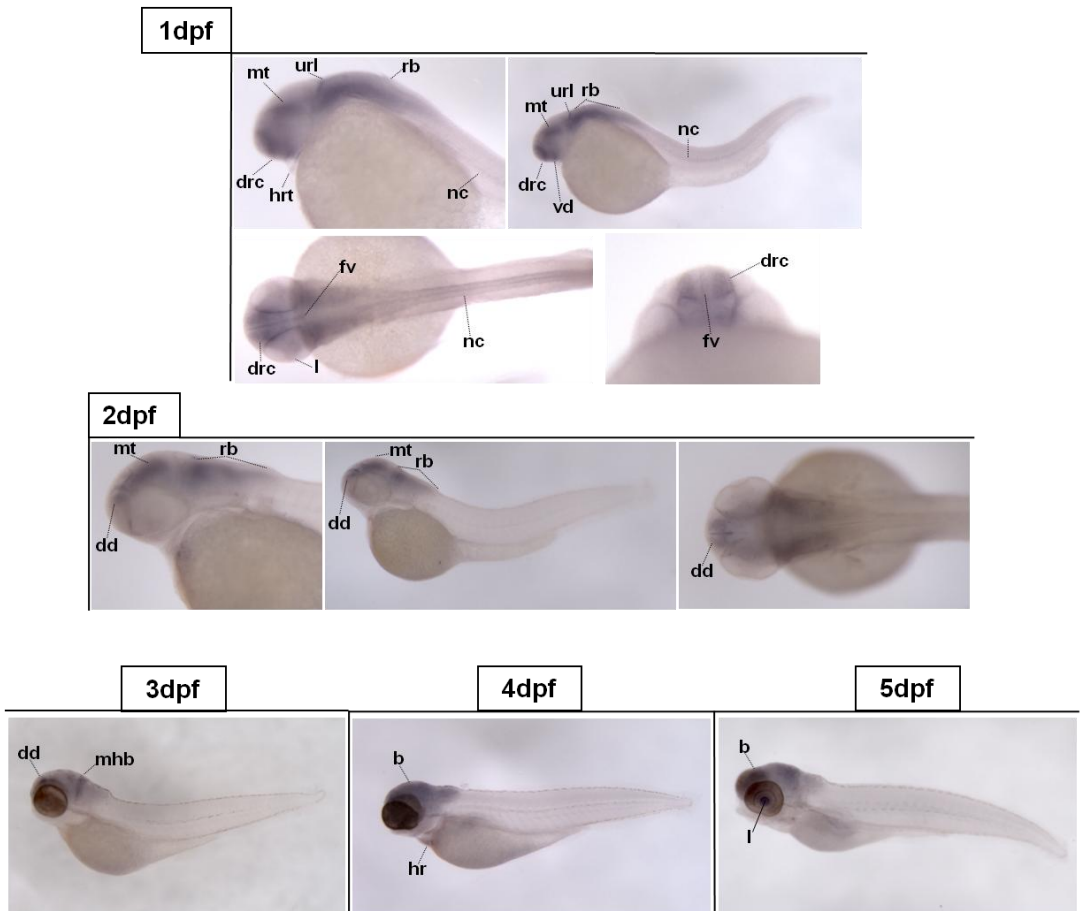

P38β

Figure 3. Whole mount in situ hybridisation showing p38β expression in wild-type zebrafish embryos. Presence of p38β RNA was detected in the brain, heart and lens. Antisense In situ probes of the full length coding sequences where used. **1dpf upper panel** Lateral view anterior to left dorsal to top in situ images. p38β expression is detected in the heart(hrt),ventral diencephalon(vd) dorsal rostral cluster of the telencephalon(drc), midbrain tegmentum(mt), the notochord(nc) the upper rhombic lip(url) and the rest of the rhombencephalon(rb)/hindbrain. **1dpf lower panel left** dorsal view anterior to left, p38β expression in the lens(l) **1dpf lower panel right** anterior view dorsal to top, show also expression of p38β in the presumptive forebrain ventricle(fv). **2dpf left and middle image** Lateral view anterior to left dorsal to top in situ **2dpf right image** dorsal view anterior to left. Expression in the dorsal diencephalon(dd), midbrain tegmentum and rhombencephalon(rb)**3,4,5dpf** Lateral view anterior to left dorsal to top. p38β expression in the dorsal diencephalon and mid-hindbrain boundary(mhb) **3dpf**, entire brain and heart **4dpf**, lens(l), telencephalon (te) and mesencephalon(me) **5dpf**.

lip. p38β continues to be expressed in the brain at 2,3,4 and 5 dpf. At 2dpf p38β expression is highest in the dorsal diencephalon, midbrain tegmentum and rhombencephalon. At 3dpf an specific expression is detected in the mid-hindbrain boundary and also dorsal diencephalon. 4 days old zf embryos show p38β expression in the entire brain and heart and at 5dpf a high p38β expression is found in the iris of the embryo.

Like most MAPK p38δ is also expressed predominantly in the brain of the developing zebrafish embryo. At 1dpf p38δ is expressed in the telencephalon and diencephalon of the forebrain and in the notochord. p38δ expression seems to concentrate more specifically in the telencephalon-diencephalon boundary and the mid-hindbrain boundary of the zebrafish brain at 2dpf. In addition, p38δ expression is also detected in the chondrocranium, pectoral fins and pharyngeal pouches. In the tail region p38δ is expressed in the somite boundaries which could possibly be the growing intersegmental veins which appear between 48- and 60 hpf. P38δ expression at the somite boundaries is also detected in 3dpf embryos. furthermore, p38δ is expressed in 3dpf embryos in the dorsal diencephalon, midbrain tegmentum, rhombomeres of the hindbrain, chondrocranium, pharyngeal arches and pectoral fins. At 3dpf p38δ expression is detecteble in the developing gut and this expression will continue to be detected at 4- and 5dpf. At 4 and 5 dpf expression of p38δ in the rhombomeres of the hindbrain and the developed pharyngeal arches becomes more evident.

Expression of the zebrafish p38α and p38γ isoforms have been described previously (Krens et al. 2006a). P38αA is expressed in the tegmentum, hindbrain, otic vesicle, pronephric duct and tail muscle at 24hpf and also in the brachial arches, cerebellum and gut at 48hpf. The p38γ is expressed in the brain at 24hpf and 48hpf. It also shows an expression at the somite boundaries at 24hpf.
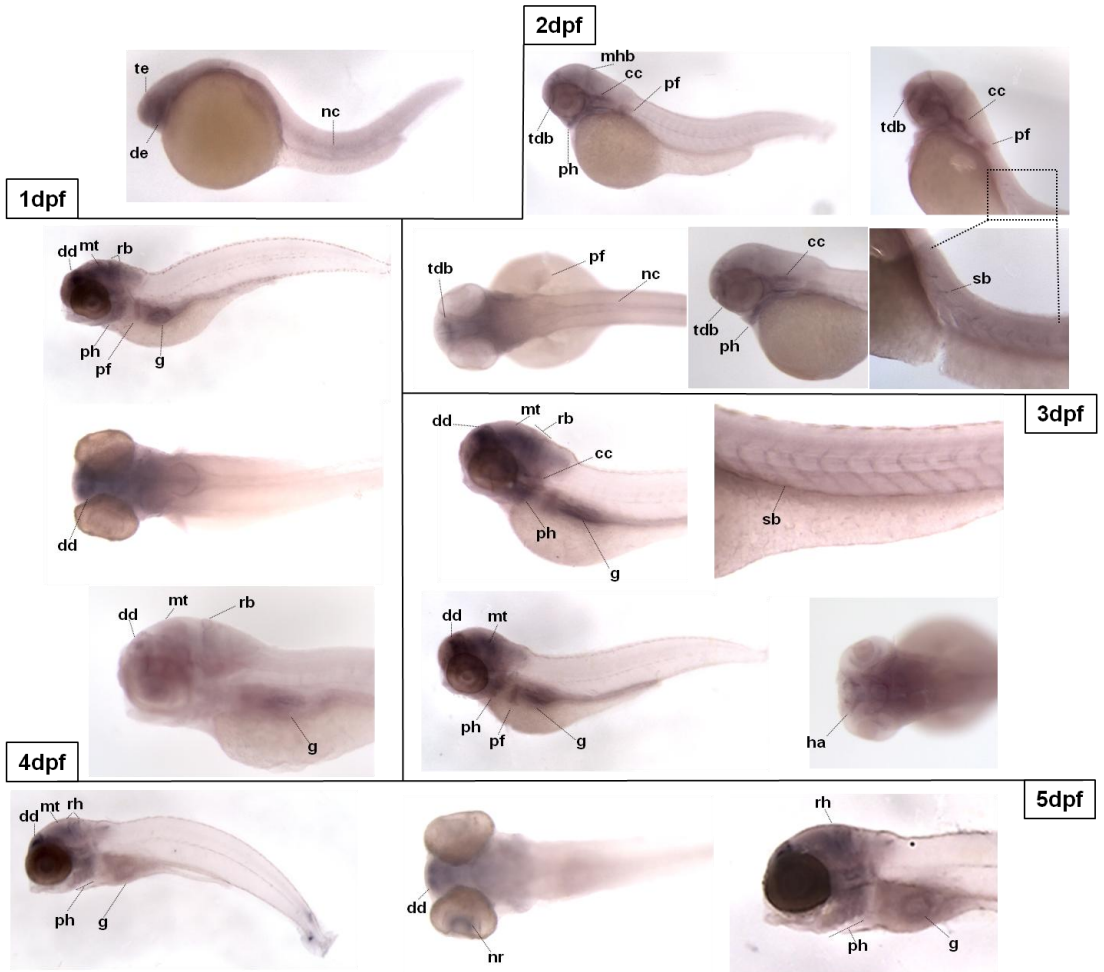
Figure 4. Whole mount in situ hybridisation showing p38δ expression in wild-type zebrafish embryos. 1dpf Lateral view anterior to left dorsal to top in situ image. expression in the telencephalon(te), diencephalon(de) and notochord(nc) **2dpf upper panel left** Lateral view anterior to left dorsal to top in situ image. p38δ expression in the pharyngeal pouches(ph), telencephalon-diencephalon boundary (tdb), mid-hindbrain boundary(mhb), chondrocranium(cc) and pectoral fins (pf). **2dpf upper panel right** Lateral view anterior to top enlargement of the anterior tail region is shown at the **2dpf lower panel right** Lateral view anterior to left dorsal to top, expression at somite boundaries (sb). **2dpf lower panel middle image** Lateral view anterior to left dorsal to top head and trunk region **2dpf lower panel left image** dorsal view anterior to left, shows p38δ expression in the notochord(nc). **3dpf upper panel left** and **3dpf lower panel left** p38δ expression in the dorsal diencephalon(dd), midbrain tegmentum (mt), rhombomeres of the hindbrain (rb), chondrocranium, pharyngeal arches, pectoral fins and the developing gut. **3dpf upper panel right** image of the middle of the tail showing expression of p38δ at the somite boundaries. **3dpf lower panel right** expression in the habenulae(ha) of the diencephalon. **4dpf top and bottom image** p38δ expression in the gut, pectoral fins, pharyngeal arches, dorsal diencephalon, midbrain tegmentum and rhombencephalon. **4dpf middle image** dorsal view anterior to left showing high expression of p38δ in the dorsal diencephalon. **5dpf left and right image** expression in the gut, pharyngeal arches, dorsal diencephalon, midbrain tegmentum and rhombomeres. **5dpf middle image** p38δ expression strongest in the dorsal diencephalon and neural retina (nr).
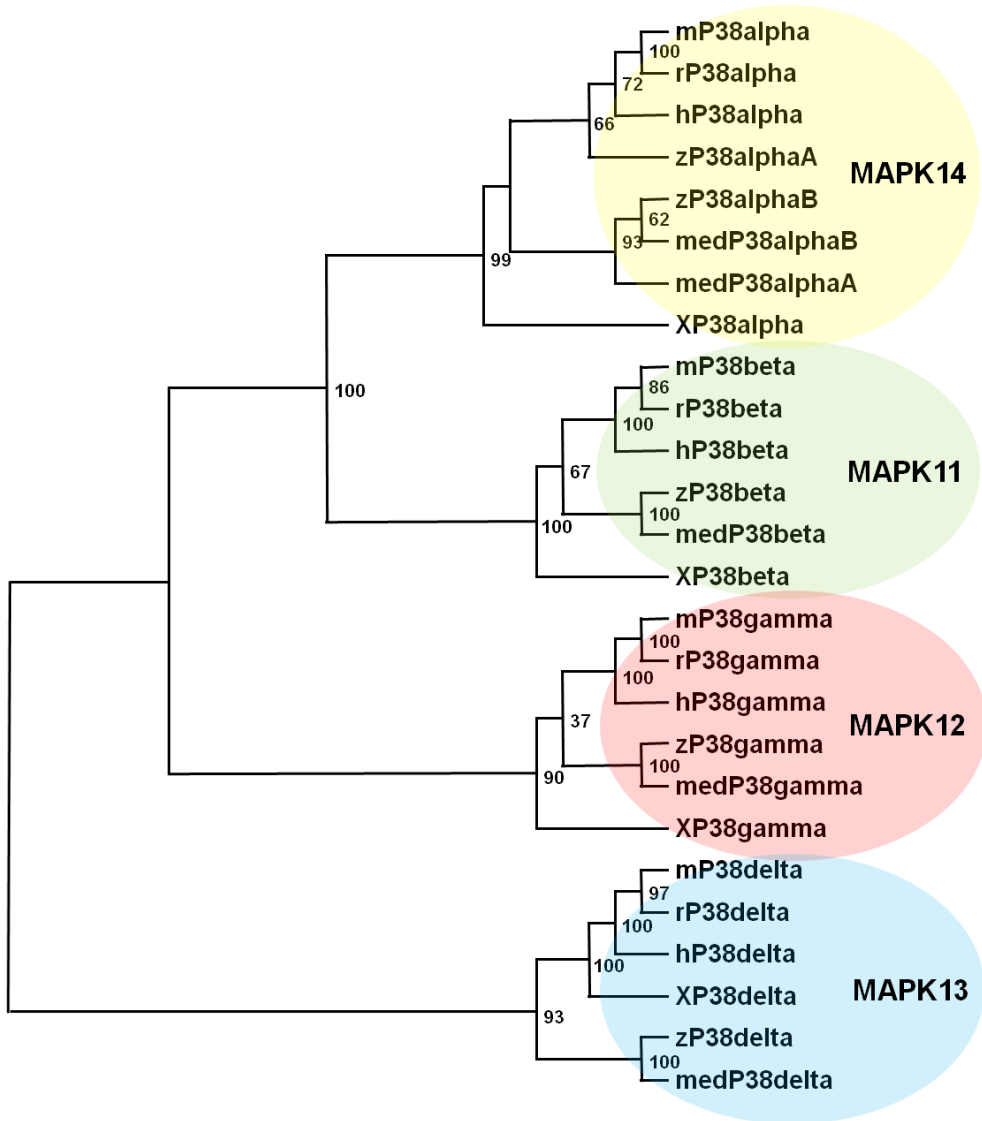
62

Figure 5. Unrooted phylogenetic tree of the zebrafish to other vertebrates P38 proteins. The phylogenetic tree was created with the ClustalW software from the DNA Data Bank of Japan(DDBJ) and the image was obtained using Treeview (http://taxonomy.zoology.gla.ac.uk/rod/treeview.html). Amino acid sequences of full length sequence predictions (ENSEMBLE) and sequencing verified coding sequences were uploaded for multiple alignment and subsequent neighbor joining analysis using default settings. The numbers indicate the occurrence of nodes during bootstrap analysis. The p-distance values are given of 1000 reiterations. Human (h), rat, (r), Mouse (m), Xenopus tropicalis (x), Zebrafish (z) and Medaka fish (med).

Phylogenetic analysis of P38 MAPKs

The unrooted phylogenetic tree based on the difference in amino acid sequences illustrates evolutionary conservation of the P38 MAPK isoforms between zebrafish, medaka, *Xenopus*, mice, rat and human(Fig5). The four zebrafish p38 isoforms cluster with their corresponding orthologues into separate branches. In addition, zebrafish and medaka are both teleost fish and the phylogenetic tree of P38 kinases shows their closely related origin since each isoform branch separates into three clusters of fish, mammalian and amphibian species.

Like in mammals, zebrafish P38α and P38β are the most similar isoforms with ~75% identity, and the catalytic domains share an even higher similarity (~80%). P38δ shows a slightly higher similarity to P38γ (61%) than when it is compared to the other isoforms: 60% with P38α and 57% P38β.

Acknowledgments

References

1. Beardmore,V.A., Hinton,H.J., Eftychi,C., Apostolaki,M., Armaka,M., Darragh,J., McIlrath,J., Carr,J.M., Armit,L.J., Clacher,C., Malone,L., Kollias,G., Arthur,J.S., 2005. Generation and Characterization of P38beta (Mapk11) Gene-targeted Mice. Mol Cell Biol, 25,10454-64.

2. Cuadrado,A., Nebreda,A.R., 2010. Mechanisms and functions of p38 MAPK signaling. Biochem. J, 429,403-417.

3. Coulthard,L.R,. White,D.E,. Jones,D.L, McDermott,M.F,. Burchill,S.A., 2009. P38(MAPK): stress responses from molecular mechanisms to therapeutics. Trends Mol Med, 15(8),369-79

4. Cuenda,A,. Rousseau,S,. 2007. P38 MAP-kinases pathway regulation, function and role in human diseases. Biochim Biophys Acta, 1773(8),1358-75.

5. Chung,K.F., 2011. p38 mitogen-activated protein kinase pathways in asthma and COPD. Chest, 139(6),1470-9.

6. Diskin,R., Lebendiker,M., Engelberg,D., Livnah,O., 2007. Structures of p38alpha active mutants reveal conformational changes in L16 loop that induce autophosphorylation and activation. J Mol Biol, 365(1),66-76.

7. Diskin,R., Engelberg,D., Livnah,O.A,. 2008. Novel lipid binding site formed by the MAP kinase insert in p38 alpha. J Mol Biol, 375(1),70-9.

8. Eckert,R.L., Efimova,T., Balasubramanian,S., Crish,J.F., Bone,F., Dashti,S., 2003. p38 Mitogen-activated protein kinases on the body surface--a function for p38 delta. J Invest Dermatol, 120(5),823-8.

9. Fearns,C., Kline,L., Gram,H., Di Padova,F., Zurini,M., Han,J., Ulevitch,RJ., 2000. Coordinate activation of endogenous p38alpha, beta, gamma, and delta by inflammatory stimuli. Leukoc Biol, 67(5),705-11.

10. Fujii,R., Yamashita,S., Hibi,M., Hirano,T.,2000. Asymmetric p38 activation in zebrafish: its possible role in symmetric and synchronous cleavage. J Cell Biol. 150(6),1335-48.

11. Holloway, B.A., Gomez de la Torre Canny, S., Ye, Y., Slusarski, D.C., Freisinger, C.M., Dosch, R., Chou, M.M., Wagner, D.S., Mullins, M.C.,2009. A novel role for MAPKAPK2 in morphogenesis during zebrafish development.PLoS Genet. 5(3),e1000413.

12. Johnson,G.L., Lapadat,R., 2002. Mitogen-Activated Protein Kinase Pathways Mediated by Erk, Jnk, and P38 Protein Kinases. Science, 298,1911-12.

13. Kim,E.K., Choi,E.J., 2010. Pathological Roles of Mapk Signaling Pathways in Human Diseases. Biochim Biophys Acta, 1802,396-405.

14. Kalender,A., Selvaraj,A., Thomas,G., 2011. A matter of energy stress: p38β meets mTORC1. Cell Res, 21(6),859-61.

15. Krens,S.F., He,S., Spaink,H.P., Snaar-Jagalska,B.E., 2006a. Characterization and Expression Patterns of the Mapk Family in Zebrafish. Gene Expr Patterns, 6,1019-26.

16. Krens,S.F., Spaink,H.P., Snaar-Jagalska, B.E.,2006b. Functions of the MAPK family in vertebrate-development.FEBS Lett. 580(21),4984-90.

17. Kimmel,C.B., Ballard,W.W., Kimmel,S.R., Ullmann,B., Schilling,T.F., 1995. Stages of Embryonic Development of the Zebrafish. Dev Dyn, 203, 253-310.

18. Lee,J.C., Laydon,J.T., McDonnell,P.C., Gallagher,T.F., Kumar,S., Green,D., McNulty,D., Blumenthal,M.J., Heys,J.R., LandvatterS.W., 1994. A Protein Kinase Involved in the Regulation of Inflammatory Cytokine Biosynthesis. Nature, 372,739-46.

19. Munoz,L., Ammit,A.J., 2010. Targeting p38 MAPK pathway for the treatment of Alzheimer's disease. Neuropharmacology, 58(3),561-8.

20. Mudgett,J.S., Ding,J.,Guh-Siesel,L., Chartrain,N.A.,Yang,L., Gopal,S., Shen,M.M., 2000. Essential Role for P38alpha Mitogen-Activated Protein Kinase in Placental Angiogenesis. Proc Natl Acad Sci U S A, 97,10454-9.

21. Nebreda,A.R., Porras,A., 2000. P38 Map Kinases: Beyond the Stress Response. Trends Biochem Sci, 25,257-60.

22. Pramanik,R., Qi,X., Borowicz,S., Choubey,D., Schultz,R.M., Han,J., Chen.G., 2003. P38 Isoforms Have Opposite Effects on Ap-1-Dependent Transcription through Regulation of C-Jun. The Determinant Roles of the Isoforms in the P38 Mapk Signal Specificity. J Biol Chem, 278,4831-9.

23. Patel,S.B., Cameron,P.M., O'Keefe,S.J., Frantz-Wattley,B., Thompson,J., O'Neill,E.A., Tennis,T., Liu,L., Becker,J.W., Scapin,G., 2009. The three-dimensional structure of MAP kinase p38beta: different features of the ATP-binding site in p38beta compared with p38alpha. Acta Crystallogr D Biol Crystallogr, 65(Pt 8),777-85.

24. Roux,P.P., Blenis,J., 2004. Erk and P38 Mapk-Activated Protein Kinases: A Family of Protein Kinases with Diverse Biological Functions. Microbiol Mol Biol Rev, 68,320-44.

25. Schindler,E.M., Hindes,A., Gribben,E.L., Burns,C.J., Yin,Y., Lin,M.H., Owen,R.J., Longmore,G.D., Kissling,G.E., Arthur,J.S., Efimova,T., 2009. p38delta Mitogen-activated protein kinase is essential for skin tumor development in mice. Cancer Res, 69(11),4648-55.

26. Thornton,T.M., Rincon,M., 2009. Non-classical p38 map kinase functions: cell cycle checkpoints and survival. Int J Biol Sci, 5(1),44-51.

27. Tanoue,T., Maeda,R., Adachi,M., Nishida,E.,2001. Identification of a docking groove on ERK and p38 MAP kinases that regulates the specificity of docking interactions. EMBO J, 20(3),466-79.

28. Wang,X., Wu,H., Miller,AH., 2004. Interleukin 1alpha (IL-1alpha) induced activation of p38 mitogen-activated protein kinase inhibits glucocorticoid receptor function. Mol Psychiatry, 9(1),65-75.

29. Wilson,K.P., Fitzgibbon,M.J., Caron,P.R., Griffith,J.P., Chen,W., McCaffrey,P.G., Chambers,S.P., Su,M.S., 1996. Crystal structure of p38 mitogen-activated protein kinase. J Biol Chem, 271(44),27696-700.

30. Westerfield,M., 2000. The Zebrafish Book: A Guide for the Laboratory Use of Zebrafish (Brachydanio Rerio). ed. by 4th. 1 vols (Eugene, OR: Univ. of Oregon Press).

31. Zarubin,T., Han,J., 2005. Activation and Signaling of the P38 Map Kinase Pathway. Cell Res, 15,11-8.

32. Zhou, X., Ferraris,J.D., Dmitrieva,N.I., Liu,Y., Burg,M.B., 2008. MKP-1 inhibits high NaCl-induced activation of p38 but does not inhibit the activation of TonEBP/OREBP: opposite roles of p38alpha and p38delta. Proc Natl Acad Sci U S A, 105(14),5620-5.

33. Zhang,Y.Y., Wu,J.W., Wang,Z.X., 2011. Mitogen-activated protein kinase (MAPK) phosphatase 3-mediated cross-talk between MAPKs ERK2 and p38alpha J Biol Chem, 286(18),16150-62.

34. Zhou,H., Zheng,M., Chen,J., Xie,C., Kolatkar,A.R., Zarubin,T., Ye,Z., Akella,R., Lin,S., Goldsmith,E.J., Han,J., 2006. Determinants that control the specific interactions between TAB1 and p38alpha. Mol Cell Biol, 26(10), 3824-34.

CHAPTER IV

The P38αA and Erk2 are essential for epiboly initiation by regulating common and separate developmental genetic programs

H. Rian, S.F.G Krens, E Salas-Vidal, H.P Spaink and B. E Snaar-Jagalska

Abstract

The P38α and Erk2 MAPKs play an essential role in morphogenetic movements during zebrafish gastrulation, in particular during epiboly. Using time-lapse imaging we demonstrated that lethality of P38α and Erk2 morphants is correlated with defective cell migration of the blastomere margin, as a result dissociated blasoderm cells. Since knock-down of either of the two MAPKs causes similar severe morphological defects, or even arresting embryonic development before the onset of epiboly, we set out to investigate their putative functional redundancy in epiboly initiation. To identify distinct and overlapping roles for Erk2 and P38 at this early stage of developmental morhogenesis, we performed transcriptome analysis of high/oblong stage P38α and Erk2 knockdown embryos.

We found common genes affected by both P38α and Erk2 knockdown and genes specifically affected by depletion of either P38α or Erk2. The common gene set and the Erk2 knock down specific gene set include transcripts regulating cell migration and adhesion properties associated with epiboly. Epithelial cell adhesion molecule (Epcam) and bloody fingers (Blf) expression is decreased by either P38α or Erk2 morpholino treatment. The Aryl hydrocarbon receptor nuclear translocator 2 (Arnt2) is specifically up-regulated in P38α morphants. Apelin receptor b (Aplnrb), c-x-c chemokine receptor 4 (Cxcr4), snail2 (Snai2), ras homolog gene family member Ab (Rhoab) and fyn oncogene related to src (Fyna) are down-regulated by Erk2 morpholino while interferon regulatory factor 6 (Irf6) is up-regulated.

Interestingly, gene ontology analysis revealed a large pool of ribosomal proteins with low expression levels and several histone protein coding transcripts where significantly up-regulated by the P38α morpholino. Imbalanced histone and ribosomal protein expression levels are associated with loss of nuclear integrity. We found also that P38α morphants fail to induce expression of P53, a key cell cycle checkpoint regulator, upon DNA damage induced by camptothecin treatment. These results show that the function of P38α in stress signalling is already put to use during initial stages of embryogenesis. Additionally, we conclude that both P38α and ERK2 regulate epiboly initiation by controlling common and distinct genetic mechanisms.

Introduction

Mitogen Activated Protein Kinase (MAPK) signalling is involved in divers cellular processes such as cell motility, cell cycle progression, survival, protein biogenesis, and differentiation. MAPK signalling cascades consist of an upstream MAPKKK (MEKK) which activates a MAPKK(MEK) to finally activate a MAPK by phosphorylation. There are 14 MAPK proteins, which are subdivided according to their dual-phosphorylation (activation) motif (T-X-Y) into the extracellular signal-regulated kinases (Erk1,2,3,4,5,6,7), c-Jun amino (N)-terminal kinases (JNK1/2/3) and P38 isoforms (α,β,γ, and δ) [1-6].

Erk2, Erk5, P38α and Jnk1/2 MAPK family members appear to be essential for vertebrate development as knock-out mice die within the first 12 days of development [7-9]. In zebrafish all 14 MAPK are conserved and previous research accomplishments have gained insight into the functions of ERK2, P38α and JNK1/2 in the first stages of development.

P38α is asymmetrically activated on one side of the blastodisc and regulates the first cell divisions during the early cleavage period. The side of P38α activity overlaps with the expressed dorsal-specific zygotic gene dharma/bozozok however dorsal-ventral axis formation is unaffected after injection with dominant negative P38α RNA suggesting that P38α is dispensable for this process [13]. In contrast, a clear function of JNK in dorsal-ventral patterning has been demonstrated with a MO knock-down approach which leads to ventralized embryos. JNK and MEKK4 are part of a dorsalization pathway that is induced by Axin/JNK and inhibited by Aida [14]. Furthermore, ERK2 and P38α are both found to be involved in epiboly movements during gastrulation: the spreading of embryonic cells of the blastoderm over surface of the yolk until fully covered and occurs from 4.3 hpf (dome stage) to 10 hpf (tail bud). Prior to epiboly, the blastula surface cells differentiates into the enveloping layer (EVL), of which the forerunner cells delaminate (later forming the Kupples vesicles) and the yolk syncycial layer (YSL), both are the essential mediators of epiboly [15].

Activated forms of ERK2 and P38α are detected at the margin of the blastoderm throughout all stages of epiboly. When the blastoderm cells reach the equator and cover the yolk cell by half, the cells at the margin are induced into mesendoderm cell fates by a combination of Nodal and Fgf signaling. [13,16]. Fgf morphogens specificallyare shown to activate downstream Erk1/2 signalling and are involved in the specification and maintenance of mesoderm cell faith by regulation of T box transcription factors [17-19]. Erk2 levels causes defects in convergent-extension movements, and a strong knock down of Erk2 leads to a full developmental arrest in blastula stage embryos [16]. In addition, the Erk2-MAPK pathway functions downstream of Fgf [16] and is a modulator in mesendoderm formation,, which is

72

apparent from reduced levels of expression of the mesodermal markers No tail, Tbx6 and Tbx16 in ERK2 depleted embryos [20]. The first evidence for a role of P38α mediated signaling in epiboly came from a large genetic screen for maternal-effect mutants that display morphological defects at or after mid blastula transition (MBT) [21,22]. In this screen, the *betty boop* mutant (bbp) was identified as *bbp* mutant show strong epiboly defects characterized by a dramatic constriction of the blastoderm margin resulting in a yolk burst. The loss of function mutation in bbp was mapped in the Mitogen Activated Protein Kinase Activated Protein Kinase 2 (Mapkapk2) gene, a specific substrate of P38 MAPKs. The same phenotype was observed by injection of dominant negative P38α RNA suggesting that this MAPK isoform plays a specific non-redundant role in regulating gastrulation cell movements [23].

Since both P38α and Erk2 knockdown results in severe morphological defects the question remains what downstream target genes are regulated by the two MAPK that are essential for early embryogenesis. Erk2 and P38α were the first identified MAPKs, initially discovered as proteins which were rapidly phosphorylated after mitogen stimulation and osmotic shock respectively. Multiple cytosolic and nuclear substrates have been identified so far which was of great value for the molecular characterization of MAPK associated cellular events [24-29]. Although both MAPK are found essential for vertebrate development the molecular mechanisms are less well documented. MAPK are known to translocate to the nucleus and influence gene expression, after extracellular stimulation. In this study, we show that depletion of P38α zebrafish embryos fail to initiate epiboly, and thus phenocopies embryos that have been depleted from ERK2 by morpholino knockdown. We compare transcriptomes of these P38α and Erk knock down embryos at high/oblong stage, prior to epiboly initiation, to identify specific and common downstream target genes that are necessary for epiboly progression.

Material & Methods

Morpholino injections
ABXTL embryos were injected between 0- and 1- cell stage with either P38αA translational blocking morpholino (ATG) 5'GTGGGTCTTTCTTTCTGCGACATGC3', P38αA splice blocking morpholino (splice)5'AGCTGCATACACGAAATATGAAAGT3', ERK2 translational blocking morpholino 5'CACCCAAAAGCACCAGGAAAAGCTC3' or a standard control morpholino 5'CCTCTTACCTCAGTTACAATTTATA3'(Genetools). Morpholino's where dissolved in 1XDanieau's buffer [58mM NaCl, 0.7mM KCl, 0.4mM MgSO4, 0.6mM Ca(NO3)2, 5.0mM HEPES pH7.6] containing 1% phenol red solution.
Time Lapse Imaging

For a time course experiment of 16:40 hours embryos were dechorionated, placed on an agar coated <u>willco</u> dish and subsequently embedded in 1% low melting agarose and covered with eggwater. From 256 cell stage onwards, embryos where repeatedly imaged every 5 minutes with 10X magnification of the DIC microscope in a room temperature of 24°C. 200 pictures were processed in a movie of 28s with ImageJ software.

<u>Protein isolation & western blotting</u>
Embryos were dechorionated in 1X pronase solution (2 mg/ml Roche Applied Science) for 7 minutes and washed several times in 1X Danieau buffer. Total protein was isolated from batch embryos first by deyolking in Ca^{2+}/Mg^{2+} free solution. Cells where collected at 500 RCF and washed twice, once in Ca^{2+}/Mg^{2+} free solution and once in PBS, before final lysis (30min incubation and vortexing in lysis buffer 1M Tris-Hcl pH7,4, 0,5M EDTA, 1 tablet protease inhibitor, 0,1M Na3VO4, 0,5M NaF).

For biochemical analysis, protein extract were diluted in SDS sample buffer red +DTT (cell signaling #7723), sonificated and heated for 10 min at 95°C. 1 µg of the proteins samples were separated in a SDS-polyacrylamide gel electrophoresis (PAGE) and transferred to nitrocellulose membrane (Schleicher & Schuell, Den Bosch, The Netherlands) by western blotting. The membranes were blocked in 5% w/v non-fat dry milk in Tris-Buffered Saline-Tween 20 (TBST). The blots were incubated with of P44/42 MAPK Kinase antibody (Cell Signaling #9102 1:1000), P38 antibody (Santa Cruz Biotechnology C-20 1:1000), pan-actin (Cell Signaling #4968 1:1000) or P53 antibody (mouse antibody, kind gift from Alyson W. MacInnes 1:1) in TBST with 3% BSA (Sigma) overnight at 4°C. Signal was detected using a 1:5000 dilution of horseradish peroxidase (HRP)-conjugated anti-rabbit or anti-mouse antibodies and the enhanced chemiluminescence method (Amersham).

<u>RNA isolation & transcriptome analysis</u>
Morpholino injected embryos of high oblong stage where snap-freezed in liquid nitrogen (without dechorionation) and stored in -80°C until all samples were collected. For RNA isolation freezed embryos where homogenized with pestle or with a bullet blender after addition of 300µl Qiazol (Qiagen). 1/5 of chloroform was added to the homogenate, mixed and transferred to phase-lock gel heavy (5-Prime) containing Eppendorf tubes of 1.5ml. The RNA liquid phase (top transparent solution) was separated from the rest of the sample by 15min at 12000 g and purified with rneasy MinElute cleanup kit (Qiagen) according to manufacture protocol. RNA quality was checked with the Agilent 2100 bioanalyzer using eukaryote total RNA pico series II protocol. RNA samples were delivered to the microarray department University Amsterdam www.microarray.nl/ who performed a

two-color microarray-based gene expression analysis with treatment (P38αMO ATG or ERK2MO ATG injected embryos) labelled Cy3 hybridized against control (stCTRMO injected embryos) labelled Cy5 on an Agilent 180k chip. For analysis, data files (MAGE and JPEG files of each hybridized chip position) were imported into Rosetta Resolver 7.2 (Rosetta Inpharmatics LLC). Two biological replicate intensity profiles were combined using the default intensity experiment builder which is implemented in the Rosetta Resolver system. P38α morpholino against standard control morpholino (252823310001_3 and 252823310002_3), ERK2 morpholino against standard control morpholino (252823310001_4 and 252823310002_4)

Q-PCR
50ng of total RNA was used for a 20µl cDNA synthesis reaction with the iScript cDNA synthesis kit (Biorad). Q-PCR reactions were performed in a 25 µl volume comprised of 1 µl cDNA, 12.5 µl of 2× iQ SYBR Green Supermix (Bio-Rad) and 10 pmol of each primer.

Gene	Reference	Forward	Referse
aplnrb	ENSDART00000129643	TCTCAGGAGTTCTTGCTGCAC	CTCACCACCAGGTTGAAGTCC
cxcr4	ENSDART00000080350	TGGCTTATTACGAACACATCGTC	TGACTGACCTCCACATCACAC
dlc	ENSDART00000018514	AACCCATCTGCTTGTCTGGC	GCGTGCACTCATCACAGAGG
nav3	ENSDART00000005847	GATTGAGAATGTGGAGTGCTGTC	TCCCATTACACACCTCTTCAGC
rpsa	ENSDART00000135945	CATTGAGGCTCCTGGCAAG	GAGCAGCTGACCAATCCTCAG
map7d1	ENSDART00000090587	AAGGAGCGGTATGAATCTGCC	CAAACTGCGGGTCTCTCTGC
admm1b	ENSDART00000081427	TGTCGCAAAGTTAACGAGTACC	AGCTGCATGAGTTGATTGTG
sall1a	ENSDART00000111842	CTCTGATGACAACATGGAAGG	TGTCTTGAGATGCATCAACTG
krt18	ENSDART00000020750	AGCTGCGCAAGAAGATCTTTG	TCTGAAGTCATCAGCTGCCAG
zgc:136359	ENSDART00000077341	AGTTGATGGATGAGATCTGGC	CAGTAGTGGCAGCTCAATCAG
rps8a	ENSDART00000078412	CAGCAAACACCAAGATTGG	ATGAGAAGTTTCCCACATCG
rpl13	ENSDART00000047391	AGTACTGAGGAGGAGCTCAAG	GCCTTCTCTTTCTTGTGCAC
rpl19	ENSDART00000018975	ACATGTACCACAGCCTGTATCTG	GATCAGCCAAGAGCTTCTTG
rpl35	ENSDART00000009241	ACAGTCATCAACCAGACACAG	AGGCTTGTACTTCTTACCCTTG

Cycling parameters were 94°C for 3 min to activate the polymerase, followed by 40 cycles of 94°C for 15 sec and 59°C for 45 sec. Fluorescence measurements were taken at the end of each cycle. Melting curve analysis was performed to verify that no primer dimers were amplified. All reactions were done in duplicate or triplicate. Data were normalized using the Genex macro provided by Bio-Rad.

Camptothecin treatment
Embryos were injected with, pronase dechorionated and washed with 1X Danieau buffer within 1hpf. At 8 cell stage (+/- 1hpf) embryos were transferred to agarose coated plates and treated with either 500nM CPT or DMSO for 8hours at 31°C. After that total protein was isolated as described above.
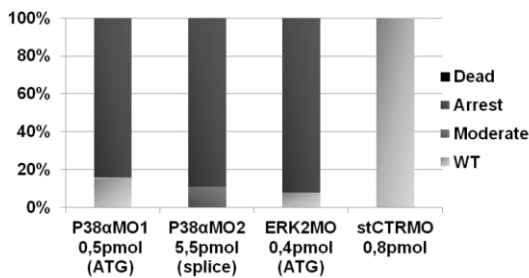
Results

Knock down of P38α causes blastula stage arrest and prevents epiboly initiation.

To study the function of P38αA in the first stages of zebrafish development the expression was blocked, by injection of a translation blocking morpholino (MO1) in zygote stage embryos. Development of (injected) embryos was followed with time lapse imaging starting from 256cell stage **(Fig1a)**. At 6hpf uninjected or control morpholino (stCTRMO) injected embryos progressed normally to shield stage. However, more than 80% of P38αA knockdown embryos arrested at blastula stage, and did not undergo epiboly resulting in embryonic lethality a few hours later. This phenotype was confirmed by a splice blocking morpholino (MO2) against P38αA **(Fig1b)**. Depletion of P38αA appeared to be more efficient with the translational blocking morpholino when compared to the P38αA splice blocking morpholino, an effect that is most likely due to the abundant maternally contributed spliced P38αA mRNA, that has been demonstrated previously [34]. Since knock-down of Erk2 also resulted in epiboly arrest we questioned whether the phenotypes of both morphants were identical and performed the time course experiment as well with Erk2 morphants. In uninjected wild type embryos epiboly started at 06:10 hpf (24°C) and the embryos remained viable and developed further until the time lapse measurement was terminated at 16:40 hpf. Embryos injected with P38α translational blocking morpholino (MO1) developed until 8:50 hpf when the animal pole started to show excessive movements in contrast to the not moving margin and eventually resulted in the burst of the yolk and death of the embryo. Two different phenotypes were distinguished among the Erk2 epiboly arrested morphants. The first phenotype was almost similar to the P38α morphants and embryos died by a yolk burst due to failed migration of marginal cells **(Fig1a ERK2MO upper panel)**. However, the deep cells of the animal pole in the Erk2 morphant curled through excessive movements and partly dissociated from the enveloping layer (EVL). In addition, the animal pole of Erk2 morphant took on a dome shape which indicates epiboly initiation. The second Erk2 morphant phenotype was much more severe since embryos died at 7:00 hpf because the cells of the animal pole started to dissociate **(Fig1a ERK2MO lower)**. Western blotting with anti-Erk1/2 and anti-P38 antibodies confirmed that P38α morpholino1 injected embryos expressed lower levels of P38 protein compared to stCTR morpholino. Erk2 morphants contained reduced Erk1/2 levels, however they also contained reduced P38 levels, possibly explaining the observed more severe phenotype in ERK2 depleted embryos **(Fig1c)**.
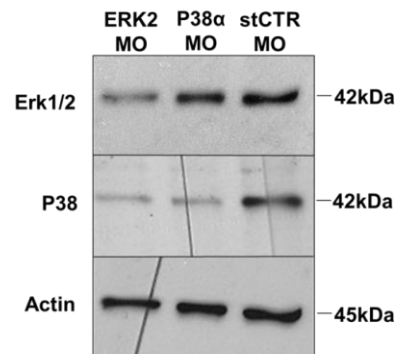
Fig1: Time lapse imaging of P38α and ERK2 morphants. P38α morphants, Erk2 morphants and WT embryos are imaged every 5 minutes starting at 256 cell stage (3hpf). Time lapse was performed with DIC microscopy using Zeiss EC Plan-Neofluar 10×/0.30 objective and extended for 16 hours and 40 minutes. **A** Fragment images of time lapse showing epiboly stage starting at 06:10hpf in WT embryos but not morpholino injected embryos. ERK2MO embryos died by a yolk burst (**upper panel**) or dissociation of the blastoderm (**lower panel**). **B** a minimum of 30 embryos for each condition was used for morpholino injections at 1-cell stage. Phenotypes were scored at 6hpf were WT embryos are developed to shield stage. Injections are performed with an ATG or a splice blocking morpholino against P38α, an Erk2 morpholino and the standard control morpholino was used as a control. **C** Western blotting with anti-Erk2 and anti-P38α antibodies on protein samples from P38αMO (ATG) and ERK2MO injected embryos prepared at high/oblong stage.

To compare the effects of Erk2 and P38α knock-down in the first hours of zebrafish development, transcriptome analysis was performed of (injected) embryos from high/oblong stage using a custom designed 180k Agilent chip. With a threshold of a twofold change relative to control morpholino (stCTR) injected embryos, a total of 454 up-regulated and 455 down-regulated genes were selected as a result of P38α knock down, whereas Erk2 morphants displayed 964 up-regulated and 418 down-regulated genes (Fig2a). The Erk2 morpholino and P38α morpholino common gene pool of 229 genes shows almost equal number of genes up-regulated (114) versus down-regulated (115). Finally, we selected 1153 and 680 genes that were specifically affected by either Erk2 or P38α knock down, respectively. The P38α morpholino specific target has an equal number of up-regulated (340) and down-regulated (340) genes. However, from the Erk2 morpholino specific set of 1153 genes the largest pool of 850 genes were up-regulated and the rest of 340 genes were down-regulated. The percentage gene frequency of different fold change
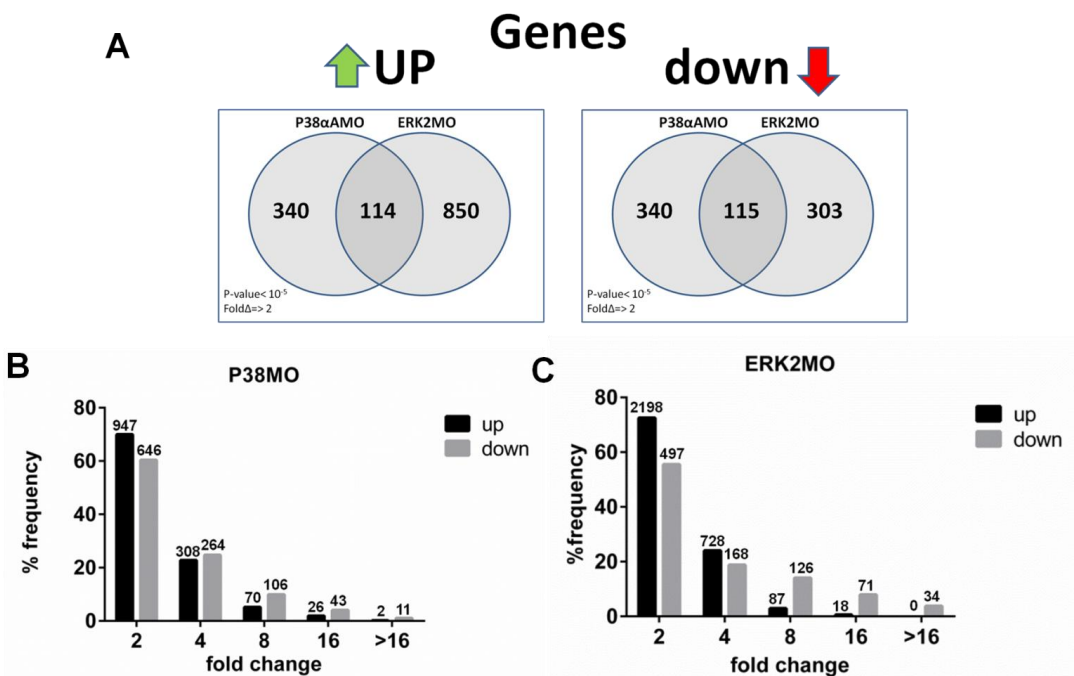
Fig2: Erk2 and P38α knock-down transcriptome analysis at high/oblong stage. A Venn diagrams of the number of genes up- or down- regulated by Erk2 and P38α translational blocking morpholinos with absolute fold change of 2 and p-value<10^{-5}. **B** Histogram of % frequency P38MO effected genes (y-axis) within a fold-change margin (x-axis) and p-value<10^{-5}. Numbers on bars represent absolute numbers of genes. Transcriptome analysis results of two independent experiments each with a pool of five embryos. **C** Histogram of ERK2MO transcriptome.

thresholds for both Erk2 and P38α knock-down were plotted. For both Erk2 and P38α knock-down significant sets of gene targets could be distinguished with fold change thresholds as high as 8 (Fig2 b and c). Interestingly, higher threshold settings resulted in more down-regulated gene expression levels than up-regulated for both Erk2 and P38α knock-down.

To address the biological processes represented by the Erk2 and P38α knockdown transcriptomes, gene ontology enrichment analysis was performed with total up-regulated and down-regulated gene sets (Fig3). 258 out of 455 P38α down-regulated genes were assigned to the gene ontology classification (GO). For Erk2 knock-down 218 out of 418 could be analyzed with GO enrichment analysis. Compared to the 180k Agilent chip both Erk2 and P38α down-regulated transcriptomes have overrepresentation of genes involved in processes of early development such as mesoderm/ectoderm development and pattern/system specification. Embryonic patterning is regulated by morphogens such as Fgf, Wnt and the Tgf-β family members Nodal and Bmp. We found various morphogen pathway components to be affected by Erk2 or P38α knock-down (**Supplemental tables1-4**). Germ line specification is dependent on positional cues, provided by
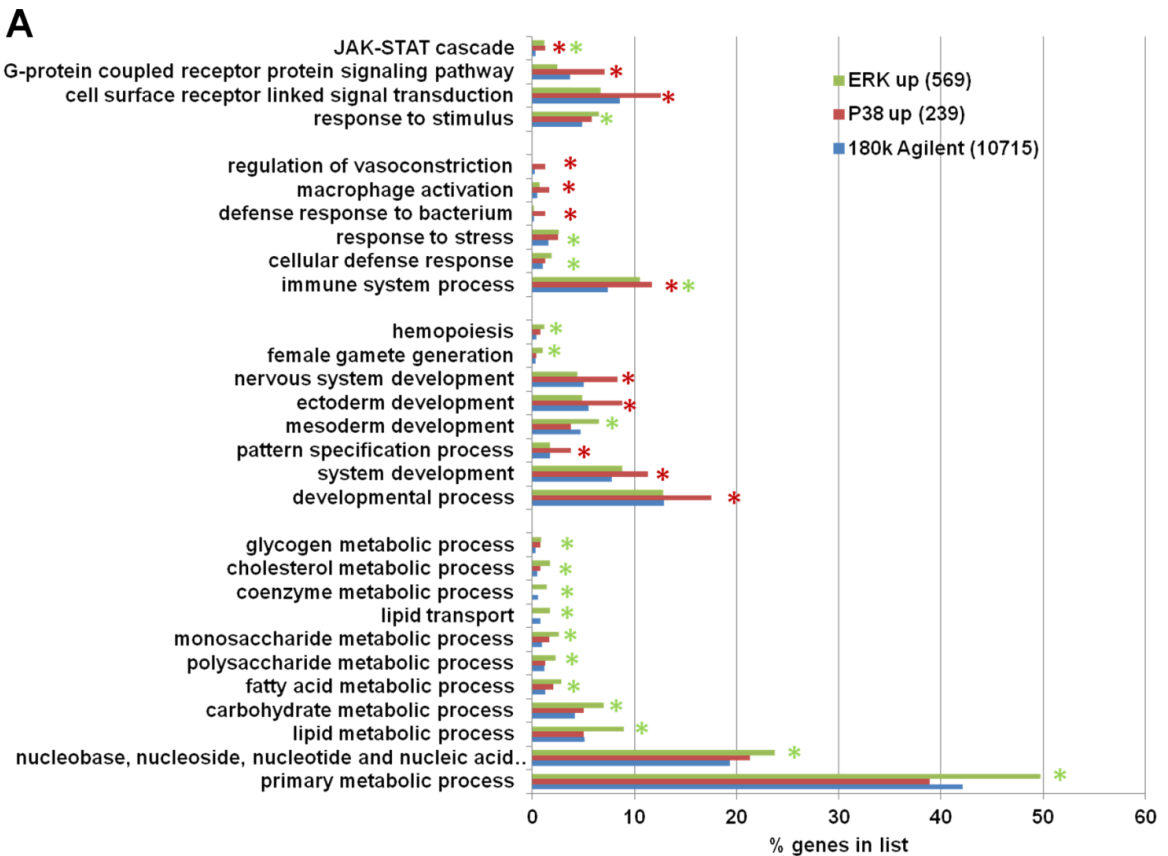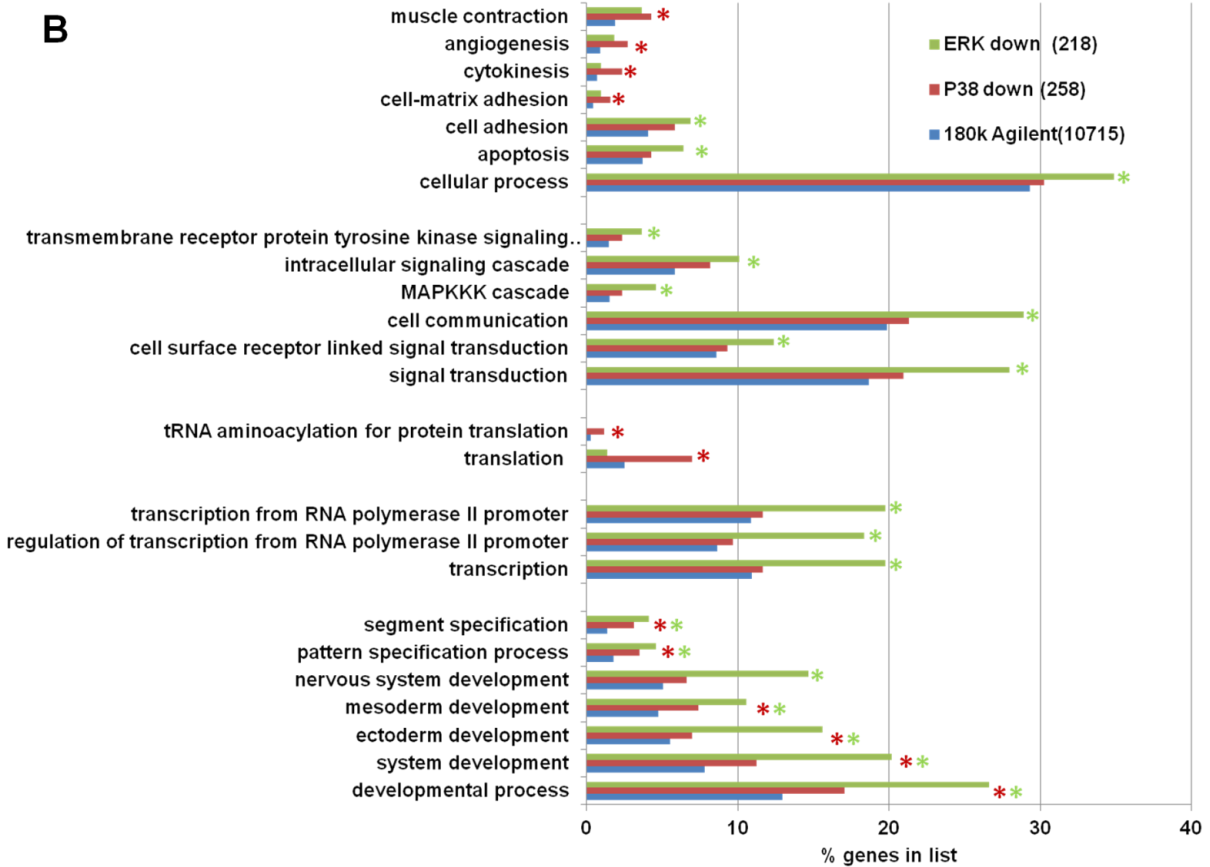
Fig3: Biological processes enriched in Erk2 and P38α knock-down transcriptome data.
A Bar graph of significantly enriched PANTHER™ GO slim biological processes compared to 180k Agilent array using upregulated gene sets of P38α morphants in red (239/454) and Erk2 morphants in green (569/964). **B** Bar graph of significantly enriched biological processes using downregulated gene sets of P38α morphants in red (258 of 455) and Erk2 morphants in green (218 of 418). * are significant overrepresented in Erk2 morphants and red * significantly overrepresented in P38α morphants. Comparison is made of %genes of the GO category in gene list of experimental condition compared to the %genes of the category in the 180k Agilent chip. Gene ontology enrichment analysis was performed with Panther software www.pantherdb.org using statistical overrepresentation function without Bonferroni correction. Only significant overrepresented biological processes in Erk2 or P38α morphant are shown with p-value ≤ 0.05 calculated with binominal statistics.

morphogens, and the same pathways are involved in regulating cell migration and adhesion properties of blastoderm cells during epiboly. We found also genes directly involved in cell adhesion to be overrepresented in both Erk2 and P38α down-regulated gene pools. Different from Erk2 morpholino, the P38αMO1 down-regulated gene pool contained overrepresentation of genes involved in protein

translation, cytokinesis, angiogenesis and muscle contraction. Erk2 knockdown resulted in the down-regulation of a large set of genes involved in transcription, predominantly transcription factors, and cell signaling cascades including the MAPK pathway.

239 (of 340) P38α morpholino1 up-regulated and 569 (of 850) Erk2 morpholino up-regulated genes were found by GO classification and enrichment analysis showed again overrepresentation of developmental genes (Fig3). Many P38α morpholino up-regulated genes seem to be involved in pattern specification and system development while the genes assigned to the mesoderm differentiation ontology were up-regulated (as well as down-regulated) by Erk2 morpholino.

Identification of common and P38α, Erk2 specific gene targets involved in cell migration and adhesion

Combined Transcriptome profiling and gene ontology analysis of epiboly arrested P38α and Erk2 knock-down embryos revealed drastic deregulation of genes regulating cell migration and adhesion underlying **(supplemental Table 5)**. Interestingly, also a number tissue specific genes expressed in the EVL, YSL or margin were down-

regulated either in both Erk2 and P38α morphants or specifically in Erk2 morphants. Erk2 and P38α morpholinos both down-regulated keratin 4 (Krt4), bloody fingers (Blf), epithelial cell adhesion molecule (Epcam), neuron navigator 3 (Nav3), and up-regulated echinoderm microtubule associated protein like 3 (Eml3) and junction plakoglobin (Jup). Epcam, and Blf are known regulators of epiboly cell movements in zebrafish [35,36]. Transcriptome data suggested that keratin 18 is specifically down-regulated by Erk2 morpholino, however keratin 4 as well as keratin 8 appeared to be dramatically down-regulated by Erk2 as well as P38α morpholino when validated with Q-pcr **(Fig4a)**. Down-regulation of Nav3, zgc136359 and Ctsh by P38α and Erk2 knock-down was also confirmed with quantitative rtPCR. In addition transcriptome data suggest that the aryl hydrocarbon receptor nuclear translocator 2 (Arnt2) is specifically up-regulated in P38α morphants which is known to regulate cell-cell adhesion during gastrulation [37]. Six previously identified epiboly critical regulators were present in the Erk2 morpholino transcriptome including apelin receptor b (Aplnrb), c-x-c chemokine receptor 4 (Cxcr4), snail2 (Snai2), ras homolog gene family member ab (Rhoab) and fyn oncogene related to src (Fyna) (down-regulated) and interferon regulatory factor 6 (Irf6) (up-regulated) [38-43]. Dlc, Cxcr4a, Aplnrb and Rpsa were indeed specifically down-regulated by Erk2 morpholino as validated with Q-pcr **(Fig4b).** Down-regulation of two P38α morphoplino specific cell adhesion regulating genes Map7d1/Zgc;172238 and Adrm1b were validated which have a yet unknown function during development **(Fig4c)**.
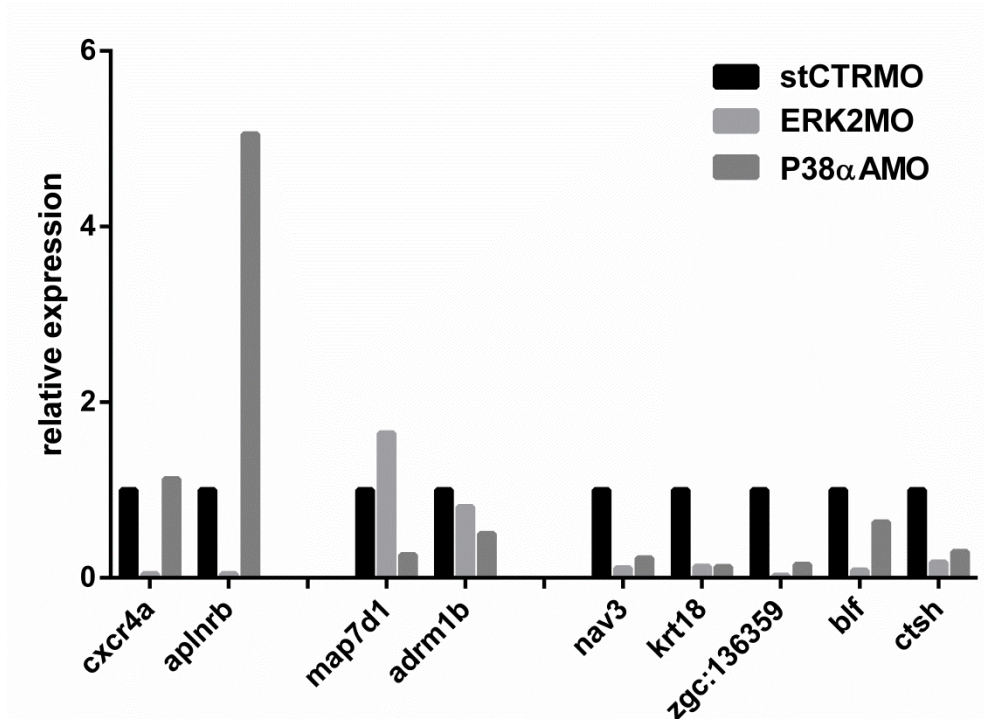
Fig4: Quantitative PCR of Erk2MO downregulated genes, P38αMO downregulated genes and common regulated genes. Graph depicts fold changes relative to stCTRMO. Results are confirmed with a second independent experiment**.**

<u>P38α induces expression of ribosomal proteins, inhibits expression of histone proteins and maintains P53 protein levels after DNA damage in the gastrulating embryo.</u>

The transcriptome data of P38α knock down embryos from high/oblong stage includes a significant number of down-regulated genes with a function in biological protein synthesis. The majority of the genes listed in supplemental **Table 6** are ribosomal proteins of which Rps8, Rpl13, Rpl19 and Rpl35 are known to have a function in nuclear stress signaling when not assembled into the ribosome [44,45]. Ribosomal proteins maintain cellular homeostasis most likely by inducing levels of P53 through binding to the P53-inhibitor MDM2 during stress. In zebrafish, Rps8, Rpl13, Rpl19 or Rpl35 recessive mutations are associated with growth impairment and tumor predisposition in zebrafish [46,47]. We identified several cancer associated ribosomal proteins downstream of P38α with transcriptome analysis followed by Q-pcr of morpholino knock-down embryos (**Fig5a**). In addition, we found a significant pool of histone protein genes being highly up-regulated. For example histone 3.2 was 16 fold higher expressed in P38α knock-down embryos (**supplemental Table 7**). Histone protein levels are tightly controlled during cell

cycle progression since elevated histone protein levels is essential for proliferation however an excess can cause
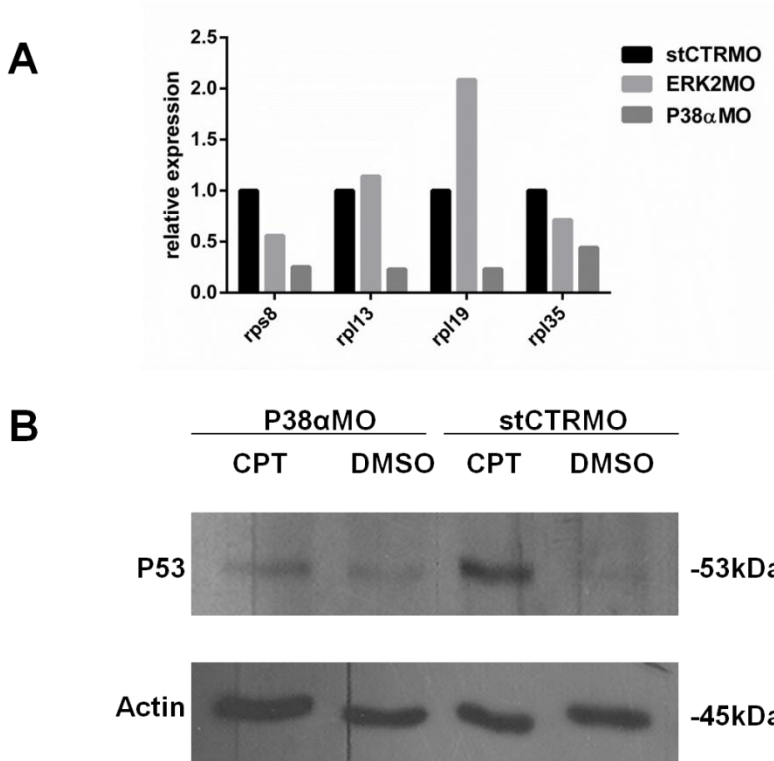
Fig5: P38α regulates expression of ribosomal proteins and maintains P53 protein levels after DNA damage during early zebrafish development. **A** Graph of quantitative real time PCR results with rps8, rpl13, rpl19 and rpl35 fold changes in Erk2 and P38 morphants compared to stCTR morpholino injected. Results are confirmed twice with independant biological experiments **B** Western blotting with ant-P53 and anti-actin antibody on protein samples from P38αMO1 or stCTRMO injected embryos treated for 7hours with either 500nM DMSO or Camptothecin.

genomic instability in the form of excessive chromosome loss, enhanced sensitivity to DNA damaging agents and cytotoxicity [48,49]. Furthermore, P38α and P53 are both stress induced proteins and functional in the same DNA-damage induced stress signaling pathway since P38α directly phosphorylates and activates P53 at Ser33 and Ser46 residues[50]. Interestingly in this report we were able to detect ribosomal protein down-regulation and histone protein up-regulation, stress associated cellular events, by knock-down of basal levels of P38α. Since we obtained these results from an early embryonic stage, were the presence of the P53 protein is questionable, we investigated the presence of P53 protein with western

blotting. We used an anti-P53 antibody in the gastrulating embryo with and without the DNA damage inducing agent camptothecin (CPT) (**Fig5b)**. P53 was indeed undetectable at 8 hpf after 7 hour treatment with DMSO, however, the level was induced by CPT in stCTRMO injected embryos. Importantly, P53 induction by CPT was reduced in P38α morphants suggesting the function of P38 in regulation of P53 protein stability during stress.

Discussion

The P38α and ERK2 MAPKs are crucial factors that regulate the first stages of vertebrate development. Knock down of either of the two MAPKs arrests embryonic development in zebrafish before the onset of epiboly. We performed transcriptome analysis of high/oblong stage P38α and ERK2 knockdown embryos to identify distinct and overlapping roles for Erk2 and P38α at this early stage of development.

Our results are in line of previous studies published by *Holloway et al.,* who discovered a role for P38α in regulation of the marginal actin ring constriction in embryos undergoing epiboly by injecting dominant negative P38α RNA [23]. Additionally, morpholino knockdown of P38α totally abolished initiation of epiboly in this study. Time-lapse imaging revealed that P38α morpholino inhibits migration of marginal cells of the blastula at a stage before 50% epiboly when the F-actin ring is normally established [51]. Previously we reported the indispensability of ERK2 for zebrafish epiboly. In this study, we elaborate on these findings by directly comparing the knock-down phenotypes of P38α and ERK2, using time-lapse imaging and transcriptome profiling. Live imaging showed that either Erk2 or P38α knock-down induced epiboly arrest due to failed migration of marginal cells. In contrast, the deep cells remained to increase in motility and protruding forces against EVL and margin resulting in lethality of embryo (see movie4 ERK2MO). The Erk2 morpholino is more potent to block epiboly, than the P38α morpholino, and injection can result in failure of EVL to maintain embryonic cell integrity and finally lead to total dissociation of the blastoderm. Therefore knock-down of either Erk2 or P38α results in failed epiboly initiation, however the phenotypes are not completely identical. In addition, western blot analysis showed lower level of Erk2 and P38α protein in Erk2 morpholino treated embryos what can account for more severe but not completely Erk2 specific phenotype of these morphants. However, it is also possible that ERK knock-down indirectly effects P38 levels.

Specific gene pools for Erk2 and P38α depleted embryos are found, which are at least three times larger than the common pool which is similarly affected by Erk2 and P38α knock-down. A number of genes that can be associated with cell migration are found in the common pool (**supplemental Table 5**) of which Blf and

84

Epcam are previously found to be essential for a proper progression of epiboly movements[35,36]. Keratin 18 is down-regulated specifically by Erk2 according to the transcriptome analysis, however with Q-pcr we found that the expression of this gene is also down-regulated by P38α morpholino, but less drastically. Keratin 4 and keratin 18 are intermediate filaments that are part of the cytoskeleton of the EVL [52]. Down-regulation of these EVL markers suggest that the EVL does not differentiate properly. As a consequence the blastoderm of Erk2 morphants dissociates, most likely through impaired cytoskeleton of the EVL and loss of cell adhesion. Within the Erk2 morpholino specific gene pool we found additional epiboly related genes such as Aplnrb, Cxcr4, Snail2, Rhoab, Fyna and Irf6. The p38α specific down-regulated gene set contains a pool of adhesion and cell migration functional genes, however only one that was previously found to be essential for epiboly. Arnt2 knock-down caused mild defects of the blastoderm during epiboly and we found it to be up-regulated in P38α morphants. Some P38α targets are conserved in mammals, also humans, of which the function is still largely unresolved. These targets such as si:dkey-30c15.12, a cadherin domain containing protein, and Map7d1, a microtubule association domain containing protein, are interesting candidates for further expression and functional studies in zebrafish. Functional studies of the adhesion regulating molecule 1 (Adrm1) have also not yet been performed in zebrafish. However *in vitro* studies have shown that adrm1 is a functional ubiquitin receptor of the proteasome complex, is inducible by interferon-γ and increases adhesion to endothelial cells when overexpressed in macrophages [53,54]. Therefore genes such as Adrm1 and Map7d1 can be studied further, with morpholino knock-down, to investigate involvement in epiboly cell movements. Theoretically it is possible that P38α exerts its function in zebrafish epiboly primarily by regulating cytosolic proteins rather than controlling gene expression. In smooth muscle and endothelial cells the P38 substrate Mapkapk2 regulates activity of heat shock protein 27 (Hsp27) an F-actin polymerization modulator [55,56].

Gene ontology analysis of P38α morpholino down-regulated gene set revealed specific enrichment of genes characterized with the GO-term 'protein translation'. The protein translation gene ontology category consists of genes predominantly coding for ribosomal proteins (RP). A possible link of P38α and RP gene expression can be found in P53 regulation during stress signaling. Both RP and P38α have a positive effect on P53 stability and are perhaps involved in a similar mechanism where stress induced P38α activity maintains RP excess [57]. RP are in excess when they exceed rRNA levels and cannot be assembled into the 40s or 60s ribosome subunits. Unbound RP have the capacity to bind Mdm2 which, in absence of stress, binds and targets P53 to the proteasome complex for degradation [44].

In line with this hypothesis, a second mechanism appeared from the transcriptome data involving suppression of histone proteins by P38α. This suggests that P38α

exerts its function in the cell cycle not only by controlling checkpoints, through P53 and RP, but also cell cycle progression by regulating expression of histone proteins. Interestingly, our transcriptome analysis reveals that the neuroepithelial cell transforming gene 1(net1) is 25 fold down-regulated in Erk2 morphants. Net1 binds RNA polymerase 1 directly and stimulates the synthesis of rRNA in yeast [58]. Therefore, Erk2 and P38α MAPK activities may form a mechanism to maintain cellular homeostasis by having opposing roles in controlling the ribosome assembly and this mechanism is established already in the first stages of development.

We have not detected P53 protein in DMSO treated stCTR morpholino injected embryos of 8hpf. Furthermore, P53 was drastically induced during initial stages of epiboly with the DNA damage, causing agent CPT in stCTR morpholino injected embryos but not in P38α morphants. These results suggest that P38α regulates P53 stability and stress associated ribosomal protein expression in the zebrafish embryo. Further study investigating the association between P38α activity, P53 stability, ribosomal protein expression and histone protein expression would be valuable to gain more understanding about the role of P38α in tumor formation.

Conclusion

Depletion of P38α prevents epiboly initiation and blocks further development of the embryo. With the help of transcriptome profiling, we found that the expression of multiple cell migration and adhesion functional genes to be disregulated, along with components of Nodal, Fgf, Wnt and Bmp morphogen pathways, which have a critical role ininterplay to regulate migratory properties of embryonic cells for developmental patterning. Many of these P38α target genes are also affected by Erk2 morpholino despite the fact that much larger gene sets do not overlap between the two conditions. Interestingly, P38α knock-down results in down-regulation of a large pool of ribosomal proteins while Erk2 Morpholino specifically down-regulates net1 a protein also involved in ribosome biogenesis. These results suggest that, in zebrafish, both ERK2 and P38α are crucial for epiboly initiation, but despite similar phenotypic outcomes have separate roles in transcriptional regulation. This is illustrated by the involvement of both ERK2 and p38 in maintenance of cellular homeostasis during early zebrafish development, however by playing seemingly opposing roles in ribosome biogenesis.

Acknowledgments:

86

Reference List

1. Cuadrado A, Nebreda AR: Mechanisms and functions of p38 MAPK signalling. *Biochemical Journal* 2010, 429:403-417.

2. Geest CR, Buitenhuis M, Groot Koerkamp MJ, Holstege FC, Vellenga E, Coffer PJ: Tight control of MEK-ERK activation is essential in regulating proliferation, survival, and cytokine production of CD34+-derived neutrophil progenitors. *Blood* 2009, 114:3402-3412.

3. Plotnikov A, Zehorai E, Procaccia S, Seger R: The MAPK cascades: Signaling components, nuclear roles and mechanisms of nuclear translocation. *Biochimica et Biophysica Acta (BBA) - Molecular Cell Research* 2011, 1813:1619-1633.

4. Roux PP, Blenis J: ERK and p38 MAPK-activated protein kinases: a family of protein kinases with diverse biological functions. *Microbiol Mol Biol Rev* 2004, 68:320-344.

5. Zhan Y, Kim S, Izumi Y, Izumiya Y, Nakao T, Miyazaki H, Iwao H: Role of JNK, p38, and ERK in platelet-derived growth factor-induced vascular proliferation, migration, and gene expression. *Arterioscler Thromb Vasc Biol* 2003, 23:795-801.

6. Zhang W, Liu HT: MAPK signal pathways in the regulation of cell proliferation in mammalian cells. *Cell Res* 2002, 12:9-18.

7. Krens SF, Spaink HP, Snaar-Jagalska BE: Functions of the MAPK family in vertebrate-development. *FEBS Lett* 2006, 580:4984-4990.

8. Adams RH, Porras A, Alonso G, Jones M, Vintersten K, Panelli S, Valladares A, Perez L, Klein R, Nebreda AR: Essential role of p38alpha MAP kinase in placental but not embryonic cardiovascular development. *Mol Cell* 2000, 6:109-116.

9. Aouadi M, Binetruy B, Caron L, Le Marchand-Brustel Y, Bost F: Role of MAPKs in development and differentiation: lessons from knockout mice. *Biochimie* 2006, 88:1091-1098.

10. Bentires-Alj M, Kontaridis MI, Neel BG: Stops along the RAS pathway in human genetic disease. *Nat Med* 2006, 12:283-285.

11. Tidyman WE, Rauen KA: The RASopathies: developmental syndromes of Ras/MAPK pathway dysregulation. *Curr Opin Genet Dev* 2009, 19:230-236.

12. Anastasaki C, Estep AL, Marais R, Rauen KA, Patton EE: Kinase-activating and kinase-impaired cardio-facio-cutaneous syndrome alleles have activity during zebrafish development and are sensitive to small molecule inhibitors. *Hum Mol Genet* 2009, 18:2543-2554.

13. Fujii R, Yamashita S, Hibi M, Hirano T: Asymmetric p38 activation in zebrafish: its possible role in symmetric and synchronous cleavage. *J Cell Biol* 2000, 150:1335-1348.

14. Rui Y, Xu Z, Xiong B, Cao Y, Lin S, Zhang M, Chan SC, Luo W, Han Y, Lu Z et al.: A beta-catenin-independent dorsalization pathway activated by Axin/JNK signaling and antagonized by aida. *Dev Cell* 2007, 13:268-282.

15. Lepage SE, Bruce AE: Zebrafish epiboly: mechanics and mechanisms. *Int J Dev Biol* 2010, 54:1213-1228.

16. Krens SF, He S, Lamers GE, Meijer AH, Bakkers J, Schmidt T, Spaink HP, Snaar-Jagalska BE: Distinct functions for ERK1 and ERK2 in cell migration processes during zebrafish gastrulation. *Dev Biol* 2008, 319:370-383.

17. Bottcher RT, Niehrs C: Fibroblast growth factor signaling during early vertebrate development. *Endocr Rev* 2005, 26:63-77.

18. Halpern ME, Ho RK, Walker C, Kimmel CB: Induction of muscle pioneers and floor plate is distinguished by the zebrafish no tail mutation. *Cell* 1993, 75:99-111.

19. Hug B, Walter V, Grunwald DJ: tbx6, a Brachyury-related gene expressed by ventral mesendodermal precursors in the zebrafish embryo. *Dev Biol* 1997, 183:61-73.

20. Krens SF, Corredor-Adamez M, He S, Snaar-Jagalska BE, Spaink HP: ERK1 and ERK2 MAPK are key regulators of distinct gene sets in zebrafish embryogenesis. *BMC Genomics* 2008, 9:196.

21. Pelegri F, Mullins MC: Genetic screens for maternal-effect mutations. *Methods Cell Biol* 2004, 77:21-51.

22. Wagner DS, Dosch R, Mintzer KA, Wiemelt AP, Mullins MC: Maternal control of development at the midblastula transition and beyond: mutants from the zebrafish II. *Dev Cell* 2004, 6:781-790.

23. Holloway BA, Gomez de la Torre Canny, Ye Y, Slusarski DC, Freisinger CM, Dosch R, Chou MM, Wagner DS, Mullins MC: A novel role for MAPKAPK2 in morphogenesis during zebrafish development. *PLoS Genet* 2009, 5:e1000413.

24. Gomez N, Cohen P: Dissection of the protein kinase cascade by which nerve growth factor activates MAP kinases. *Nature* 1991, 353:170-173.

25. Ulevitch RJ: Recognition of bacterial endotoxins by receptor-dependent mechanisms. *Adv Immunol* 1993, 53:267-289.

26. Cargnello M, Roux PP: Activation and function of the MAPKs and their substrates, the MAPK-activated protein kinases. *Microbiol Mol Biol Rev* 2011, 75:50-83.

27. Cuadrado A, Nebreda AR: Mechanisms and functions of p38 MAPK signalling. *Biochem J* 2010, 429:403-417.

28. Hall JP, Cherkasova V, Elion E, Gustin MC, Winter E: The osmoregulatory pathway represses mating pathway activity in Saccharomyces cerevisiae: isolation of a FUS3 mutant that is insensitive to the repression mechanism. *Mol Cell Biol* 1996, 16:6715-6723.

29. Yoon S, Seger R: The extracellular signal-regulated kinase: Multiple substrates regulate diverse cellular functions. *Growth Factors* 2006, 24:21-44.

30. Schuck S, Soloaga A, Schratt G, Arthur JS, Nordheim A: The kinase MSK1 is required for induction of c-fos by lysophosphatidic acid in mouse embryonic stem cells. *BMC Mol Biol* 2003, 4:6.

31. Soloaga A, Thomson S, Wiggin GR, Rampersaud N, Dyson MH, Hazzalin CA, Mahadevan LC, Arthur JS: MSK2 and MSK1 mediate the mitogen- and stress-induced phosphorylation of histone H3 and HMG-14. *EMBO J* 2003, 22:2788-2797.

32. Plotnikov A, Zehorai E, Procaccia S, Seger R: The MAPK cascades: Signaling components, nuclear roles and mechanisms of nuclear translocation. *Biochimica et Biophysica Acta (BBA) - Molecular Cell Research* 2011, 1813:1619-1633.

33. Zebisch A, Czernilofsky AP, Keri G, Smigelskaite J, Sill H, Troppmair J: Signaling through RAS-RAF-MEK-ERK: from basics to bedside. *Curr Med Chem* 2007, 14:601-623.

34. Krens SF, He S, Spaink HP, Snaar-Jagalska BE: Characterization and expression patterns of the MAPK family in zebrafish. *Gene Expr Patterns* 2006, 6:1019-1026.

35. Slanchev K, Carney TJ, Stemmler MP, Koschorz B, Amsterdam A, Schwarz H, Hammerschmidt M: The epithelial cell adhesion molecule EpCAM is required for epithelial morphogenesis and integrity during zebrafish epiboly and skin development. *PLoS Genet* 2009, 5:e1000563.

36. Sumanas S, Zhang B, Dai R, Lin S: 15-zinc finger protein Bloody Fingers is required for zebrafish morphogenetic movements during neurulation. *Dev Biol* 2005, 283:85-96.

37. Hsieh CS, Ko CY, Chen SY, Liu TM, Wu JS, Hu CH, Sun CK: In vivo long-term continuous observation of gene expression in zebrafish embryo nerve systems by using harmonic generation microscopy and morphant technology. *J Biomed Opt* 2008, 13:064041.

38. Blanco MJ, Barrallo-Gimeno A, Acloque H, Reyes AE, Tada M, Allende ML, Mayor R, Nieto MA: Snail1a and Snail1b cooperate in the anterior migration of the axial mesendoderm in the zebrafish embryo. *Development* 2007, 134:4073-4081.

39. Jopling C, den HJ: Fyn/Yes and non-canonical Wnt signalling converge on RhoA in vertebrate gastrulation cell movements. *EMBO Rep* 2005, 6:426-431.

40. Mizoguchi T, Verkade H, Heath JK, Kuroiwa A, Kikuchi Y: Sdf1/Cxcr4 signaling controls the dorsal migration of endodermal cells during zebrafish gastrulation. *Development* 2008, 135:2521-2529.

41. Sabel JL, d'Alencon C, O'Brien EK, Van OE, Lutz K, Cuykendall TN, Schutte BC, Houston DW, Cornell RA: Maternal Interferon Regulatory Factor 6 is required for the differentiation of primary superficial epithelia in Danio and Xenopus embryos. *Dev Biol* 2009, 325:249-262.

42. Scott IC, Masri B, D'Amico LA, Jin SW, Jungblut B, Wehman AM, Baier H, Audigier Y, Stainier DY: The g protein-coupled receptor agtrl1b regulates early development of myocardial progenitors. *Dev Cell* 2007, 12:403-413.

43. Zhu S, Liu L, Korzh V, Gong Z, Low BC: RhoA acts downstream of Wnt5 and Wnt11 to regulate convergence and extension movements by involving effectors Rho kinase and Diaphanous: use of zebrafish as an in vivo model for GTPase signaling. *Cell Signal* 2006, 18:359-372.

44. Suzuki A, Kogo R, Kawahara K, Sasaki M, Nishio M, Maehama T, Sasaki T, Mimori K, Mori M: A new PICTure of nucleolar stress. *Cancer Sci* 2012, 103:632-637.

45. Martin DE, Soulard A, Hall MN: TOR regulates ribosomal protein gene expression via PKA and the Forkhead transcription factor FHL1. *Cell* 2004, 119:969-979.

46. Lai K, Amsterdam A, Farrington S, Bronson RT, Hopkins N, Lees JA: Many ribosomal protein mutations are associated with growth impairment and tumor predisposition in zebrafish. *Dev Dyn* 2009, 238:76-85.

47. Macinnes AW, Amsterdam A, Whittaker CA, Hopkins N, Lees JA: Loss of p53 synthesis in zebrafish tumors with ribosomal protein gene mutations. *Proc Natl Acad Sci U S A* 2008, 105:10408-10413.

48. Marzluff WF, Duronio RJ: Histone mRNA expression: multiple levels of cell cycle regulation and important developmental consequences. *Curr Opin Cell Biol* 2002, 14:692-699.

49. Alabert C, Groth A: Chromatin replication and epigenome maintenance. *Nat Rev Mol Cell Biol* 2012, 13:153-167.

50. Kim SJ, Hwang SG, Shin DY, Kang SS, Chun JS: p38 kinase regulates nitric oxide-induced apoptosis of articular chondrocytes by accumulating p53 via NFkappa B-dependent transcription and stabilization by serine 15 phosphorylation. *J Biol Chem* 2002, 277:33501-33508.

51. Heisenberg CP, Tada M: Zebrafish gastrulation movements: bridging cell and developmental biology. *Semin Cell Dev Biol* 2002, 13:471-479.

52. Pei W, Noushmehr H, Costa J, Ouspenskaia MV, Elkahloun AG, Feldman B: An early requirement for maternal FoxH1 during zebrafish gastrulation. *Dev Biol* 2007, 310:10-22.

53. Chen W, Hu XT, Shi QL, Zhang FB, He C: [Silencing of Adrm1 by RNA interference suppresses proliferation of colorectal cancer cells]. *Zhonghua Zhong Liu Za Zhi* 2009, 31:815-819.

54. Chen W, Hu XT, Shi QL, Zhang FB, He C: Knockdown of the novel proteasome subunit Adrm1 located on the 20q13 amplicon inhibits colorectal cancer cell migration, survival and tumorigenicity. *Oncol Rep* 2009, 21:531-537.

55. Kacimi R, Chentoufi J, Honbo N, Long CS, Karliner JS: Hypoxia differentially regulates stress proteins in cultured cardiomyocytes: role of the p38 stress-activated kinase signaling cascade, and relation to cytoprotection. *Cardiovasc Res* 2000, 46:139-150.

56. Rousseau S, Houle F, Landry J, Huot J: p38 MAP kinase activation by vascular endothelial growth factor mediates actin reorganization and cell migration in human endothelial cells. *Oncogene* 1997, 15:2169-2177.

57. Bulavin DV, Saito S, Hollander MC, Sakaguchi K, Anderson CW, Appella E, Fornace AJ, Jr.: Phosphorylation of human p53 by p38 kinase coordinates N-terminal phosphorylation and apoptosis in response to UV radiation. *EMBO J* 1999, 18:6845-6854.

58. Shou W, Sakamoto KM, Keener J, Morimoto KW, Traverso EE, Azzam R, Hoppe GJ, Feldman RM, DeModena J, Moazed D et al.: Net1 stimulates RNA polymerase I transcription and regulates nucleolar structure independently of controlling mitotic exit. *Mol Cell* 2001, 8:45-55.

59. Whitmarsh AJ: Regulation of gene transcription by mitogen-activated protein kinase signaling pathways. *Biochim Biophys Acta* 2007, 1773:1285-1298.

Supplemental tables 1-7

Nodal									
Gene name	Ensemble	nr probes	**P38αMO**			**ERK2MO**			
			Δ fold	p-value		Δ fold	p-value		
smad1	ENSDART00000033566	2	5,3	2,1E-04	⬆	4,2	9,9E-13	⬆	
ndr2	ENSDART00000058969	1	-2,7	4E-17	⬇	1,3	0,2721	X	
Jun	ENSDART00000063912	1	2,3	3,0E-07	⬆	-1,1	8,0E-01	X	
JunB	ENSDART00000109640	6	1,1	8,4E-01	X	3,3	7,3E-43	⬆	
bambi	ENSDART00000077732	1	-1,2	1,0E-04	X	-2,1	3,8E-12	⬇	
oep	ENSDART00000042441	1	1,6	1,0E-05	X	1,9	2,0E-12	⬆	
eng2a/Dharma	ENSDART00000031700	4	1,5	6,2E-01	X	9,2	2,8E-06	⬆	
stat3	ENSDART00000080854	1	1,4	1,3E-01	X	2,7	2,5E-17	⬆	

sTable 1

WNT									
Gene name	Ensemble	nr probes	**P38αMO**			**ERK2MO**			
			Δ fold	p-value		Δ fold	p-value		
dia1	ENSDART00000015374	4	3,6	0,0E+00	⬆	3,1	1,1E-40	⬆	
drl	ENSDART00000097364	7	-3,7	0,0E+00	⬇	-11,6	1,5E-20	⬇	
wnt2	ENSDART00000060259	2	2,6	3,2E-11	⬆	1,9	4,3E-02	X	
fzd8a	ENSDART00000066835	1	2,3	1,9E-07	⬆	-1,1	8,3E-01	X	
fzd1	ENSDART00000060789	1	2,6	1,3E-07	⬆	1,2	4,0E-01	X	
fzd9	ENSDART00000024087	2	2,6	4,5E-11	⬆	1,4	2,7E-04	X	
limk2	ENSDART00000020532	1	-2,8	8,1E-14	⬇	-1,1	6,6E-01	X	
tcf4	ENSDART00000009237	1	-3,9	1,6E-06	⬇	-2,7	2,5E-04	X	
sfrp2	ENSDART00000102498	1	4,6	4,0E-08	⬆	1,6	2,1E-01	X	
ctbp2	ENSDART00000114215	1	4,4	1,3E-10	⬆	-2,0	1,3E-01	X	
wnt11r	ENSDART00000099880	1	-1,2	2,9E-01	X	-2,1	3,2E-09	⬇	
wnt3l	ENSDART00000098394	2	-1,2	7,6E-01	X	3,7	2,8E-07	⬆	
fzd4	ENSDART00000112320	1	1,2	4,3E-01	X	-3,8	1,8E-07	⬇	
has2	ENSDART00000053754	2	1,1	5,9E-01	X	-8,0	4,6E-09	⬇	
stat3	ENSDART00000080854	1	1,4	1,3E-01	X	2,7	2,5E-17	⬆	
Stat5.2	ENSDART00000077952	1	2,1	5,0E-05	X	2,3	6,4E-09	⬆	
dact1	ENSDART00000058001	3	1,0	9,2E-01	X	-13,7	0,0E+00	⬇	
gsk3b	ENSDART00000018228	2	1,2	2,3E-01	X	2,6	3,3E-07	⬆	

sTable 2

92

			P38αMO			ERK2MO		
BMP								
Gene name	**Ensemble**	**nr probes**	**Δ fold**	**p-value**		**Δ fold**	**p-value**	
smad1	ENSDART00000033566	2	5,3	2,1E-04	⬆	4,2	9,9E-13	⬆
gata3	ENSDART00000025153	5	-2,6	1,4E-06	⬇	-21,9	1,6E-40	⬇
vent	ENSDART00000017456	1	4,2	1,2E-09	⬆	-2,9	1,5E-29	⬇
noggin 1	ENSDART00000081766	4	1,3	4,5E-04	X	-3,1	9,5E-11	⬇
nog2	ENSDART00000063231	1	-2,9	1,2E-01	X	3,3	8,5E-06	⬆
chd	ENSDART00000045110	1	-1,9	8,0E-05	X	-2,6	1,0E-05	⬇
fst	ENSDART00000051065	3	3,1	6,0E-05	X	5,0	1,3E-06	⬆
fstl1	ENSDART00000081824	1	-1,2	7,0E-01	X	6,7	4,4E-06	⬆
bmp2b	ENSDART00000100482	3	1,6	6,2E-03	X	-6,5	1,4E-09	⬇
bmp7b	ENSDART00000092214	1	2,2	1,7E-02	X	3,8	1,0E-10	⬆
bmper	ENSDART00000097348	3	-1,1	7,9E-01	X	-9,1	0,0E+00	⬇
admp	ENSDART00000037557	3	-1,2	1,2E-01	X	-10,5	3,0E-15	⬇
bambi	ENSDART00000077732	2	-1,2	1,4E-01	X	-2,2	1,7E-18	⬇
snai2	ENSDART00000058571	3	-1,7	2,0E-04	X	-3,0	4,8E-08	⬇
dlc	ENSDART00000018514	3	1,3	5,2E-01	X	-15,0	4,0E-43	⬇
id3	ENSDART00000077087	2	1,1	5,7E-01	X	-2,6	1,1E-11	⬇
gata2a	ENSDART00000082420	1	-1,2	3,5E-01	X	-6,7	5,4E-11	⬇
otul	ENSDART00000064320	2	1,5	3,0E-05	X	3,6	9,7E-16	⬆

sTable 3

			FGF					
			P38αMO			ERK2MO		
Gene name	Ensemble	nr probes	Δ fold	p-value		Δ fold	p-value	
mych	ENSDART00000115049	1	2,4	2,2E-20	↑	-1,2	1,7E-01	X
mych	ENSDART00000115049	1	1,1	6,2E-01	X	-4,6	6,2E-21	↓
RALA	ENSDART00000027587	4	-3,1	3,1E-09	↓	-6,5	8,6E-13	↓
DUSP14	ENSDART00000080338	2	3,2	1,2E-06	↑	4,1	5,5E-10	↑
RASSF4	ENSDART00000100803	1	2,0	8,5E-06	↑	2,2	9,1E-40	↑
hrasl	ENSDART00000015040	1	-2,4	7,1E-20	↓	-1,9	4,2E-17	↓
fgf4	ENSDART00000108971	2	-2,8	3,7E-06	↓	-34,1	0,0E+00	↓
MAPK organizer 1	ENSDART00000109873	2	2,0	1,9E-25	↑	1,3	4,9E-04	X
mapk12	ENSDART00000018502	1	3,9	8,0E-10	↑	1,6	1,7E-01	X
mapk14a	ENSDART00000040362	1	-2,2	3,2E-37	↓	-1,5	4,6E-08	X
mapksp1	ENSDART00000079669	4	2,5	4,3E-11	↑	1,3	9,8E-02	X
rasgef1bb	ENSDART00000064968	1	-2,1	1,6E-12	↓	1,4	2,7E-04	X
a-raf	ENSDART00000076687	1	5,9	2,3E-08	↑	2,9	1,5E-03	X
b-raf	ENSDART00000023894	1	-4,7	1,1E-27	↓	-2,2	7,0E-05	X
SPRY2	ENSDART00000052423	2	4,7	2,9E-06	↑	1,2	7,1E-01	X
Spry4	ENSDART00000099528	4	-3,0	1,1E-08	↓	-2,6	1,1E-02	X
eef2k	ENSDART00000052001	1	-3,6	1,2E-06	↓	-2,7	1,3E-02	X
cFOS-like	ENSDART00000043298	1	3,4	6,8E-11	↑	1,5	1,8E-01	X
c-jun	ENSDART00000063912	1	2,3	3,0E-07	↑	-1,1	8,0E-01	X
Jun dimerization protein	ENSDART00000014166	3	-2,1	4,1E-09	↓	1,1	6,6E-01	X
CRTC1	ENSDART00000113356	1	-2,2	1,0E-16	↓	1,1	5,3E-01	X
pea3	ENSDART00000013033	1	3,9	3,2E-07	↑	2,1	2,5E-02	X
fgf17	ENSDART00000029630	4	-1,4	1,3E-01	X	-44,3	1,1E-25	↓
fgf3	ENSDART00000111524	2	1,2	5,3E-01	X	-8,5	1,3E-08	↓
fgfr1b	ENSDART00000004803	1	-1,2	6,6E-01	X	-2,7	6,0E-31	↓
fgfr4	ENSDART00000100286	3	-1,7	6,3E-02	X	-43,6	1,1E-25	↓
12b6 ras-like	ENSDART00000015755	2	-1,2	7,8E-02	X	-2,3	1,0E-05	↓
rasl11b	ENSDART00000015755	1	-1,2	4,5E-02	X	-2,4	5,3E-06	↓
rasa1	ENSDART00000051518	1	1,5	1,8E-08	X	2,2	6,5E-15	↑
spry2	ENSDART00000114948	1	1,3	3,9E-01	X	2,0	4,0E-26	↑
dusp1	ENSDART00000014515	1	1,5	6,8E-07	X	2,1	4,4E-07	↑
DUSP6	ENSDART00000104496	16	-1,4	1,4E-02	X	-89,5	0,0E+00	↓
mycn	ENSDART00000024104	6	1,4	2,4E-01	X	-8,6	1,2E-20	↓
bad	ENSDART00000077219	1	1,6	5,4E-12	X	2,0	8,6E-07	↑
srf	ENSDART00000076035	1	1,0	9,9E-01	X	2,2	3,0E-06	↑
JunB	ENSDART00000109640	6	1,1	8,4E-01	X	3,3	7,3E-43	↑
ATF4	ENSDART00000055609	3	-1,5	4,5E-04	X	-3,3	2,2E-06	↓

sTable 4

94

	Ensemble	nr probes	P38αMO Δ fold	p-value		ERK2MO Δ fold	p-value	

Cell migration

	Ensemble	nr probes	Δ fold	p-value		Δ fold	p-value	
			P38αMO			**ERK2MO**		
nav3	ENSDART00000036886	1	-5,8	0,0E+00	↓	-5,9	0,0E+00	↓
blf	ENSDART00000063318	2	-2,1	1,4E-30	↓	-12,8	0,0E+00	↓
EpCAM/ zgc:110304	ENSDART00000110637	2	-100,8	0,0E+00	↓	-58,8	3,5E-33	↓
krt4	ENSDART00000012644	2	-2,6	5,7E-10	↓	-8,7	4,2E-45	↓
ncam1	ENSDART00000017229	1	-2,4	2,6E-09	↓	-2,7	3,4E-08	↓
ncam2	ENSDART00000100681	1	-2,4	4,2E-27	↓	-3,5	3,4E-13	↓
net1	ENSDART00000049066	6	-2,4	3,9E-06	↓	-13,3	3,3E-09	↓
zic3	ENSDART00000105761	3	-6,7	6,1E-06	↓	-64,1	0,0E+00	↓
EML3	ENSDART00000080834	1	2,1	2,5E-22	↑	3,0	2,1E-21	↑
arpc5b	ENSDART00000010329	5	2,2	1,2E-15	↑	2,7	1,5E-10	↑
tgfb2	ENSDART00000030271	1	2,2	3,1E-07	↑	3,7	6,9E-21	↑
jup	ENSDART00000003891	1	2,3	1,8E-15	↑	2,6	2,8E-24	↑
stka	ENSDART00000054823	3	-2,4	2,9E-36	↓	-1,3	2,3E-03	X
Spry4	ENSDART00000099528	3	-3,0	1,1E-08	↓	-2,6	1,1E-02	X
zgc:172238	ENSDART00000090587	9	-7,7	0,0E+00	↓	-2,5	4,7E-02	X
map1a	ENSDART00000067321	1	-3,9	7,8E-07	↓	-2,8	7,5E-03	X
mibp	ENSDART00000114380	2	-2,3	1,9E-11	↓	-1,4	8,5E-03	X
adrm1a	ENSDART00000081433	4	-4,0	7,3E-39	↓	-1,4	3,9E-04	X
adrm1b	ENSDART00000081427	2	-2,2	1,6E-11	↓	1,3	1,1E-02	X
flot2a	ENSDART00000109770	1	-7,5	3,7E-06	↓	-8,9	1,2E-04	X
cldn10	ENSDART00000081900	1	-2,4	5,9E-07	↓	1,4	1,7E-04	X
actn3a	ENSDART00000005682	2	-4,7	0,0E+00	↓	1,7	1,9E-01	X
pcdh2ab1	ENSDART00000081898	1	-2,8	6,3E-08	↓	1,1	2,3E-01	X
rhoj	ENSDART00000002507	1	2,0	7,9E-07	↑	1,8	5,1E-02	X
rnd1l	ENSDART00000109712	1	3,7	8,8E-11	↑	1,3	5,9E-01	X
twf1l	ENSDART00000065006	2	2,8	1,5E-32	↑	1,2	3,2E-01	X
si:dkey-30c15.12	ENSDART00000081386	1	8,4	3,8E-18	↑	3,6	1,7E-02	X
cldna	ENSDART00000102086	2	6,0	5,2E-16	↑	-1,1	7,4E-01	X
arnt2	ENSDART00000031712	1	2,5	2,4E-12	↑	1,3	1,0E-01	X
rhoh	ENSDART00000102646	1	3,1	4,9E-10	↑	1,7	1,4E-01	X
aplnrb	ENSDART00000053264	3	1,2	5,5E-01	X	-17,3	2,2E-20	↓
cxcr4a	ENSDART00000080350	1	1,2	7,8E-02	X	-9,7	3,6E-39	↓
epd	ENSDART00000049895	5	-1,4	3,4E-03	X	-16,8	4,6E-35	↓
delta C	ENSDART00000018514	3	1,3	5,2E-01	X	-15,0	4,0E-43	↓
snail2/slug	ENSDART00000058571	2	-1,7	2,0E-04	X	-3,0	4,8E-08	↓
rhoab	ENSDART00000024009	15	-1,9	6,5E-03	X	-4,0	6,6E-09	↓
krt18	ENSDART00000020750	1	-1,2	6,1E-01	X	-5,3	3,7E-08	↓
rpsa	ENSDART00000114282	4	-1,4	1,2E-02	X	-3,1	5,9E-31	↓
fyna	ENSDART00000046414	1	-1,8	5,8E-06	X	-2,2	1,2E-36	↓
irf6	ENSDART00000063562	1	2,1	1,7E-04	X	2,0	2,7E-14	↑
adam9	ENSDART00000109805	1	1,5	6,2E-06	X	2,2	5,1E-06	↑
limk2	ENSDART00000020532	2	1,8	8,2E-18	X	2,1	3,9E-07	↑
hmmr	ENSDART00000031785	2	1,7	4,0E-06	X	2,3	1,8E-37	↑
clauding	ENSDART00000015547	2	1,5	2,9E-03	X	2,1	9,3E-12	↑

sTable 5

			Protein Translation					
Gene symbol	Ensemble	Nr. probes	P38αMO			ERK2MO		
			Δ fold	p-value		Δ fold	p-value	
rpl3	ENSDART00000011251	2	-2,2	6,4E-25	↓	-1,5	9,5E-03	X
rpL9	ENSDART00000054340	6	-2,3	1,2E-35	↓	-1,7	4,3E-04	X
rpl10	ENSDART00000032744	3	-2,9	1,2E-13	↓	-1,6	1,3E-04	X
rpl13	ENSDART00000047391	1	-2,5	3,1E-06	↓	-1,1	1,9E-01	X
rpl19	ENSDART00000018975	2	-4,4	7,5E-13	↓	-1,3	4,5E-04	X
rpl23a	ENSDART00000003001	3	-3,2	7,5E-11	↓	-1,5	9,5E-02	X
rpl24	ENSDART00000019227	1	-3,2	1,2E-08	↓	-1,4	3,0E-02	X
rpl35	ENSDART00000009241	3	-2,6	1,9E-26	↓	-1,9	1,6E-12	X
rps2	ENSDART00000113070	1	-3,2	1,1E-09	↓	-1,6	6,6E-02	X
rps8	ENSDART00000078412	7	-7,0	2,3E-17	↓	1,4	4,7E-03	X
mrps15	ENSDART00000048727	1	-3,1	1,4E-12	↓	1,0	8,4E-01	X
mrpl24	ENSDART00000010862	2	-2,9	9,1E-18	↓	1,1	7,4E-01	X
mrpl37	ENSDART00000091479	2	-2,1	5,7E-07	↓	-1,1	3,9E-01	X
eif2b2	ENSDART00000060689	3	-2,3	1,7E-07	↓	-1,2	1,1E-01	X
cwc22	ENSDART00000023684	1	-2,0	2,1E-10	↓	-1,0	5,9E-01	X
tyw3	ENSDART00000055737	3	-6,2	4,2E-23	↓	-1,1	3,4E-01	X
yars	ENSDART00000052126	4	-3,6	1,1E-18	↓	1,1	1,3E-01	X
farsa	ENSDART00000033738	4	-2,8	0,0E+00	↓	-1,3	3,8E-02	X
iars	ENSDART00000004423	1	-2,0	1,7E-13	↓	-1,8	5,0E-05	X
hars2	ENSDART00000065566	2	-2,1	6,7E-25	↓	-1,2	7,8E-02	X
pus3	ENSDART00000062722	3	-2,7	6,1E-20	↓	-1,3	9,1E-04	X
NSA2	ENSDART00000021976	3	-5,3	2,9E-08	↓	-1,0	8,8E-01	X
eif3s7	ENSDART00000011052	1	-2,9	1,0E-05	↓	-1,1	3,5E-01	X
eef2k	ENSDART00000052001	1	-3,6	1,2E-06	↓	-2,7	1,3E-02	X
fhla	ENSDART00000105767	1	2,2	1,1E-10	↑	1,1	8,0E-01	X
eef1a1	ENSDART00000075340	1	3,1	6,8E-14	↑	1,7	1,2E-01	X
eif2ak3	ENSDART00000113051	2	1,7	3,6E-04	X	2,7	8,2E-06	↑
eif3h	ENSDART00000110583	1	-1,1	6,7E-01	X	2,5	1,8E-14	↑
eef1b2	ENSDART00000065373	1	-1,5	1,0E-01	X	2,3	6,3E-22	↑
eif4a3	ENSDART00000014887	1	2,2	2,5E-11	↑	2,5	5,8E-07	↑
IGFN1	ENSDART00000114121	1	3,2	1,4E-07	↑	5,8	2,8E-06	↑

sTable 6

Epigenetic modification									
	Ensemble	**nr probes**	**P38αMO**			**ERK2MO**			
			Δ fold	**p-value**		**Δ fold**	**p-value**		
h2afx	ENSDART00000040328	6	7,2	2,3E-25	⬆	-3,5	5,7E-36	⬇
zgc:163047	ENSDART00000103024	1	11,2	0,0E+00	⬆	-2,7	1,2E-07	⬇
histone H4-like	ENSDART00000114073	6	5,5	0,0E+00	⬆	-2,9	0,0E+00	⬇
prmt1	ENSDART00000012630	1	2,0	2,0E-14	⬆	2,1	2,7E-22	⬆
ppme1	ENSDART00000016219	1	2,4	2,3E-12	⬆	2,7	5,7E-12	⬆
Histone H3.2	ENSDART00000111408	8	15,9	9,4E-42	⬆	-3,6	8,5E-02	X
Histone H2B 1/2	ENSDART00000097813	6	7,0	0,0E+00	⬆	-2,5	8,7E-04	X
Histone H2B 1/2	ENSDART00000109316	3	4,2	1,0E-14	⬆	-1,3	7,0E-02	X
histone H2a	ENSDART00000109856	1	4,4	3,5E-08	⬆	-2,4	5,1E-02	X
histone H3	ENSDART00000115371	1	15,2	0,0E+00	⬆	-1,4	5,0E-01	X
sirt5	ENSDART00000112030	3	-2,2	4,0E-06	⬇	-1,6	6,9E-03	X
sirt3	ENSDART00000051973	1	-2,1	3,8E-14	⬇	-1,1	7,4E-01	X
arnt2	ENSDART00000051813	1	2,5	2,4E-12	⬆	1,3	1,0E-01	X
gamt	ENSDART00000104360	3	-2,2	9,6E-08	⬇	1,0	5,8E-01	X
mri1	ENSDART00000111671	1	3,7	1,0E-05	⬆	1,5	1,9E-01	X
mybbp1a	ENSDART00000038767	5	-3,1	1,1E-39	⬇	1,3	3,9E-04	X
mych	ENSDART00000115049	2	2,4	2,2E-20	⬆	-1,2	1,8E-01	X
rbb4	ENSDART00000048144	4	1,5	3,0E-02	X	4,3	3,0E-38	⬆
rbb4l	ENSDART00000008144	1	1,5	3,3E-07	X	2,0	3,5E-28	⬆
histh1l	ENSDART00000124705	1	1,1	9,3E-01	X	-2,8	2,8E-11	⬇
asf1bb	ENSDART00000064194	6	1,6	1,4E-04	X	3,8	2,6E-17	⬆
TGS1	ENSDART00000097868	2	1,7	2,7E-03	X	2,7	3,3E-26	⬆
METTL9	ENSDART00000084076	1	1,3	2,3E-01	X	2,2	4,7E-15	⬆
kdm2aa	ENSDART00000083127	1	1,5	1,3E-03	X	2,4	7,6E-06	⬆
cMyca	ENSDART00000067178	6	1,1	9,2E-01	X	6,3	3,3E-19	⬆

sTable 7

CHAPTER V

Identification of P38α target genes involved in the physiological angiogenesis

Hanan Rian, Shuning He, Herman. P Spaink and B. Ewa Snaar-Jagalska

Abstract

Developmental angiogenesis is one of the physiological processes were P38α MAPK signalling is found to be crucial. The formation of intersegmental blood vessels (ISVs) in the zebrafish embryos serves as a paradigm to study angiogenesis in vivo. Here we investigated the role of P38α in the embryonic angiogenesis and further focussed on the identification of the target genes.

To study the role of P38α in angiogenesis we performed knock-down experiments with gene specific morpholinos. Unsaturated knock-down of P38α in zebrafish resulted in a delayed formation of intersegmental vessels and expansion of the intermediate cell mass. Scanning confocal microscopy of Tg(fli:EGFP) embryos revealed absence of filopodia on the tip cells of growing ISV indicating defective endothelial cell migration in P38α morphants. The P38 morpholino phenotype with defective angiogenesis was confirmed by the P38 inhibitor BIRB796. When applied at the 4-8 somite stage the inhibitor completely blocked sprouting of the ISV. To identify P38α target genes involved in physiological angiogenesis we compared the P38α knock-down transcriptome with the GFP+ enriched gene set of Tg(fli:EGFP). T-cell activation RhoGTPase activating protein b (Tagapb) was affected by P38α morpholino and among the pool of GFP+ enriched genes. The vascular endothelial zinc finger 1a (Vezf1) affected by P38 morpholino, was not specifically expressed in the vasculature however was reported previously to play a role in angiogenesis. Furthermore the runt-related transcription factor 1 (Runx) transcription factor was upregulated in P38 morphants which plays an important role in definitive hematopoesis.

Introduction

The virulence component of anthrax lethal toxin lethal factor (LF) is an zinc-metalloprotease that cleaves the NH(2) termini of mitogen-activated protein kinase kinase 1 and 6 (Mekk) causing severe vascular damage.[1,2] This association of MAPK with vascular morphogenesis is further supported by numerous *in vitro* and *in vivo* studies which lead to the overall conclusion that Erk2, Erk5 and P38α MAPK are separately indispensible for angiogenesis: the branching of vasculature from preexisting blood vessels. In contrast, MAPK have not been reported to be involved in vasculogenesis: the formation of blood vessels from endothelial cell precursors (angioblasts). P38α is in particular involved in regulation of cell migration and permeability of endothelial cells[3]. Targeted P38α deletion causes placental angiogenesis defects and subsequent cardiovascular defects in the embryo resulting in lethality starting at E10.5.[4,5]

The P38α MAPK, and the other isoforms β, δ, γ of the P38 MAPK subfamily, are also known as stress activated protein kinases since activity is induced by stressors such endotoxins, hypoxia, cytokines, DNA damaging factors etc.[6] However P38α activity can be stimulated by growth factors and besides a role in stress signaling is also involved in physiological and developmental processes[7]. P38α and P38β, show a wide tissue expression and can be activated by Mek3 and Mek6 which are in turn activated by an Mapkkk (Mekk) [7-10]. Multiple Mekks are identified to function in the Mekk-Mek3/6-P38α/β cascade[11]. Mekk3, functional in both the P38α as Mek5-Erk5 cascade, was identified as an essential gene for vascular morphogenesis. Knock-out of Mekk3 in mice is lethal, starting at E11, due to extensive defects in blood vessel formation in the embryo, placenta and yolk sac [12].

Several *In vitro* studies have contributed to identification of the molecular signaling events of angiogenesis depending on P38α. P38α activation is triggered by the angio-proliferative factors as vascular endothelial growth factor (Vegf) or fibroblast growth factor 2 (Fgf2) which regulate different aspects of angiogenesis: endothelial tip cell sprouting, proliferation, lining, migration and tube formation. P38α regulates the expression of Vegf post transcriptionally by increasing mRNA half-life and is functional downstream of Vegf in endothelial cells as well [13]. Phosphorylation of the Tyrosine-1214 residue of Vegfr2 (kdrl, flk1), through ligand binding, leads to activation of P38α and subsequent Mapk activated protein kinase 2 (Mk2)-Hsp27 to drive actin remodeling in stress fibers [14,14-16]. Furthermore, Nck, Fyn, Pak2 and Cdc42 are found to function upstream of P38α when stimulated by Vegfr2 [17]. Alternatively, Raftk/Pyk2 and Src have been reported to increase P38α activity and regulate migration of endothelial cells in response to Vegf[18]. A negative feedback signal has also been reported. Vegfr2 induces expression of MiR-20a which blocks

expression of Mekk3 mRNA leading to decreased P38α activity and eventually inhibition of endothelial cell migration[19]. The Vegf-A bound Vegfr2 stimulates P38α activation when complexed with the co-receptor Neuropillin-1 (Nrp1) leading to vessel branching in subcutaneous matrigel plugs. Excessive vessel branching in matrigel plugs was observed after stimulation with Vegf-A165 a splice variant that complexes Vegfr2 with both coreceptors Nrp1 and heparin sulphate proteoglycan (Hspg) also leading to P38α activition[20]. Vegf-A165 induced endothelial cell organization and pericyte association was disturbed in subcutaneous matrigel plugs treated with the P38 inhibitor SB203580.

On the contrary, P38 stimulated with Fgf2 in endothelial cells has been suggested to have a negative effect on angiogenesis. Fgf2 caused a sustained P38 activity in vascular endothelial cells in vivo in the chick chorioallantoic membrane and inhibition with the P38 inhibitor SB202190 enhances neovascularisation. Based on this experiment Fgf2 stimulated P38 is suggested to inhibit endothelial cell survival, proliferation and differentiation in collagen gel cultures of bovine capillary endothelial cells [21].

Furthermore, P38 is likely to be involved in inflammation linked angiogenesis mediated by Interleukin 1β[22]. Endothelial tube formation and migration induced by Interleukin 1β was depending on Traf6 complex formation with caveolin-1 and subsequent P38-MK2 activation. TRAF6 activation of P38-Mapk is could have been mediated via the transforming growth factor (Tgf)-β-activated kinase 1 (Tak1)/Tak1-binding protein 1 (Tab1)/Tab2 signaling complex [23].

Targeted knock-out studies in mice have clearly demonstrated that the P38α is essential for angiogenesis and could not be compensated by the other P38 isoforms. Most studies of P38α dependant angiogenesis, tough mostly performed *in vitro* using non-selective P38 inhibitors, have identifyed some of the molecular events upstream of P38. Since P38α is able to affect the activity of many substrates including transcription factors the downstream signalling and gene expression during angiogenesis is still an unexplored area. At 1 day post fertilization the zebrafish forms the intersegmental vessels (ISV) allowing study of angiogenesis that can be visualized in detail. The growth of ISV along the somite boundaries is often assayed as measure for physiological angiogenesis. Since we have recently developed P38α specific antisense oligonucleotides (morpholinos) to knock-down P38α, we used this new tool to study the role of P38α in embryonic angiogenesis.

Material & Methods

Zebrafish husbandry
Zebrafish (Danio rerio) wild type line was maintained under standard conditions and guidelines given in the zebrafish book (Westerfield 200). Embryos were kept at 28°C or 31°C to adjust required speed of development for experiment.

Morpholino microinjection and life imaging
Tg(fli:EGFP)^{y1} (Lawson et al., 2002) embryos were injected between 0- and 1- cell stage with either P38αA translational blocking morpholino (ATG) 5'GTGGGTCTTTCTTTCTGCGACATGC3', or standard control morpholino 5'CCTCTTACCTCAGTTACAATTTATA3'(Genetools). Morpholino's where dissolved in 1XDanieau's buffer [58mM NaCl, 0.7mM KCl, 0.4mM MgSO$_4$, 0.6mM Ca(NO$_3$)$_2$, 5.0mM HEPES pH7.6] containing 1% phenol red solution. Injected embryos were kept at 28°C for live imaging.

Chemical Inhibitor treatment of *Tg(fli1:egfp)^{y1}*
The Pan-P38 inhibitor Birb-796 was dissolved in DMSO and used to block P38 activity in *Tg(fli:EGFP)^{y1}* embryos. Because the inhibitor cannot pass through the chorion sufficiently, embryos have been mechanically dechorionated in Danieau buffer into agarose coated dishes. 100 μM Birb796 was added at 4-7 somite stage before sprouting of ISVs (around 24somite stage). Embryos were kept at 28°C and staged in hours post fertilization (hpf) according to (Kimmel et al. 1995) for live imaging.

Protease dissociation of *Tg(fli1:egfp)^{y1}* and FACS
GFP+ cells were isolated from untreated *Tg(fli:EGFP)^{y1}* of 24hpf kept o/n at 28°C or 31°C. Embryos have been bleached and dechorionated prior to deyolking and dissociation. Dechorionation was performed by enzymatic digestion with Pronase (2 mg/ml Roche Applied Science) for 7 mintutes with subsequent washing in 1XDanieau's buffer. Dissociation was performed as previously reported (Covassin et al. 2006). On average 220 embryos per condition was sufficient for 1x10^7 cells which on average would be sufficient for 1.4 μg of GFP$^+$ RNA. Dissociated cells were centrifuged for 5 min at 500 RCF and resuspended in Leibovitz medium L15 without phenol red, 1% fetal calf serum, 0.8 mM CaCl2, penicillin 50 U/mL and streptomycin 0.05 mg/mL. The cell suspension was filtered through a 50 μm CellTrics filter (Partec) for FACS (BD FACS AriaII cell sorter using a 70-100 μm nozzle). sorted GFP+ and GFP- cells were collected in 1/3 volume L15, 0.8 mM CaCl2, 10% fetal calf serum, 10% zebrafish embryo extract, penicillin 50 U/mL and streptomycin 0.05 mg/mL. Cells were immediately collected and lysed in QIAzol reagent for RNA isolation. On average 200 embryos per condition was sufficient for 1x10^7 GFP$^+$ cells for a yield of 1.4 μg of RNA.
104

RNA isolation for q-PCR or transcriptome analysis

1/5 of chloroform was added to the Qiazol cell lysis, mixed and transferred to phase-lock gel heavy (5-Prime) containing eppendorf tubes of 1.5ml. The RNA liquid phase (top transparent solution) was separated from the rest of the sample by 15min at 12000 g and purified with rneasy minelute cleanup kit (Qiagen) according to manufacture protocol.

50ng of RNA was used for cDNA synthesis for qPCR expression analysis of fli and flt4 (primers Covassin et al.2006) relative to 18S rRNA (primers Tang et al. 2007).RNA samples were delivered to the microarray department University Amsterdam www.microarray.nl/ who performed a RNA quality check with the Agilent 2100 bioanalyzer using eukaryote total RNA pico series II protocol.

A two-color microarray-based gene expression analysis with treatment (GFP+) labelled Cy3 hybridized against control (GFP-) labelled Cy5 on an Agilent 180k chip. For analysis, data files (MAGE and JPEG files of each hybridized chip position) were imported into Rosetta Resolver 7.2 (Rosetta Inpharmatics LLC). Three biological replicate intensity profiles were combined using the default intensity experiment builder which is implemented in the Rosetta Resolver system. 28°C GFP+ against GFP- (252823310038_2, 252823310039_4, 252823310040_2) and 31°C GFP+ against GFP- (252823310038_3, 252823310039_1, 252823310040_4).

0.1pmol P38α morpholino or standard control morpholino was injected in zebrafish embryos and RNA was isolated at 24hpf (31°C). RNA samples were used for transcriptome analysis with a common reference design (common reference=pool of all P38α morpholino and standard control samples) A two-color microarray-based gene expression analysis with treatment (P38α morpholino or standard control morpholino) labelled Cy5 hybridized against control (common reference) labelled Cy3 on an Agilent 180k chip. Three biological replicate intensity profiles were combined using the default intensity experiment builder P38α morpholino against common reference (P38α morpholino against common reference 252823310118_1, 252823310118_3, 252823310119_1), (standard control morpholino against common reference 252823310118_2, 252823310118_4, 252823310119_2).

Results

P38α regulates growth of ISV and is essential for zebrafish angiogenesis

P38αA is widely expressed in the most tissues and has an early developmental function in epiboly. Saturated knock-down with gene specific translational blocking morpholinos causes severe morphological abnormalities and lethality (**chapter IV**). Therefore we studied the role of P38α in embryonic angiogenesis under unsaturated knock-down conditions. We performed a titration experiment in Tg(fli:EGFP) with our previously designed morpholino to obtain the pool of embryos displaying vascular defects and minor morphological defects for further analysis. In the wild type embryos the intersegmental vessels (ISV) in the trunk arise from the lateral posterior mesoderm (LPM), and migrate to the dorsal aorta. From the dorsal aorta the ISV grow along the vertical somite boundaries dorsally at 20 somite stage. Reaching the dorsal most portion of the trunk the ISV form a T shape. Tips of neighbouring vessels connect into the dorsal longitudinal anastomotic vessels (DLAV) which runs horizontally. Unsaturated knock-down of P38α resulted in a significant delayed growth of ISV **Fig1a**.
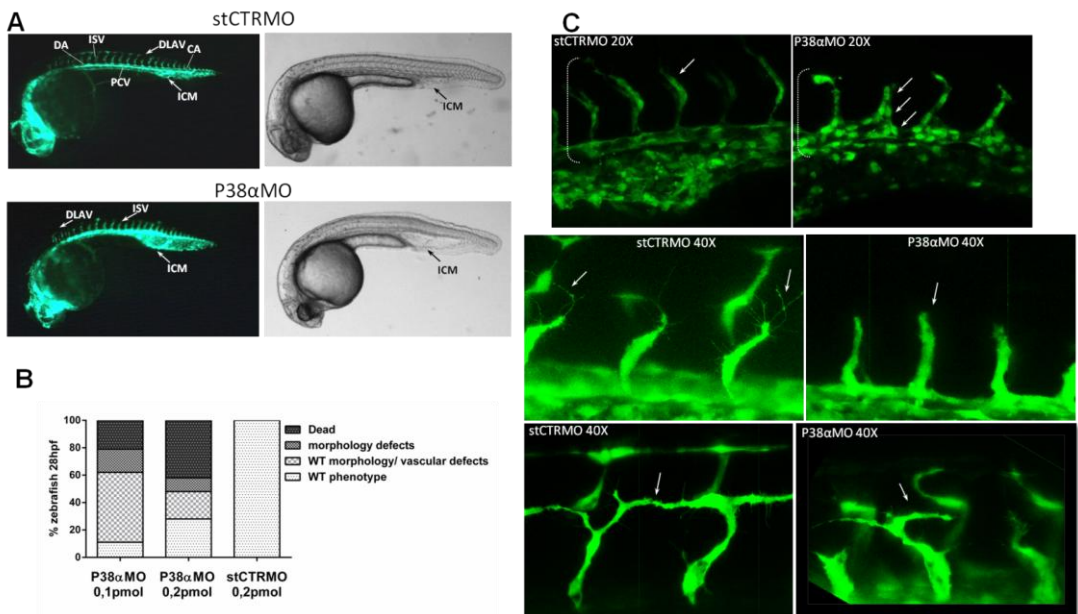
Fig1. Unsaturated morpholino knock-down of P38α delays development of ISV. **A:** Transmission and florescent stereo images of 1,5dpf (28˚C) Tg(Fli:eGFP) embryos injected with P38α or standard control morpholino. **B:** Optimization of unsaturated knock-down to obtain the pool of embryos displaying vascular defects and minor morphological defects. **C:** Confocal images showing ISV of Tg(Fli:eGFP) embryos injected with standard control morpholino **left** or P38α morpholino **right** 20X magnification: **upper panel**. Endothelial cells of P38α morphants display an aberrant morphology (more packed and less stretched). 1,5dpf P38α morphs have sprouted ISV that lack filopodia: **middle panel**. Formation of DLAV is delayed in P38α morphs: **lower panel**.
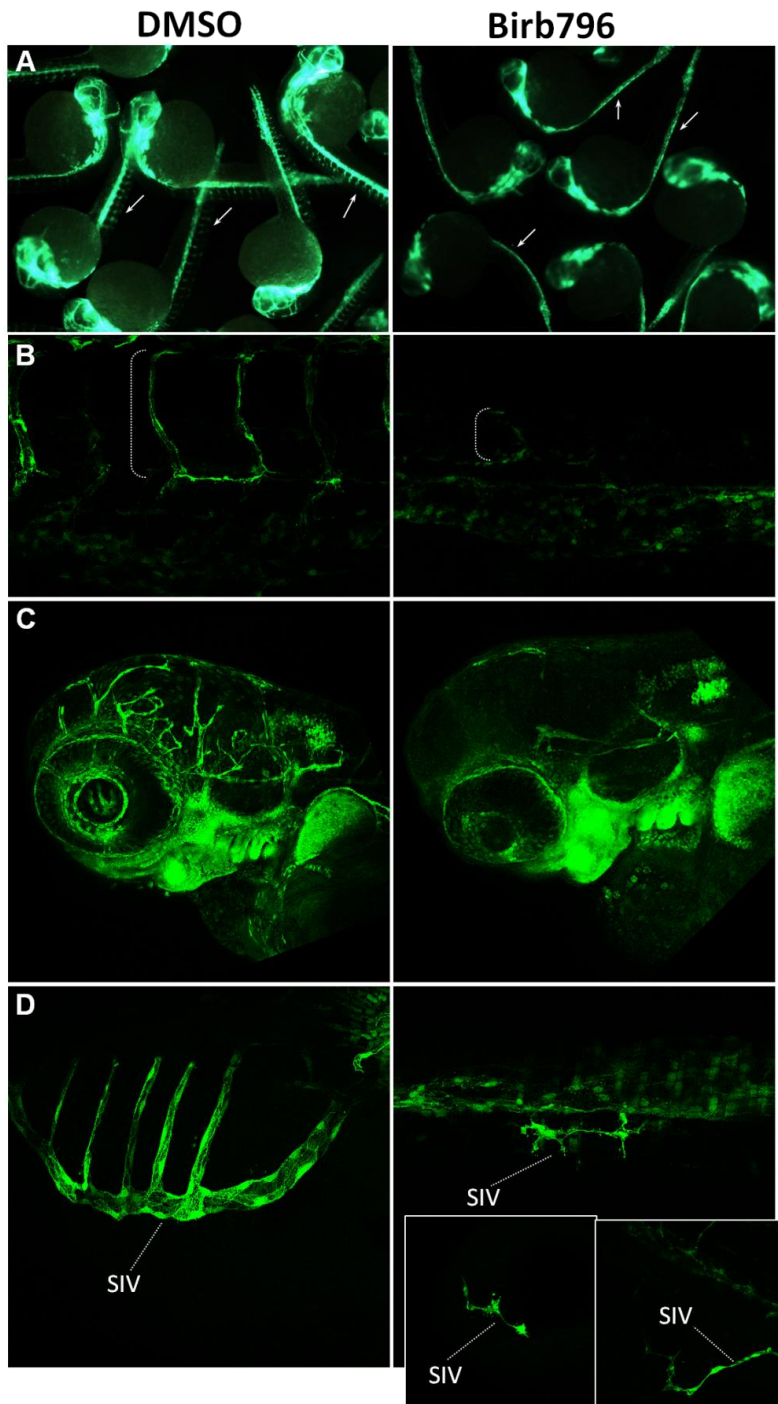
Fig2. The P38 inhibitor Birb798 blocks angiogenesis in the tail, head and formation of the SIV complex. Left: DMSO treated embryos, **Right**: Birb796 treated embryos. **A-B** Tg(Fli:eGFP) embryos treated with Birb796 lack sprouting of ISV at 1,5dpf. **A** Stereo images and **B** Confocal images 40X magnification **C** At 3,5dpf also brain, eye vasculature where underdeveloped 10X magnification and **D** the SIV was absent or malformed. 20X magnification.

With 0.1 pmol P38α morpholino a significant pool of embryos can be distinguished displaying morphological defects where the ISV have not grown into DLAV compared to standard control morpholino injected embryos **Fig1b**. In addition, an enlargement of the intermediate cell mass (ICM) was clearly visible in P38α morpholino injected embryos. Scanning confocal microscopy revealed absence of the filopodia on the tip cells of growing ISV indicating defective endothelial cell migration in P38α morphants **Fig1c**. Endothelial cells of ISV appeared also more stretched in control embryos than in P38α morphants. The P38 morpholino phenotype on sprouting ISV was confirmed by the pan P38 inhibitor BIRB796 **Fig2**. When applied between 4-7 somite stage the inhibitor blocked sprouting of ISV from the dorsal aorta **Fig2a-b**. BIRB796 was also applied at 2dpf resulting in undeveloped head/eye vasculature. After this treatment the subintestinal vein (SIV) complex was malformed or completely absent at 3,5dpf **Fig2c-d**.
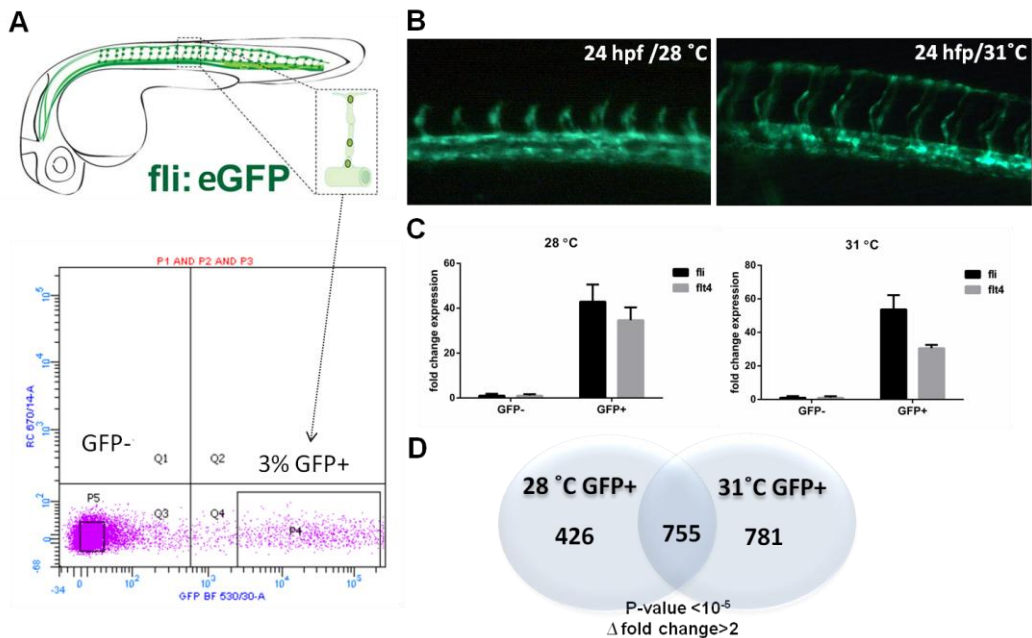
Fig3. GFP+ cells are FACs sorted from embryos for transcriptome profiling to discover endothelial genes important for physiological angiogenesis. **A** Single unattached cells were sorted (P1, P2 and P3) of which approximately 3% was GFP+ (P4) and 97% GFP- (P5). **B** WT 24hpf dissociation time point; Tg(Fli;GFP) embryos were kept o/n at either 28°C or 31°C. **C** Bar graph of Q-pcr results comparing fli and flt4 expression in RNA samples from sorted cells. Graphs are calculated from the mean of a biological duplicate. **D** number of transcripts identified and the number of overlapping transcripts. Threshold settings fold change >2 and p-value <10^{-5}.

Transcriptional analysis of fli expressing cells isolated from Tg(Fli:GFP)

To characterize the transcriptome of Fli expressing cells RNA from FACS sorted GFP+ cells was hybridized against GFP- RNA from Tg(Fli:GFP) on a 180k Agilent chip **Fig3**. Two stages of ISV development were analyzed at 24hpf. The first pool of embryos was kept overnight at 28°C and at 24hpf the ISV were still growing and did not connect to form the DLAV. In contrast, the second pool was kept overnight at 31°C and at 24hpf the ISV were fully grown and DLAV was formed **Fig3b.** Expression analysis of Fli1 and Flt4 with Quantitative PCR, comparing GFP+ against GFP-, confirmed successful sorting of endothelial cells and RNA quality used for transcriptome analysis **Fig3c**. In the 28°C grown embryos a total of 1181 genes were expressed with a fold change above 2 ($p<10^{-5}$) in GFP+ cells compared to GFP- cells. The transcriptome of the 31°C grown embryos consist of 1536 genes of which 755 overlapped with the 28°C embryo transcriptome.
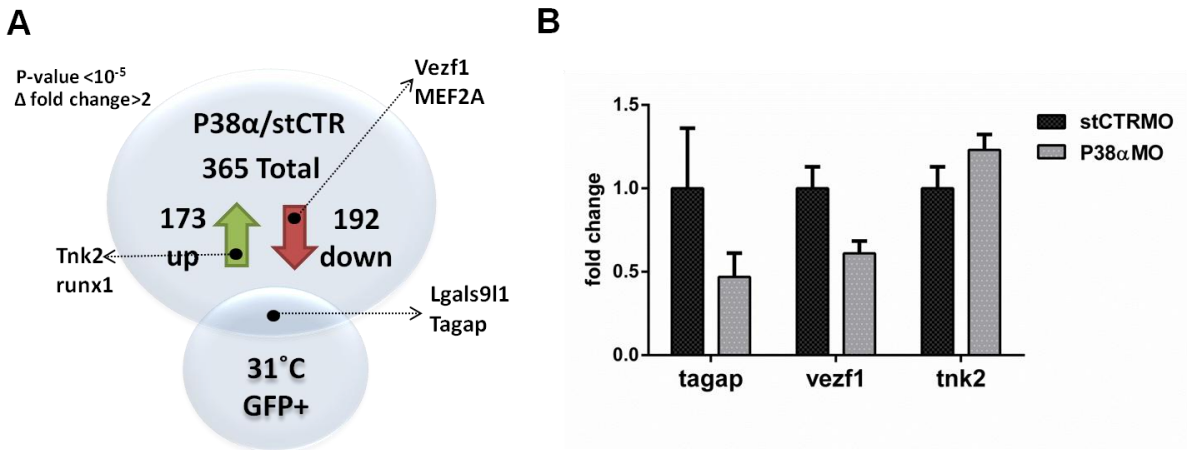
Fig4. Transcriptome profiling of P38α morphants displaying vascular defect. A Number of identified genes in 0.1pmol P38α morpholino injected embryos with some selected genes of interest. results are from a biological triplicates. **B** Bar graph of Q-PCR expression analysis of Tagap, Vezf1 and Tnk2. Means are calculated from a biological triplicate. Expression levels are normalized against the 18s reference gene.

Identification of P38α target genes involved in physiological angiogenesis

To identify the P38α target genes involved in physiological angiogenesis P38α morphants with delayed growth of ISV were snap-frozen in liquid nitrogen for transcriptome analysis. Standard control morpholino injected embryos were taken as a control. Under this unsaturated knock-down condition a total of 365 genes were identified as P38α dependant of which 173 upregulated and 192 downregulated compared to standard control morpholino. Tyrosine kinase, non-receptor, 2 (Tnk2) and runt-related transcription factor 1 (Runx1) were identified among the upregulated genes. The downregulated genes contained vascular

endothelial zinc finger 1 (Vezf1) and myocyte enhancer factor 2A (Mef2A). Embryos in this experiment were kept overnight at 31˚C. The P38α transcriptome could therefore be compared with the 31˚C transcriptome of sorted Fli:GFP+. The overlap contained 2 genes lectin, galactoside-binding, soluble, 9 (galectin 9)-like 1 (Lgal29l1) and T-Cell Activation GTPase-Activating Protein b (Tagapb) both downregulated. Results were validated with Q-PCR which was successful for all genes except Runx1 which is located at the telomere of chromosome 1 and specific primers could not be designed. Lgals9l1 and Mef2a displayed inconsistency between biological triplicates and Tnk2 showed a small fold change of 1,2. Tagap and Vezf1 were significantly downregulated in P38α morphants compared to standard control morpholino.

Discussion

The zebrafish contains all of the 14 MAPK identified so far in mammals including the four P38α isoforms. As the rodent and human cell culture experiments indicated previously, the angiogenesis process depends on P38α activation. In this study, we investigated the role of P38α in zebrafish embryonic angiogenesis. We observed that targeted knock-down of P38α, with gene specific morpholino in Tg(fli:EGFP) delayed the growth of intersegmental vessels significantly. Birb796, a chemical inhibiting all P38 isoforms, abolished the sprouting of ISV as well and was even more potent in inhibiting angiogenesis then the morpholino. The concentration of the morpholino was downscaled in order to prevent morphological abnormalities and therefore the downregulation of P38α mRNA was only partly effective. In addition, the possibility exists that all four P38 isoforms redundantly regulate angiogenesis in the zebrafish and therefore the phenotypes after Birb796 treatment were more severe. With transgenic zebrafish technology using a dominant negative mutant of P38α (and other isoforms) the specificity of the angiogenic phenotype can be further investigated. Also, by using promotors or control elements of endothelial specific marker expression such as fli, kdrl the question can be answered whether the defective growth of ISV is a result of P38α knockdown in the endothelial cells or due to knockdown in the surrounding tissue.

When visualizing the ISV in more detail we found in P38α morphants the lack of filopodia sprouts that are normally present on the tip cells. Since P38α influences the activity of transcription factors we performed transcriptome analysis to characterize this defect at the level of gene expression. Sorting out GFP+ cells from Tg(fli:EGFP) for transcriptome analysis against GFP- provided a gene list of hematopoietic, pharyngeal and endothelial marker genes. This list obtained using 180k Agilent chip is more complete then previously published list by group of Lawson and can be used as reference in the future research[24]. From comparison

110

of the P38α morpholino transcriptome with the GFP+/GFP- transcriptome we selected Tagapb as the endothelial expressed gene (zfin in situ data) downregulated by P38α morpholino.

Interestingly we also found the transcription factor Runx1 to be 6 fold upregulated in P38α morphants. Runx1 is critical for definitive haematopoiesis and known to prime the hemangioblast (blood precursor) or hemogenic endothelium for differentiation into hematopoietic stem cells [25-27]. Hemogenic endothelium is a unique population of vascular cells that could give rise to blood cells. Perhaps the increase of Runx1 expression is related to the expansion of the intermediate cell mass we observed in P38α morphants. In zebrafish at 24hpf Runx1 expression is present in the dorsal aorta, posterior blood island (ICM) but also in the nervous system. Explaining why we did not find Runx1 mRNA enriched in GFP+ cells sorted from Tg(fli:EGFP). Mammalian Runx1 has previously been found functional in neuronal axon outgrowth and guidance a process which greatly resembles the navigation of blood vessels during angiogenesis[28]. Multiple axonal guidance cues, such as the semaphorins, are also involved in the blood vessel guidance[29]. Since P38α is expressed in the most tissues and also associated with neurite outgrowth it is likely to regulate downstream genes critical for angiogenesis even tough not exclusively expressed in endothelial cells[30]. Vezf1 is selected from the P38α morpholino transcription profile and are interesting for further functional studies in zebrafish. Vezf1 is a zinc finger transcription factor that regulates endothelial sprouting and organizes the vascular network [31].

Conclusion

Similarly as in mammals, zebrafish angiogenesis depends on P38 activity. However the endothelial cell autonomous specific function of P38α needs to be further addressed.   P38α morpholino reduces the expression of Tagapb of which expression is concentrated in endothelial cells. Furthermore, the expression of Runx1 is increased in P38α morphants. P38α signalling leads therefore to the suppression of this gene in endothelial, hematopeotic or hematopeitic endothelial cells. Since the molecular mechanisms of hemogenic endothelium differentiation is not well defined yet it is worth investigating the role of P38α in this process.

Reference List

1. Bolcome RE, III, Chan J: Constitutive MEK1 activation rescues anthrax lethal toxin-induced vascular effects in vivo. *Infect Immun* 2010, 78:5043-5053.

2. Chopra AP, Boone SA, Liang X, Duesbery NS: Anthrax lethal factor proteolysis and inactivation of MAPK kinase. *J Biol Chem* 2003, 278:9402-9406.

3. Depeille PE, Ding Y, Bromberg-White JL, Duesbery NS: MKK signaling and vascularization. *Oncogene* 2007, 26:1290-1296.

4. Adams RH, Porras A, Alonso G, Jones M, Vintersten K, Panelli S, Valladares A, Perez L, Klein R, Nebreda AR: Essential role of p38alpha MAP kinase in placental but not embryonic cardiovascular development. *Mol Cell* 2000, 6:109-116.

5. Mudgett JS, Ding J, Guh-Siesel L, Chartrain NA, Yang L, Gopal S, Shen MM: Essential role for p38alpha mitogen-activated protein kinase in placental angiogenesis. *Proc Natl Acad Sci U S A* 2000, 97:10454-10459.

6. Whitmarsh AJ: A central role for p38 MAPK in the early transcriptional response to stress. *BMC Biol* 2010, 8:47.

7. Roux PP, Blenis J: ERK and p38 MAPK-activated protein kinases: a family of protein kinases with diverse biological functions. *Microbiol Mol Biol Rev* 2004, 68:320-344.

8. Krens SF, Spaink HP, Snaar-Jagalska BE: Functions of the MAPK family in vertebrate-development. *FEBS Lett* 2006, 580:4984-4990.

9. Krens SF, He S, Spaink HP, Snaar-Jagalska BE: Characterization and expression patterns of the MAPK family in zebrafish. *Gene Expr Patterns* 2006, 6:1019-1026.

10. Pearson G, Robinson F, Beers GT, Xu BE, Karandikar M, Berman K, Cobb MH: Mitogen-activated protein (MAP) kinase pathways: regulation and physiological functions. *Endocr Rev* 2001, 22:153-183.

11. Morrison DK: MAP kinase pathways. *Cold Spring Harb Perspect Biol* 2012, 4.

12. Yang J, Boerm M, McCarty M, Bucana C, Fidler IJ, Zhuang Y, Su B: Mekk3 is essential for early embryonic cardiovascular development. *Nat Genet* 2000, 24:309-313.

13. Rousseau S, Houle F, Landry J, Huot J: p38 MAP kinase activation by vascular endothelial growth factor mediates actin reorganization and cell migration in human endothelial cells. *Oncogene* 1997, 15:2169-2177.

14. Lamalice L, Houle F, Jourdan G, Huot J: Phosphorylation of tyrosine 1214 on VEGFR2 is required for VEGF-induced activation of Cdc42 upstream of SAPK2/p38. *Oncogene* 2004, 23:434-445.

15. Gee E, Milkiewicz M, Haas TL: p38 MAPK activity is stimulated by vascular endothelial growth factor receptor 2 activation and is essential for shear stress-induced angiogenesis. *J Cell Physiol* 2010, 222:120-126.

16. Issbrucker K, Marti HH, Hippenstiel S, Springmann G, Voswinckel R, Gaumann A, Breier G, Drexler HC, Suttorp N, Clauss M: p38 MAP kinase--a molecular switch between VEGF-induced angiogenesis and vascular hyperpermeability. *FASEB J* 2003, 17:262-264.

17. Lamalice L, Houle F, Huot J: Phosphorylation of Tyr1214 within VEGFR-2 triggers the recruitment of Nck and activation of Fyn leading to SAPK2/p38 activation and endothelial cell migration in response to VEGF. *J Biol Chem* 2006, 281:34009-34020.

18. McMullen M, Keller R, Sussman M, Pumiglia K: Vascular endothelial growth factor-mediated activation of p38 is dependent upon Src and RAFTK/Pyk2. *Oncogene* 2004, 23:1275-1282.

19. Pin AL, Houle F, Guillonneau M, Paquet ER, Simard MJ, Huot J: miR-20a represses endothelial cell migration by targeting MKK3 and inhibiting p38 MAP kinase activation in response to VEGF. *Angiogenesis* 2012, 15:593-608.

20. Kawamura H, Li X, Goishi K, van Meeteren LA, Jakobsson L, Cebe-Suarez S, Shimizu A, Edholm D, Ballmer-Hofer K, Kjellen L et al.: Neuropilin-1 in regulation of VEGF-induced activation of p38MAPK and endothelial cell organization. *Blood* 2008, 112:3638-3649.

21. Matsumoto T, Turesson I, Book M, Gerwins P, Claesson-Welsh L: p38 MAP kinase negatively regulates endothelial cell survival, proliferation, and differentiation in FGF-2-stimulated angiogenesis. *J Cell Biol* 2002, 156:149-160.

22. Jagielska J, Kapopara PR, Salguero G, Scherr M, Schutt H, Grote K, Schieffer B, Bavendiek U: Interleukin-1 assembles a proangiogenic signaling module consisting of caveolin-1, tumor necrosis factor receptor-associated factor 6, p38-mitogen-activated protein kinase (MAPK), and MAPK-activated protein kinase 2 in endothelial cells. *Arterioscler Thromb Vasc Biol* 2012, 32:1280-1288.

23. Morioka S, Inagaki M, Komatsu Y, Mishina Y, Matsumoto K, Ninomiya-Tsuji J: TAK1 kinase signaling regulates embryonic angiogenesis by modulating endothelial cell survival and migration. *Blood* 2012, 120:3846-3857.

24. Covassin L, Amigo JD, Suzuki K, Teplyuk V, Straubhaar J, Lawson ND: Global analysis of hematopoietic and vascular endothelial gene expression by tissue specific microarray profiling in zebrafish. *Dev Biol* 2006, 299:551-562.

25. Crosier PS, Kalev-Zylinska ML, Hall CJ, Flores MV, Horsfield JA, Crosier KE: Pathways in blood and vessel development revealed through zebrafish genetics. *Int J Dev Biol* 2002, 46:493-502.

26. Kalev-Zylinska ML, Horsfield JA, Flores MV, Postlethwait JH, Vitas MR, Baas AM, Crosier PS, Crosier KE: Runx1 is required for zebrafish blood and vessel

development and expression of a human RUNX1-CBF2T1 transgene advances a model for studies of leukemogenesis. *Development* 2002, 129:2015-2030.

27. Sakai E, Kitajima K, Sato A, Nakano T: Increase of hematopoietic progenitor and suppression of endothelial gene expression by Runx1 expression during in vitro ES differentiation. *Exp Hematol* 2009, 37:334-345.

28. Marmigere F, Montelius A, Wegner M, Groner Y, Reichardt LF, Ernfors P: The Runx1/AML1 transcription factor selectively regulates development and survival of TrkA nociceptive sensory neurons. *Nat Neurosci* 2006, 9:180-187.

29. Autiero M, De SF, Claes F, Carmeliet P: Role of neural guidance signals in blood vessel navigation. *Cardiovasc Res* 2005, 65:629-638.

30. Watanabe H, Hongu T, Yamazaki M, Kanaho Y: Phospholipase D2 activation by p38 MAP kinase is involved in neurite outgrowth. *Biochem Biophys Res Commun* 2011, 413:288-293.

31. Zou Z, Ocaya PA, Sun H, Kuhnert F, Stuhlmann H: Targeted Vezf1-null mutation impairs vascular structure formation during embryonic stem cell differentiation. *Arterioscler Thromb Vasc Biol* 2010, 30:1378-1388.

CHAPTER VI

General Discussion

General discussion

The Mitogen activated protein kinase (MAPK)family is engaged in complex networks of signal transduction orchestrating cellular behaviours such as proliferation, differentiation, migration and apoptosis. MAPK signalling depends highly on the cellular environment as the cascades can respond to different extracellular cues. What adds also to signalling complexity is the presence of various MAPK family members and isoforms which can be functionally redundant in one cellular context while differing in another context where they can even antagonize each other. In addition, several factors such as the presence and abundance of activated receptors, presence of scaffold or adaptor proteins, or crosstalk with other pathways, collectively fine tune the duration and magnitude of MAPK signals to direct a precise cellular response. Giving this complexity, precise elucidation of the molecular mechanisms underlying MAPK associated cellular processes or pathologies remains challenging.

The use of multiple experimental models is valuable to discover MAPK conserved functions among species. In this thesis the zebrafish model is used for further understanding the role of MAPK protein family in embryogenesis. Since most MAPK proteins are conserved within vertebrates the zebrafish is a suitable model to study functional redundancies and specialisations between different members during development. Firstly we have approached this study by applying probes to display specific tissue expression of different MAPK genes. Secondly, we have developed tools to up-regulate and down-regulate MAPK cascades by generating mutants with increased kinetic activity and by using morpholino knockdown, dominant negative mutants or chemical inhibitors.

ChapterII

Activated forms of the upstream ERK kinases RAF and RAS were used for the study of cell transformation and for discovery of anti-cancer drugs. Being part of the RAS-RAF-MEK1/2-ERK1/2 cascade, ERK2 is often hyperactivated in tumors harbouring oncogenic EGFR, RAF and RAS mutations[1]. However this cascade is a core module within a complex signalling network involving positive and negative signalling loops, isoform availability and crosstalk with other cascades. To understand isoform specific signalling differences between ERK1 and ERK2 in development and tumor formation we constructed intrinsically activated forms refractory to inhibition (chapter II). Since naturally occurring activating mutations in ERK have never been identified in cancer patients, developing artificial constitutively activated mutants was necessary. Giving its physiological functional importance and involvement in severe pathologies, ERK2 was an interesting subject for former

structural studies using crystallographic methods[2;3]. The activated (phosphorylated) structure and inactivated (unphosphorylated) ERK2 structure were solved and an overlap revealed the conformational changes, resulting from phosphorylation of the dual phosphorylation site, that facilitate kinase activity and make the protein more accessible for substrate binding. Phosphorylation of the dual phosphorylation site of ERK2 triggers a complex reorganization of hydrogen bounds between amino acids resulting i.a. in the positioning of the activesite. Increasing ERK2 kinetic activity with a simple strategy was impossible and mutational screening for constitutive active mutants were carried out to identify mutations that mimic this effect. *Brunner et al.* was successful in developing an active mutant of the Drosophila ERK2 ortholog Rolled by mutating the docking domain on ERK2 recognised by inhibiting phosphatases (D330N zebrafish)[4]. This mutation was called the sevenmaker mutation and the mutation site was conserved among various species. Furthermore, other gain-of function mutations were published from yeast genetic screens of Fus3. *Emrick et al.2001* measured the *in vitro* kinetic activity of yeast ERK2 double and triple mutant combinations relative to ERK2 basal activity and we have selected the most potent combinations for generating similar constitutively active zebrafish ERK2 mutants[5].

We inserted the same mutations in ERK1 and we found the triple mutant, including the sevenmaker mutation (D352N zebrafish), to increase ERK1 phophorylation *in vitro*. However, we could not measure any differences in the phosphorylation of P90RSK or CREB which are known ERK1/2 substrates. ERK1 and ERK2 are more than 80% identical, yet when targeted for gene disruption ERK2 deficiency appears to results in dramatic effects while ERK1 seems to be dispensable for cell physiology. Two hypotheses are proposed stating i) that differences in expression levels between the low expressed ERK1 and the abundantly present ERK2 is the main and exclusive reason for the observed functional differences[6] or ii) that ERK1 signalling to the nucleus is less efficient than ERK2 and acts as a partial agonist in the ERK1/2 cascade[7]. A partial agonist binds the same upstream activators as the full agonist (ERK2), however, this is less efficient to transmit the signal further downstream of the cascade. The slow ERK1 activity becomes more significant in situations of prolonged cascade stimulation and high demand of activated ERK1/2. In support for this second hypothesis, ERK1 depletion in wild-type conditions is compensated by increased phosphorylation of ERK2 and has no effect on cell proliferation. However, proliferation of oncogenic H-Ras^{Q61L} transformed cells with hyperactivated ERK2 was inhibited by ERK1 overexpression. This suggests that ERK1, as a partial agonist of ERK2, protects cells from excessive proliferation. Differences in ERK1 and ERK2 downstream signaling can be explained by the demonstrated less efficient cytoplasmic/nuclear translocation of ERK1[8;9].

The partial agonist model may also explain the relationship between two other MAPK protein studied in this thesis, the P38α and P38β isoforms, which are 75% homologous and share upstream and downstream kinases. P38α is essential for embryonic development while mice lacking P38β survive normally and do not show any obvious phenotype[10;11]. P38α plays a key role in various developmental processes (myoblast differentiation, neural differentiation, survival, cell migration, proliferation and cytokine production) while P38β function within the Mekk3/6-P38α/β cascade seems to be insignificant[12]. Over activation of P38s is believed to be part of the cause for various inflammatory diseases, including inflammatory bowel diseases and rheumatoid arthritis, as well as for congestive heart failure and breast cancer[13-15]. It would be interesting and valuable to know if P38β acts as a partial agonist of P38α signalling during these processes especially in cytokine biogenesis. There are gain- of function mutations published for all P38 isoforms potentially useful to engineer the corresponding zebrafish proteins[16;17]. Transgenic zebrafish stably expressing such mutated P38 MAPKs will be valuable for future developmental and disease studies.

ChapterIII

All P38 MAPK isoforms are maternally expressed and, except for P38δ, the level of expression, remains constant during embryonic development. P38δ mRNA was detected for the first time at 16 cell stage. Interestingly, we found all P38 isoforms to be expressed in the brain of the zebrafish including the P38α and P38β isoforms of which expression was demonstrated previously in the adult mouse brain[18]. These results suggest that the P38 pathway may play an important role in the development and/or normal physiology of the brain. P38α/β is found to play a role in synaptic plasticity in the hippocampus[19;20]. The functions of the other isoforms in the brain are not known yet. The transcriptome data of the P38α morpholino knock-down embryos (Chapter IV) included a gene pool associated to the nervous system such as Neuropillin 2b, Fgf4, Elavl3, Actn3a, Stathmin, Ceruloplasmin, Lhx5, Ncam and Gbx-2 which were down-regulated and the upregulated Emx1, Crx, Camk4, Mxtx1, Bdnf protein, Her8a, Her11, Endothelin type A, Dishevelled 1b (dvl1b), Vega2, opcml, Isl1, Asl1b, reticulon 1, Jagged 1b, Fbln5 and zic3. This genes list includes possible direct target genes of P38α functioning in the nervous system development and neuronal physiology and when validated will give more insight into the role of P38α in this process. It would be interesting to compare with transcriptome data of other MAPK family members to reveal specificity.

 In future research it would be interesting to perform quantitative PCR analysis to detect P38 isoform expression relative to each other. Once having developed reliable P38 isoform specific probes, primers and antibodies expression data can be

obtained in different *in vivo* contexts. Expression analysis can be combined with functional studies involving treatment of zebrafish with stressors such inflammatory cytokines, bacteria, wounding, irradiation etc. to determine possible changes in expression. To analyze protein translation and activation isoform specific antibodies are necessary. These are currently available for the P38α isoform. Structural alignment of the P38 isoforms revealed a mutation prone domain which can be exploited to develop specific antibodies. The P38α and P38β isoforms share the highest sequence similarity and since phospho-P38α specific antibodies have been developed it should also be possible to obtain such antibodies for the β, δ and γ isoforms.

Chapter IV

The function of ERK2 in development was investigated in mouse, drosophila, sea urchin, xenopus and zebrafish models leading to the key finding of a conserved ERK2 cascade downstream of FGF regulating trophoblast differentiation and gastrulation cell movements in the first embryonic stages[21]. Later on the pathway is involved in formation of branchial arches, migrating neural crest cells, the midbrain/hindbrain boundary and forebrain[22]. The role of P38α in developmental processes has been predominantly studied in the relation to skeletal muscle development[23]. However, in zebrafish we have previously demonstrated the expression of all P38 isoforms, including P38α, in specific regions of the developing brain suggesting a role of this MAPK subfamily in development of the central nervous system as well. As already mentioned several genes important for neurogenesis were affected by P38α morpholino knock-down (Chapter IV). Some of these genes, Zic3, Fgf4, Elavl3, Her11, Stmn, Lhx5, Ncam, Vega2, Asl1b are also present in the ERK2 morpholino transcriptome which also includes Flh, Zic2, Hxb8a, Tcf12, Rx3, Gsc, Barhl2, Efna-L1, Cp, Irx1b, Rtn3, Dlc, Cxcr4, Dlx1a, irx7, Otx1a, Acha from the ERK2 specific pool. Neural crest cells arise from the edges of the nascent central nervous system, a domain called the neural plate border (NPB). ERK2 and P38α might be both involved in this process by stringing along in regulation of zic3 expression as Zic2 and Zic3 proteins function in specification of the NPB. Finally, both the P38 and ERK2 MAPK are expressed at the margin of the blastoderm prior and during epiboly and knock-down results in arrested embryos failing to initiate this process. We found a number of epiboly functional genes concurrent and specifically affected by P38α and ERK2 morpholino knockdown. Altogether our transcriptome data indicates that ERK2 function in development is partly redundant with the P38α MAPK which is an interesting finding for further validation using other genetic tools. It remains a question whether the specific pools of target genes deduced from P38α/ERK2 knock down comparisons contain genes that are regulated by the other MAPK family members.

Unlike other vertebrates, the zebrafish contains two copies of the P38α gene and we have found that morpholino knock-down of P38αA or P38αB results in epiboly arrested phenotypes (data not shown). As expected, reduced presence of P38α protein but not Erk2 was detected in P38αA morphants with western blotting using a gene duplicate aspecific antibody. However, a down-regulation of P38α was detected in Erk2 morphants and since the anti-P38α antibody does not distinguish between the two genes it was not clear from the biochemical analysis data which one is down-regulated in Erk2 morphants. We have performed transcriptome analysis of P38αB morphants (data not shown) and the transcriptome largely overlaps with Erk2 transcriptome data. Considering that we do identify a large pool of P38αA specific regulated genes it is likely that P38αB is down-regulated in Erk2 morphants and not P38αA. Data presented in this report and further discussion is about the P38αA gene unless otherwise indicated.

Chapter V

Using genetic and chemical tools we demonstrated that P38α is functional in zebrafish angiogenesis. With unsaturated P38 morpholino knockdown conditions we found 4 genes (Annexin1, Tnk2, Runx1, Vezf1) to be effected. Three of them are previously implicated in angiogenesis and one (Tagap) with expression enriched in the vasculature having an undescribed function in this process. The concentration of the morpholino was down scaled to circumvent severe morphological defects with the disadvantage that many P38α regulated genes were most likely not picked up by microarray transcriptomics. However, this limited number of effected genes is interesting for further validation experiments to identify P38α target genes and understand the role of this MAPK family in angiogenesis. P38α was proposed to have a tumor suppression function by activating several cell cycle checkpoint proteins including P53[24;25]. The role of P38α in tumor progression has two sides since P38α promotes tumor angiogenesis and metastasis. A detailed understanding of cell type specific P38α signalling will be valuable for designing new drug that intervene in steps in cancer development in which the P38 proteins play a role.

We have isolated GFP+ cells of pharmacological treated Tg(fli:EGFP) embryos by FACS for transcriptional profiling. This method would be valuable to determine cell type specific effects after pharmacological treatment. Zebrafish xeno-transplants are being used for high-throughput chemical screens for anti-cancer drugs. With the growing repertoire of zebrafish transgenic lines, that mark specific cell types or stages of immature differentiating cells based on identified marker genes, the treatment effects can be analyzed in detail. We treated Tg(fli:EGFP) embryos with Birb796, an P38 inhibitor severely impeding angiogenesis, in the trunk and head.

cDNA samples of sorted GFP+ cells were hybridised on a 180k Agilent array for transcriptome analysis. We also hybridised samples from GFP+ cells against GFP-cells and obtained a pool of genes of which expression is enriched in pharyngeal arch, hematopoietic or endothelial cells. These comparisons indentified a high number of genes with high fold changes compared to control samples representing tissues from the entire organism which could be validated with Q-pcr. Q-pcr analysis of Fli, Flt4 and Tbx6 indicates that after FACS sorting different ratios of endothelial and blood cell populations were obtained. The ratio differences could have been the result of a sampling error that presumably overshadows the treatment effect but did not interfere with the detection of transcripts with significantly high fold changes. Optimalization of sampling conditions to obtain samples with constant ratios of cell populations is therefore necessary for this experiment.

Conclusion

The capacity to predict treatment outcomes is highly depending on understanding molecular mechanisms of disease associated cellular processes. Tools to manipulate activity, or study expression and activity of one particular protein allow researchers to draw a precise map of the molecular events. Giving the existence of multiple MAPK variants and the divers cellular processes that are regulated, extensive input and different approaches of research is necessary to tackle the yet unknown facts regarding this protein family. How is MAPK signalling translated into different cellular behaviours such as proliferation, differentiation and migration? What are the mechanisms that control MAPK signalling localization, duration and amplitude in such a way to favour and sustain a particular cellular state. Finally how does deregulation of these mechanisms lead to disease.

This thesis was produced within the scope of the research interest of the Molecular Cell Biology department of Leiden University in the Netherlands which has a background investigating the MAPK pathway in development and cancer using the zebrafish. With the current study we provided new tools to mimic uncontrolled ERK2 activity found in tumours and to investigate the exact role of this MAPK family member in cell transformation. We have completed cloning and expression analysis of the P38 MAPK subfamily in zebrafish and provided a basis for research on isoform specific functions. Both P38α and ERK2 are essential for zebrafish epiboly and by comparing the transcriptome profiles of knock-down embryos we identified epiboly associated genes of which are commonly or specifically regulated by the two MAPK. Finally we have demonstrated that P38α is also functional in migration of endothelial cells during angiogenesis and we identified candidate target genes that are possible involved in this process. Using different approaches we aimed to

make use of the many advantages of the zebrafish and combine the fields of developmental and tumour biology by focusing on the MAPK pathway.

Reference List

1. Roberts PJ, Der CJ. Targeting the Raf-MEK-ERK mitogen-activated protein kinase cascade for the treatment of cancer. Oncogene 2007;26:3291-3310.

2. Canagarajah BJ, Khokhlatchev A, Cobb MH, Goldsmith EJ. Activation mechanism of the MAP kinase ERK2 by dual phosphorylation. Cell 1997;90:859-869.

3. Zhang F, Strand A, Robbins D, Cobb MH, Goldsmith EJ. Atomic structure of the MAP kinase ERK2 at 2.3 A resolution. Nature 1994;367:704-711.

4. Brunner D, Oellers N, Szabad J et al. A gain-of-function mutation in Drosophila MAP kinase activates multiple receptor tyrosine kinase signaling pathways. Cell 1994;76:875-888.

5. Emrick MA, Hoofnagle AN, Miller AS, Ten Eyck LF, Ahn NG. Constitutive activation of extracellular signal-regulated kinase 2 by synergistic point mutations. J.Biol Chem. 2001;276:46469-46479.

6. Lefloch R, Pouyssegur J, Lenormand P. Single and combined silencing of ERK1 and ERK2 reveals their positive contribution to growth signaling depending on their expression levels. Mol.Cell Biol 2008;28:511-527.

7. Vantaggiato C, Formentini I, Bondanza A et al. ERK1 and ERK2 mitogen-activated protein kinases affect Ras-dependent cell signaling differentially. J.Biol 2006;5:14.

8. Harrington HA, Komorowski M, Beguerisse-Diaz M, Ratto GM, Stumpf MP. Mathematical modeling reveals the functional implications of the different nuclear shuttling rates of Erk1 and Erk2. Phys.Biol 2012;9:036001.

9. Shankaran H, Ippolito DL, Chrisler WB et al. Rapid and sustained nuclear-cytoplasmic ERK oscillations induced by epidermal growth factor. Mol.Syst.Biol 2009;5:332.

10. Kuida K, Boucher DM. Functions of MAP kinases: insights from gene-targeting studies. J.Biochem. 2004;135:653-656.

11. Mudgett JS, Ding J, Guh-Siesel L et al. Essential role for p38alpha mitogen-activated protein kinase in placental angiogenesis. Proc.Natl.Acad.Sci.U.S.A 2000;97:10454-10459.

12. Aouadi M, Binetruy B, Caron L, Le Marchand-Brustel Y, Bost F. Role of MAPKs in development and differentiation: lessons from knockout mice. Biochimie 2006;88:1091-1098.

13. Cuadrado A, Nebreda AR. Mechanisms and functions of p38 MAPK signalling. Biochem.J. 2010;429:403-417.

14. Kyriakis JM, Avruch J. Mammalian MAPK signal transduction pathways activated by stress and inflammation: a 10-year update. Physiol Rev. 2012;92:689-737.

15. Tourian L, Jr., Zhao H, Srikant CB. p38alpha, but not p38beta, inhibits the phosphorylation and presence of c-FLIPS in DISC to potentiate Fas-mediated caspase-8 activation and type I apoptotic signaling. J.Cell Sci. 2004;117:6459-6471.

16. Askari N, Diskin R, Avitzour M et al. Hyperactive variants of p38alpha induce, whereas hyperactive variants of p38gamma suppress, activating protein 1-mediated transcription. J.Biol Chem. 2007;282:91-99.

17. Avitzour M, Diskin R, Raboy B et al. Intrinsically active variants of all human p38 isoforms. FEBS J. 2007;274:963-975.

18. Maruyama M, Sudo T, Kasuya Y et al. Immunolocalization of p38 MAP kinase in mouse brain. Brain Res. 2000;887:350-358.

19. Guan Z, Kim JH, Lomvardas S et al. p38 MAP kinase mediates both short-term and long-term synaptic depression in aplysia. J.Neurosci. 2003;23:7317-7325.

20. Aouadi M, Bost F, Caron L et al. p38 mitogen-activated protein kinase activity commits embryonic stem cells to either neurogenesis or cardiomyogenesis. Stem Cells 2006;24:1399-1406.

21. Krens SF, Spaink HP, Snaar-Jagalska BE. Functions of the MAPK family in vertebrate-development. FEBS Lett. 2006;580:4984-4990.

22. Samuels IS, Saitta SC, Landreth GE. MAP'ing CNS development and cognition: an ERKsome process. Neuron 2009;61:160-167.

23. Keren A, Bengal E, Frank D. p38 MAP kinase regulates the expression of XMyf5 and affects distinct myogenic programs during Xenopus development. Dev.Biol 2005;288:73-86.

24. Hui L, Bakiri L, Mairhorfer A et al. p38alpha suppresses normal and cancer cell proliferation by antagonizing the JNK-c-Jun pathway. Nat.Genet. 2007;39:741-749.

25. Hui L, Bakiri L, Stepniak E, Wagner EF. p38alpha: a suppressor of cell proliferation and tumorigenesis. Cell Cycle 2007;6:2429-2433.

CHAPTER VII

Nederlandse samenvatting

De functies van P38 en ERK kinasen in de vroege ontwikkeling van de zebrafish

Mitogen activated protein kinases (MAPK) vormen een eiwitfamilie, die een rol speelt in de signaaltransductie van de cel. Het zijn kinase enzymen die de overdracht van een fosfaat groep van ATP naar substraten katalyseren en het substraat wordt daarbij geactiveerd. De MAPK eiwitfamilie komt voor in alle eukaryoten en er zijn maar liefst 14 isovormen geïdentificeerd in gewervelden. MAPK functioneren in cascades van eiwitten die signalen overdragen vanuit het celmembraan naar andere compartimenten van de cel om een cellulaire respons te genereren t.g.v. veranderingen in de micro-omgeving. De nucleus is een van de cellulaire organen waar MAPK zich naartoe verplaatsen na activatie. MAPK beïnvloeden in de nucleus de activiteit van transcriptie factoren en daarmee de expressie van genen. Er zijn drie MAPK subgroepen te onderscheiden namelijk de extracellular signal regulated kinases (Erk1,2,3,4,5,6,7), de c-Jun amino-terminal kinases (Jnk1/2/3) en de P38 MAPK (α,β,γ, and Δ).

Er is tot heden ongeveer dertig jaar onderzoek verricht om de functies van MAPK eiwitten in diverse cellen en onder verschillende condities te achterhalen en er is aanzienlijk veel informatie verworven. Extracellulaire stimulansen, membraaneiwitten (receptoren), substraten en overige eiwit interacties die de cascade beïnvloeden zijn geïdentificeerd en goed in kaart gebracht voor enkele isovormen. Het meeste informatie is verworven met betrekking tot Erk2 en P38α MAPK. Deze twee MAPK zijn met name interessant omdat ze essentieel zijn gebleken voor verschillende cellulaire functies. Afwijkende Erk2 en P38α activiteit wordt geassocieerd met verschillende aandoeningen. Erk2 reguleert, als gevolg van stimulering met groeifactoren, de celdeling en in verschillende vormen van kanker (bijvoorbeeld melanoma) is de Erk2 cascade hyperactief aanwezig. De P38α MAPK cascade wordt voornamelijk door stress signalen gestimuleerd zoals endotoxinen, DNA beschadigende radiatie, osmotische stress, en functioneert o.a in de aanmaak van cytokinen. Cytokinen zijn eiwitten die een belangrijke functie vervullen in het immuunsysteem maar ook ontstekingen kunnen veroorzaken. P38α is betrokken bij verschillende ontsteking gerelateerde aandoeningen zoals rheumatoid arthiritis. Tevens vervullen Erk2 en P38α een essentiële rol in de vroege ontwikkeling van zoogdieren. Muis embryos waarvan het Erk2 of P38α ontbreekt overlijden in een zeer vroeg stadium gedurende de eerste 11 dagen na fertilisatie. Alhoewel er veel bekend is over beide eiwitten is het nog onduidelijk hoe verschillende MAPK isovormen gemeenschappelijk betrokken zijn bij cellulair processen die vaak door een combinatie van meerdere signaaltransductie cascades worden gereguleerd. Door verder onderzoek te doen naar specifieke en overeenkomstige functies van MAPK isovormen ontstaat er meer duidelijkheid over de rol van eiwitfamilies in de

ontwikkeling en handhaving van (specifieke) karaktereigenschappen van cellen. Om MAPK gerelateerde aandoeningen beter te begrijpen en behandelingen te ontwikkelingen, is het tevens van belang om de functies van afzonderlijke MAPK te onderzoeken.

Wij zijn daarom geïnteresseerd in de specifieke rol van MAPK in embryologische processen om uiteindelijk meer inzicht te krijgen in de pathogenese van tumoren. Tumor en embryonale cellen hebben de capaciteit om continue te delen en de cellulaire mechanismen die bedoeld zijn om de celdeling te beperken ontbreken. Daarbij zijn het ongespecialiseerde cellen die niet volledig gedifferentieerd zijn tot een celtype met een specifieke functionaliteit zoals erytrocyt, endotheelcel of een hepatocyt. Wanneer muizen getransplanteerd worden met embryonale stamcellen ontstaan er teratomas, tumoren bestaande uit verschillende soorten weefsels. Ook op moleculair niveau blijken bepaalde eiwitten met een essentiële functie in embryologie betrokken te zijn bij de metastasering van tumoren. De MAPK eiwitfamilie is bijvoorbeeld betrokken bij zowel embryologische processen als kanker en door deze eiwitfamilie als uitgangspunt te nemen kunnen we een relatie leggen tussen deze twee processen op moleculair niveau. We gebruiken de zebravis vanwege de praktische voordelen die het een geschikt model organisme maken voor embryologisch en kanker onderzoek. Een zebravis paar kan 200-300 bevruchte eitjes leggen na een periode van 10 uur donker wat de mogelijkheid biedt om een significant aantal embryo's van een gewenste embryonale stadium te verzamelen voor een experiment. De ontwikkeling van zebravis embryo's geschied extern van de zebravis waardoor de morfogenese microscopisch gevolgd kan worden. Binnen een dag zijn de meeste organen ontwikkeld en is het bevruchte eitje uitgegroeid tot een herkenbaar visje. Zebravis embryo's zijn transparant en kunnen geïnjecteerd worden met stoffen of getransplanteerd worden met (tumor) cellen. Dit proefschrift is een vervolg van eerder verricht onderzoek van Dr. Krens (Proefschrift: The mitogen activated protein kinases in zebrafish development) en omvat de resultaten van vier verschillende projecten naar de rol van MAPK eiwitten in de ontwikkeling van zebravissen.

Om de hyperactiviteit van Erk2 in tumor cellen na te bootsen hebben we, met het project beschreven in hoofdstuk II, mutanten ontwikkeld met een verhoogde kinetische activiteit. Dit is gebeurd door specifieke puntmutaties te introduceren in Erk2, bedoeld om de eiwitstructuur zodanig te veranderen dat autofosforylering mogelijk wordt en inactiveren wordt belemmerd. Constructen met genen coderend voor gemuteerde en wild type Erk2 zijn getransfecteerd in zebravis fibroblast cellen en ik heb aangetoond dat de mutanten een verhoogde capaciteit hebben om reeds bekende substraten te fosforyleren. Daarnaast is de verhoogde kinetische activiteit gevalideerd in zebravis embryo's. Er is mRNA gesynthetiseerd, gebruik makend van

de Erk2 constructen, en geïnjecteerd in embryo's van transgene zebravissen die het groen fluorescerend eiwit (GFP) produceren onder controle van de promotor van het Dusp6 gen. De Dusp6 promotor wordt beïnvloed door signalen van de ERK2 cascade en een verandering in de activiteit van deze cascade is kwantitatief vast te leggen in deze transgene zebravissen door het GFP signaal te detecteren. De mutant met drie geïntroduceerde punt mutaties heeft een sterke verhoging van het GFP signaal veroorzaakt en is verder gebruikt om de effecten van verhoogde Erk2 activiteit te bepalen m.b.v. peptide microarrays. Lysaten van embryo's geïnjecteerd met RNA coderend voor de drievoudige mutant veroorzaken een verhoogde fosforylering van het CDK1 eiwit dat betrokken is bij de celdeling. Hierdoor concluderen wij dat de drievoudige mutant gebruikt kan worden om Erk2 hyperactivatie te creëren in specifieke cellijnen van de zebravis om mogelijke gevolgen voor celdeling en cel transformatie te bestuderen.

In hoofdstuk III hebben we het expressiepatroon van P38β en P38δ gedurende de ontwikkeling van de zebravis bestudeerd. P38β RNA is detecteerbaar vanaf de zygote, wordt maternaal overgedragen en blijft detecteerbaar gedurende een reeks aan stadia, tussen zygoot tot vijf dagen post fertilisatie, van ontwikkeling. P38β expressie is gelokaliseerd in het brein, hart en de lens. P38δ wordt niet maternaal overgedragen en het expressiepatroon is meer variabel tijdens de vroege zebravis ontwikkeling. P38δ komt tot expressie in het chondrocranium, borstvinnen, brein, voorlopers van de kieuwen, darm, en mogelijk de groeiende venen.

P38α en Erk2 zijn twee MAPK die essentieel zijn voor cel migratie processen die belangrijk zijn voor de gastrulatie een proces waarbij embryonale cellen differentiëren tot drie kiemlagen het mesoderm, ectoderm en endoderm. In hoofdstuk IV is aangetoond dat het injecteren van stoffen die de translatie van Erk2 of P38α RNA blokkeren resulteert in een volledige remming van de celmigratie van embryonale cellen, en daardoor ook de gastrulatie. Omdat beide MAPK betrokken zijn bij dit proces hebben we verder onderzocht hoe de stoffen de embryos zodanig beïnvloeden dat de ontwikkeling wordt geremd. Met transcriptome microarrays hebben we genen geidentificeerd die een rol spelen in de embryonale celmigratie. De genen worden ofwel door Erk2 en P38α gemeenschappelijk gereguleerd danwel afzonderlijk. Tevens was de expressie van een aanzienlijk aantal genen coderend voor ribosomale eiwitten verlaagd in embryos geinjecteerd met gemanipuleerd P38α expressie en niet in embryos met afwijkend Erk2 eiwit gehalte. Dit duidt op een specifieke interactie functie tussen de twee MAPK in signaaltransductie gedurende stress wat al ontwikkeld is in embryonale stadia.

In hoofdstuk V is aangetoond dat P38α tevens een belangrijke rol speelt in de migratie van endotheel cellen, die de binnenkant van bloedvaten uitlijnen. De groei

van nieuwe bloedvaten kan bestudeerd worden m.b.v transgene zebravissen bevattende GFP gemarkeerde endotheel cellen. Gedoseerde toediening van P38α blokerende stoffen aan zebravissen veroorzaken afwijkingen in de vorming van het bloedvatenstelsel tijdens de ontwikkeling door obstructie van angiogenese (bloedvaten vertakkingen). P38α is ook betrokken bij de angiogenese van zoogdieren (muizen) tijdens ontwikkeling. Wij hebben aangetoond dat de functie van P38α in angiogenese evolutionair geconserveerd is in zebravissen. De specifieke rol van P38α in deze context kan daarom verder bestudeerd worden m.b.v het zebravis model. Tevens hebben we op transcriptie niveau gekeken naar de effecten van P38α manipulatie in endotheel cellen en we hebben daarbij een aantal gen kandidaten geidentificeerd die een rol spelen in angiogenese en mogelijk gereguleerd worden door de P38α MAPK cascade.

Curriculum vitae

&

Publicaties

C.V

Hanan Rian werd geboren op 31 januari 1984 te Winterswijk. In 2002 behaalde zij haar Havo diploma aan de Openbare scholengemeenschap de Driemark in Winterswijk. Hanan ging vervolgens Biologie & Medisch laboratoriumonderzoek studeren aan de Saxion Hogeschool in Enschede. Na het behalen van haar Bachelor titel ging zij in 2006 Moleculaire Cel Biologie studeren aan Universiteit Leiden voor een Master diploma. Hanan heeft haar masterstage verricht bij de onderzoeksgroep van Dr.B.E. Snaar-Jagalska van het Instuut voor Biologie en werd aangenomen voor dit promotieonderzoek na het behalen van haar diploma in december 2008.

Publicatie

Hanan Rian, S. F. Gabriel Krens, Herman P. Spaink, and B. Ewa Snaar-Jagalska, "Generation of Constitutive Active ERK Mutants as Tools for Cancer Research in Zebrafish," ISRN Cell Biology, vol. 2013, Article ID 867613, 11 pages, 2013. doi:10.1155/2013/867613